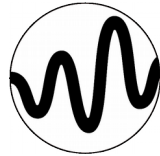




UNIVERSITY OF
BIRMINGHAM



Gravitational-wave astronomy & black hole astrophysics

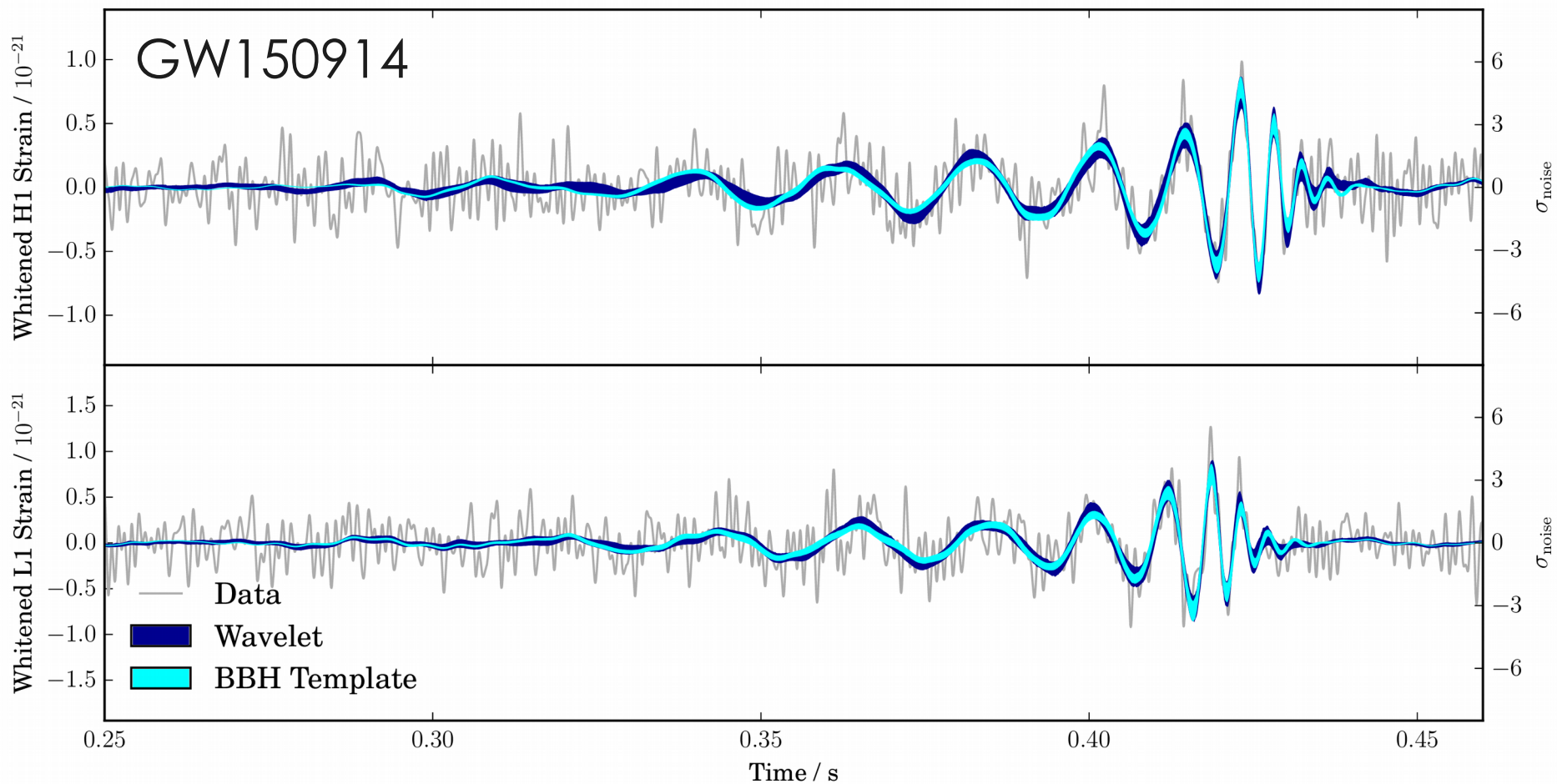
Christopher Berry

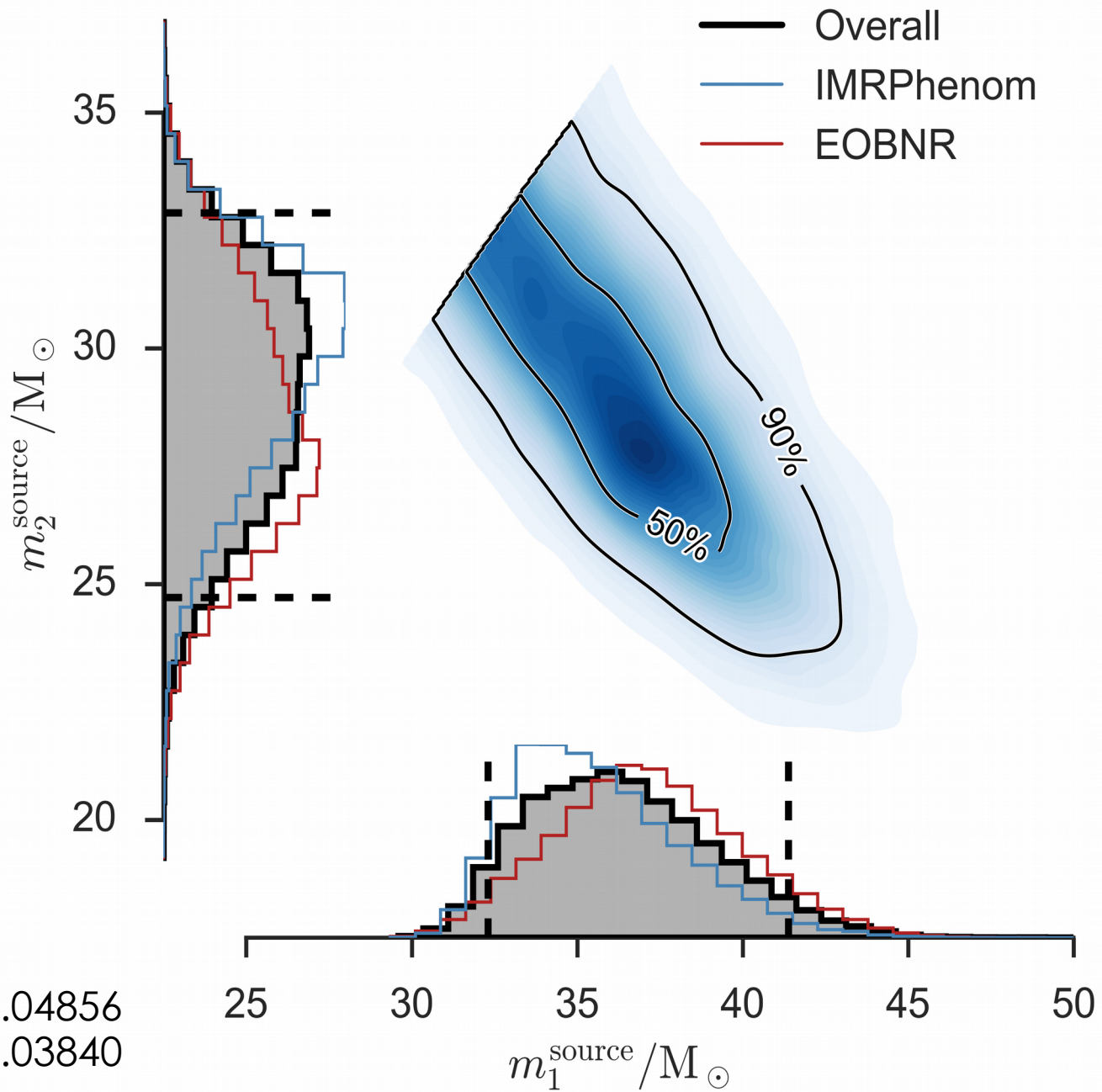
University of Birmingham

@cplberry

On behalf of the
LIGO Scientific & Virgo Collaborations

DCC G1800621
IOP APP & HEPP 2018





LVC
arXiv:1606.04856
arXiv:1602.03840

How to infer source properties

Our measurements so far

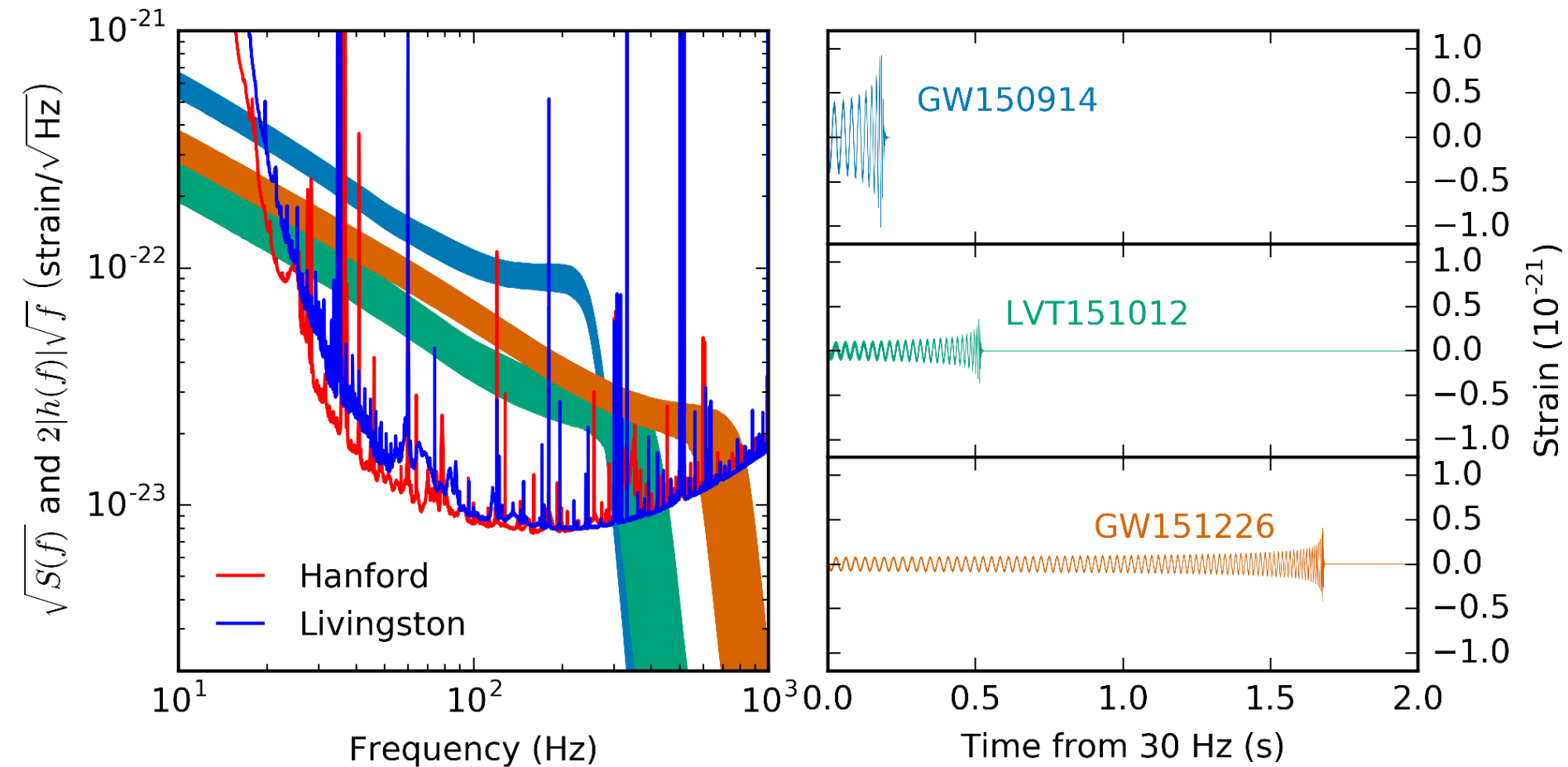
How we can use gravitational-wave
observations

How to infer source properties

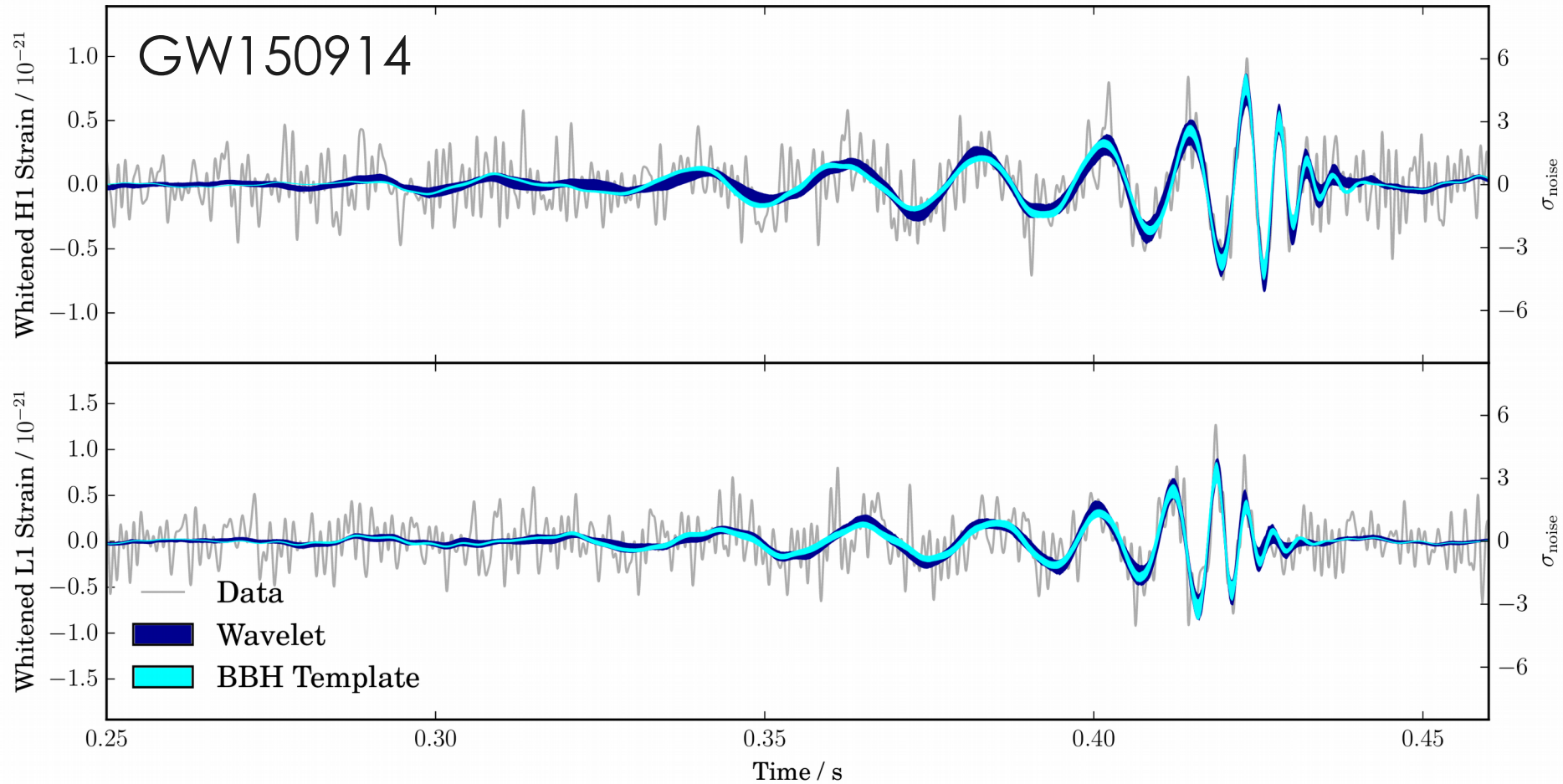
Our measurements so far

How we can use gravitational-wave observations

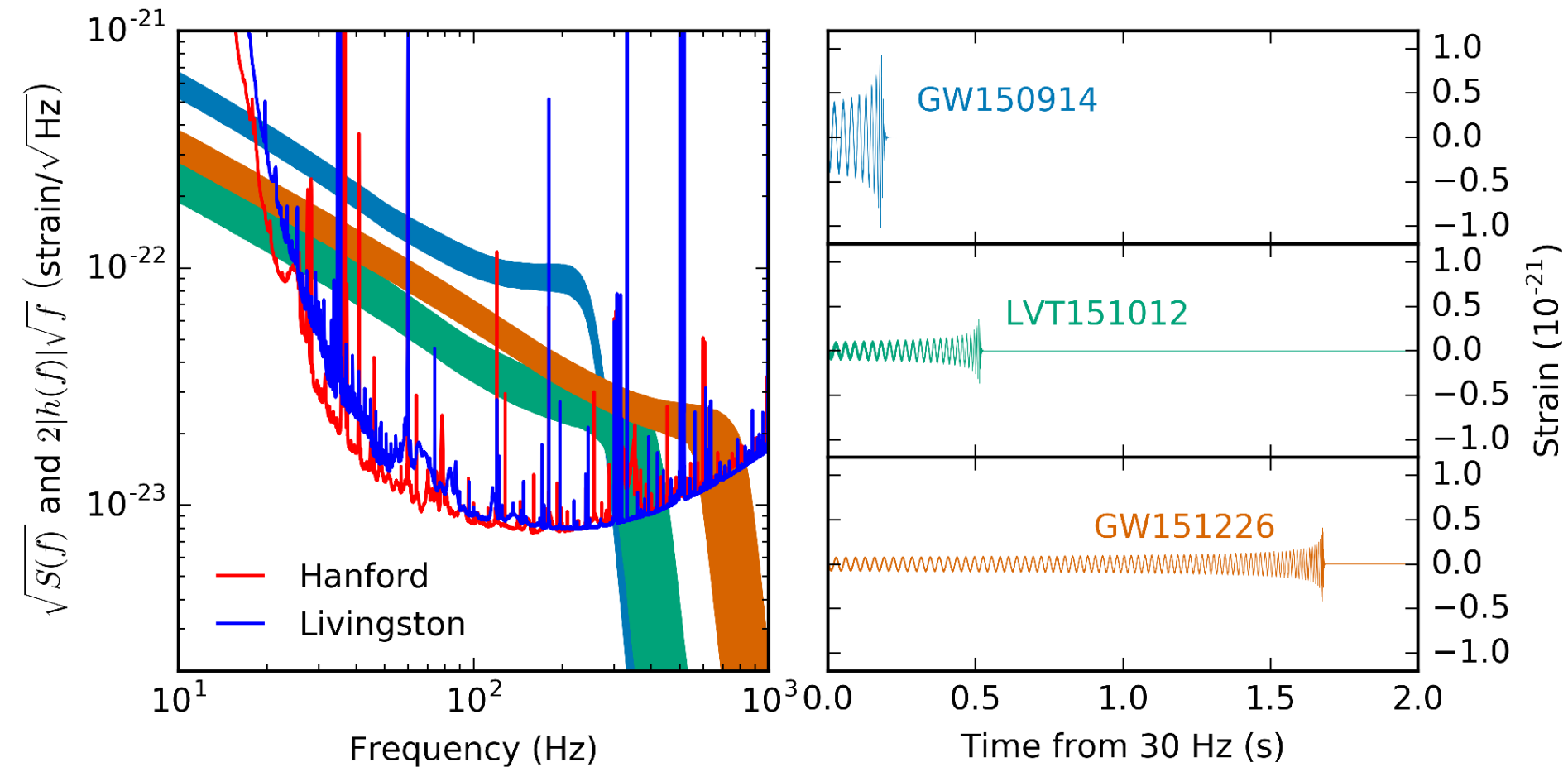
Measurement

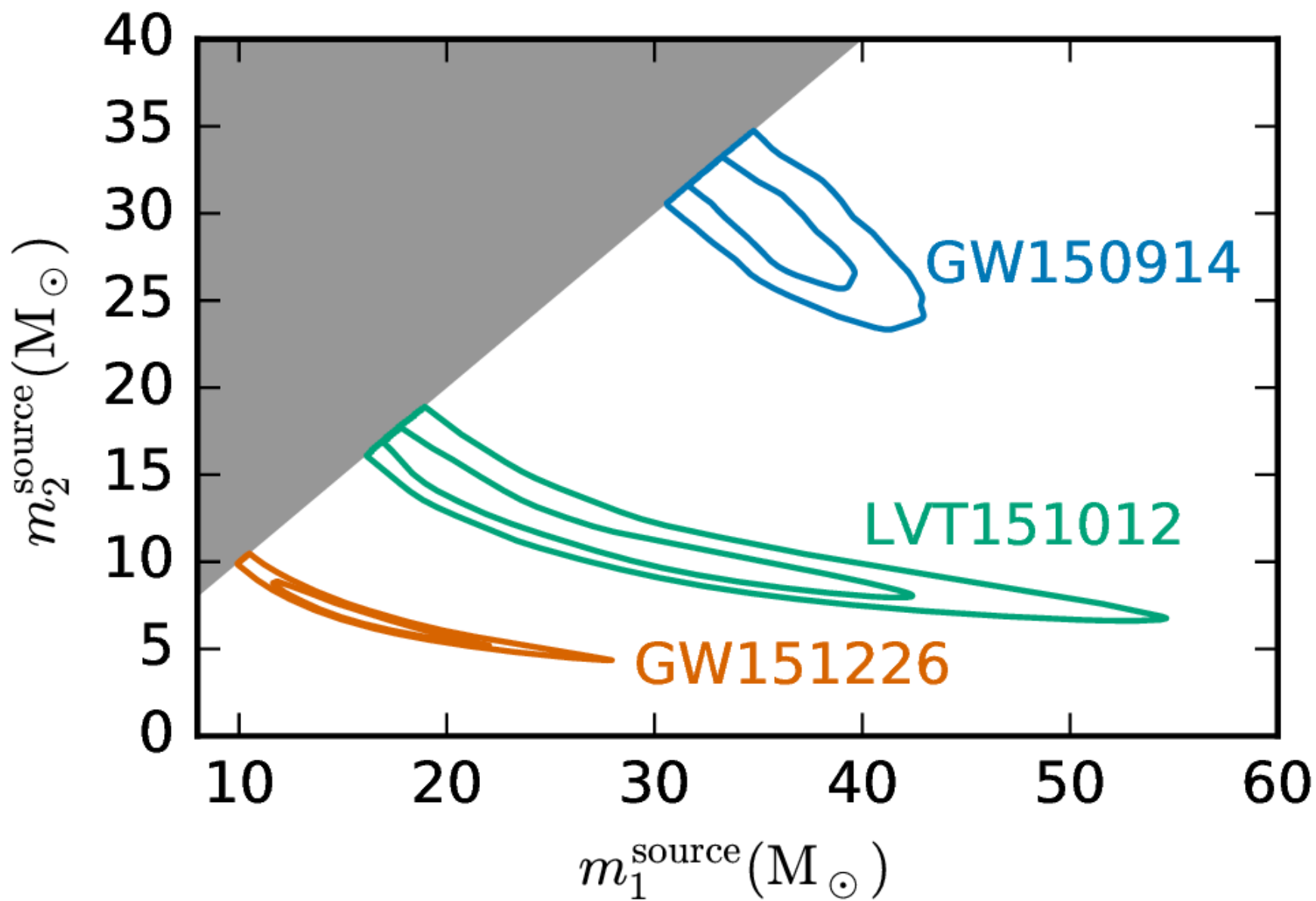


Waveform



Measurement





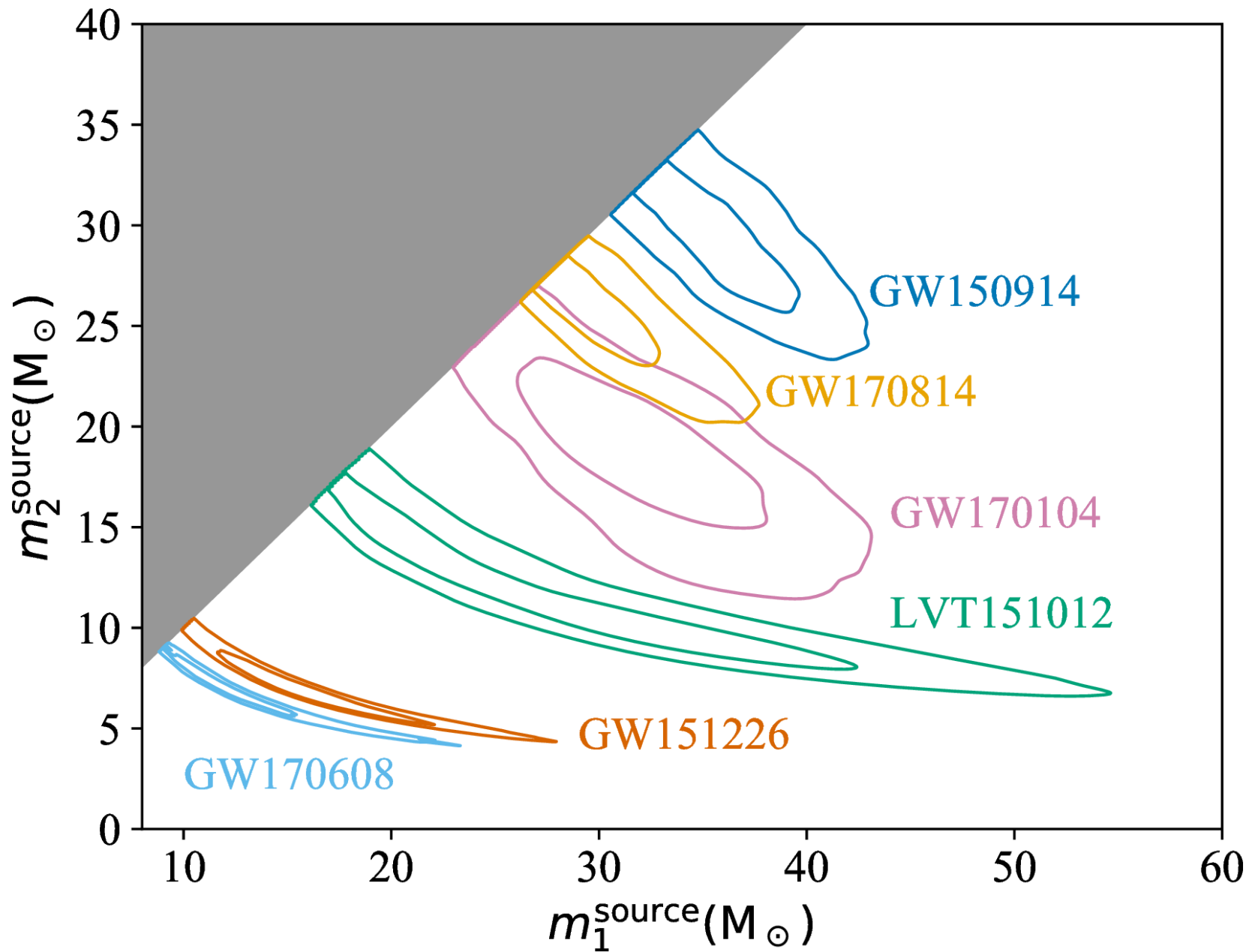
How to infer source properties

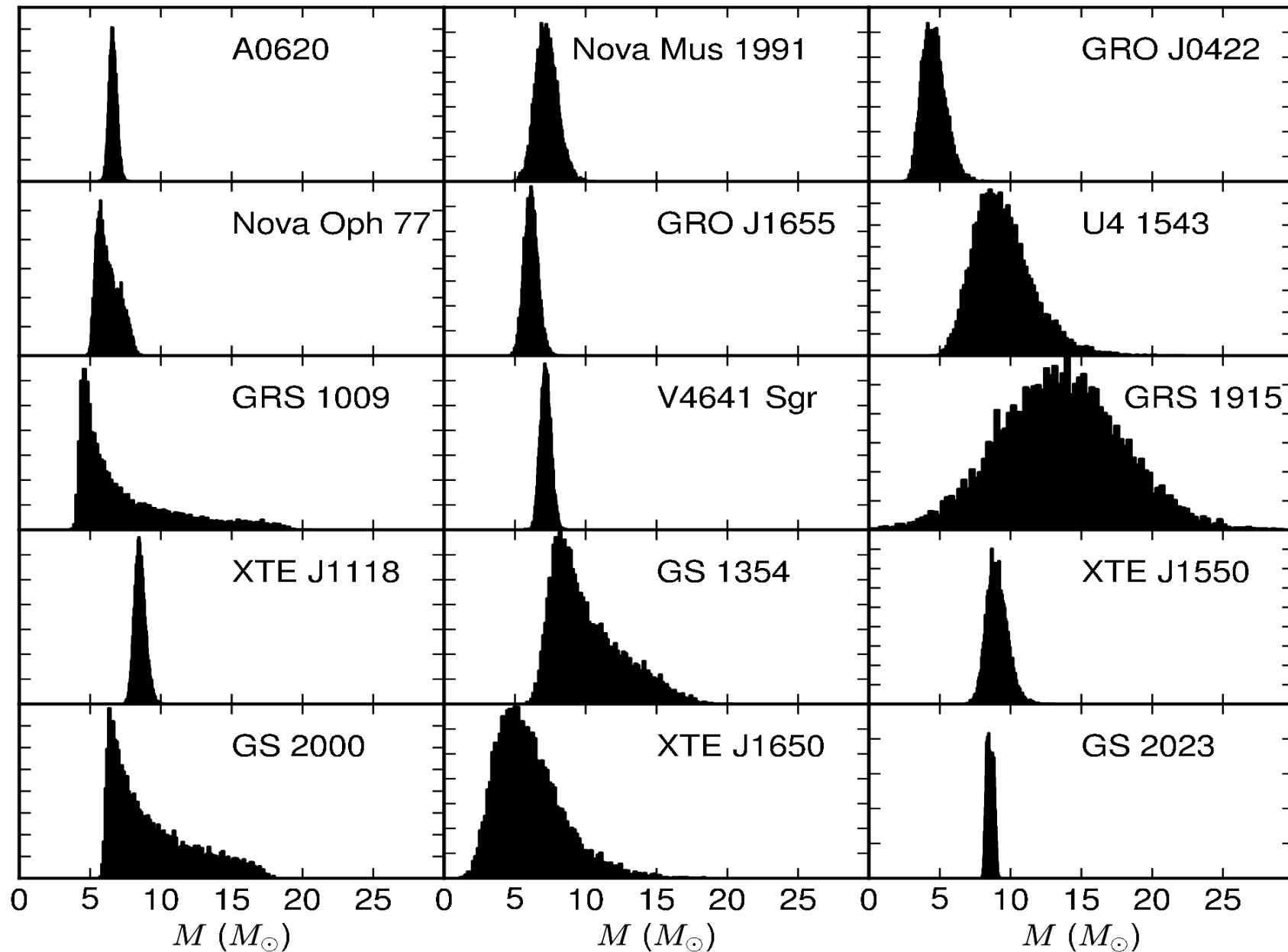
Our measurements so far

How we can use gravitational-wave
observations

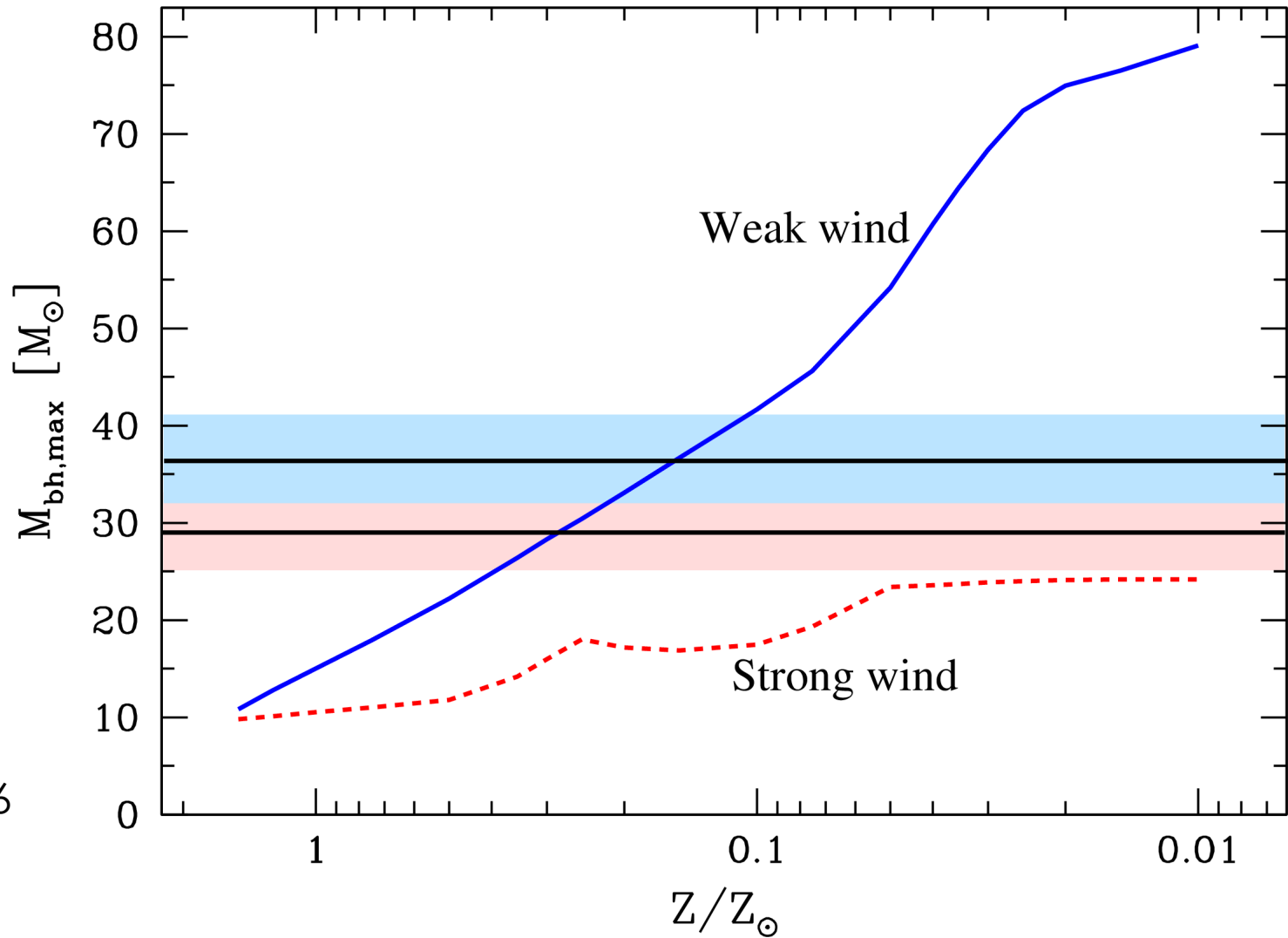


Credit: ButterflyLove1

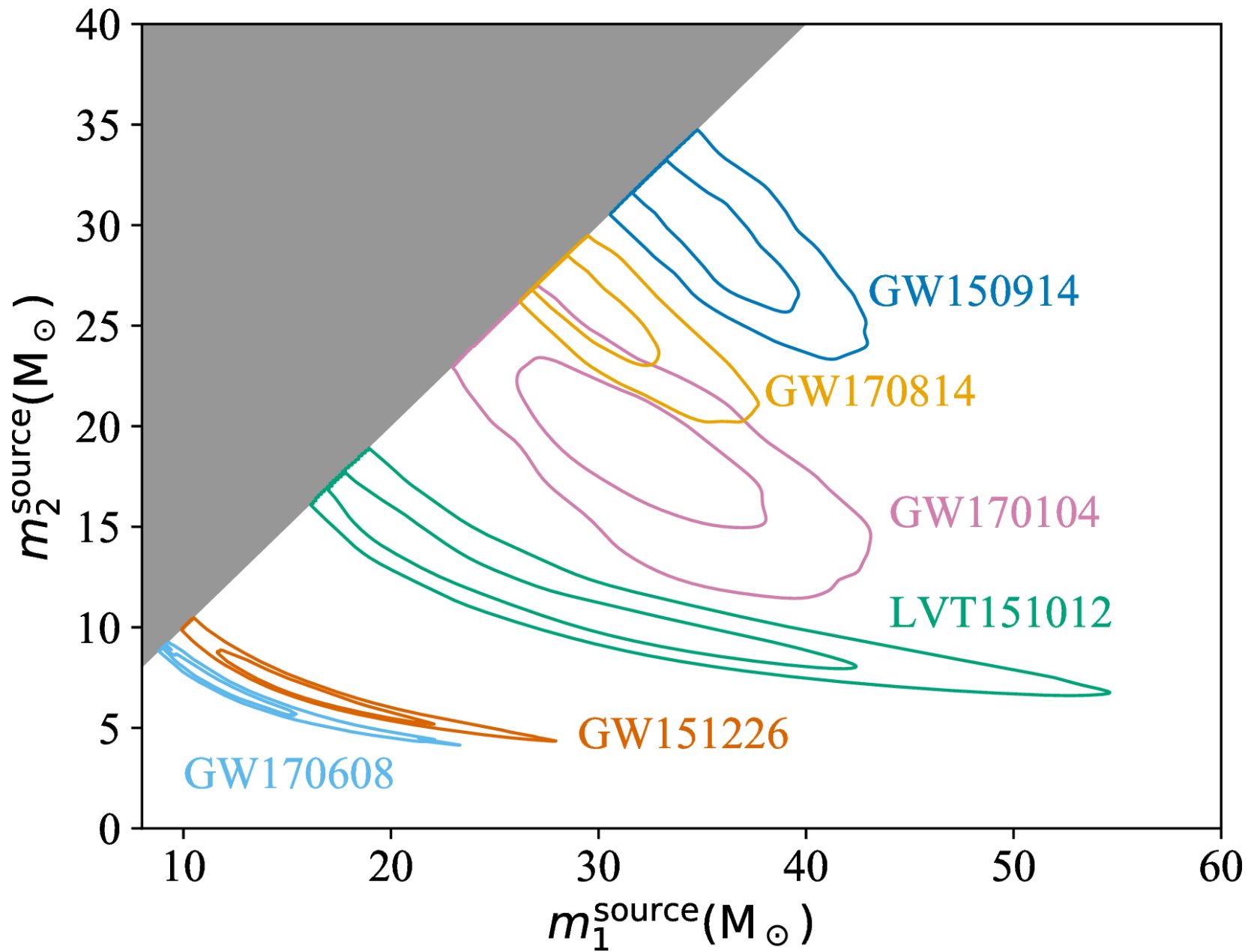




Metallicity



LVC
arXiv:1602.03846
Belczynski *et al.*
arXiv:0904.2784



No hair theorem

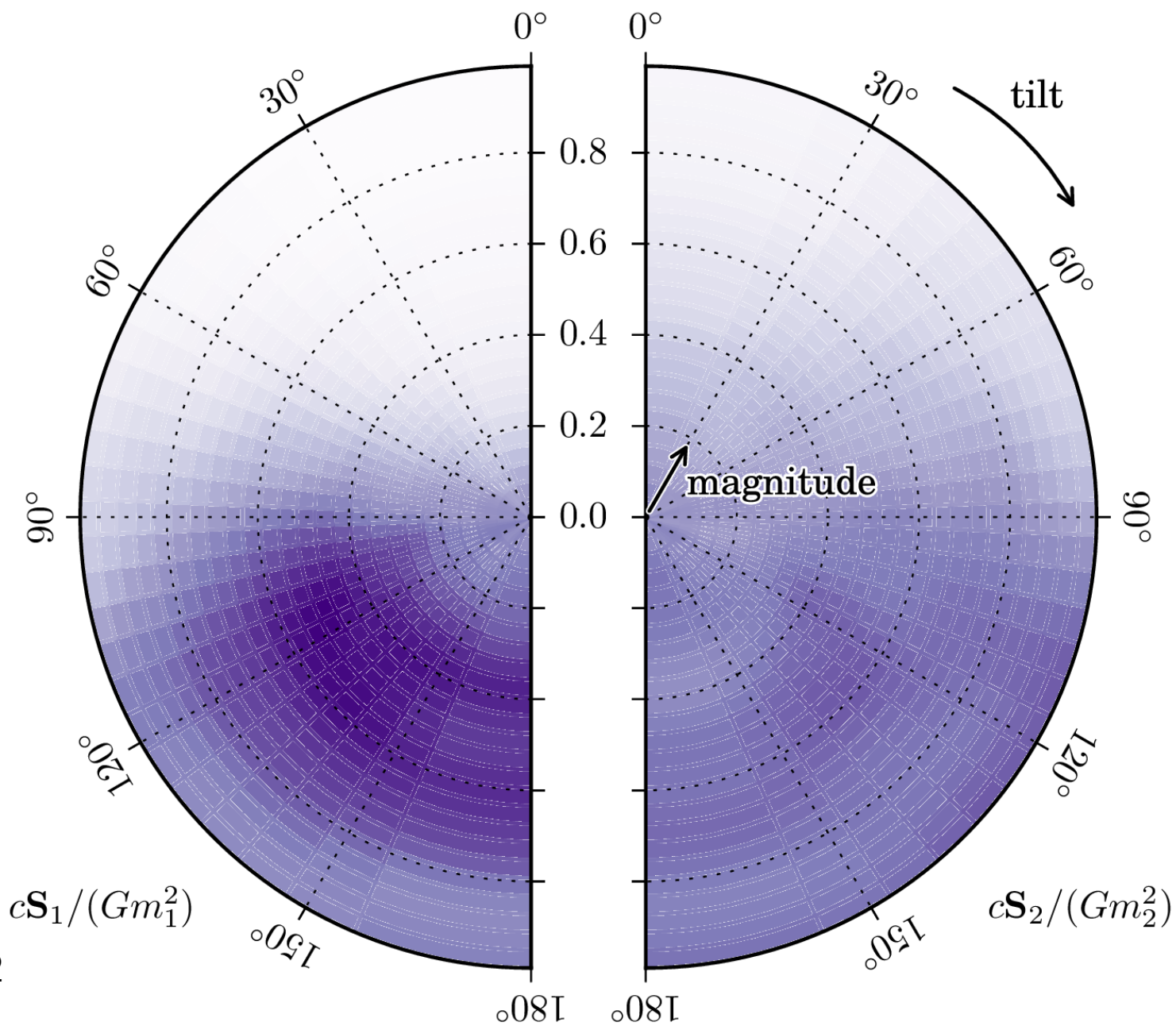


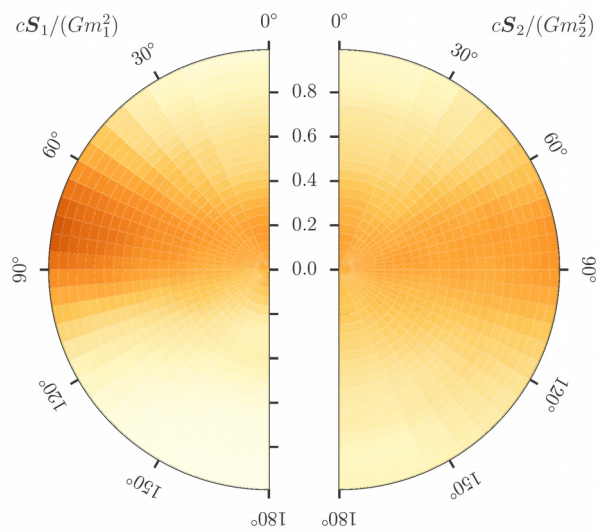
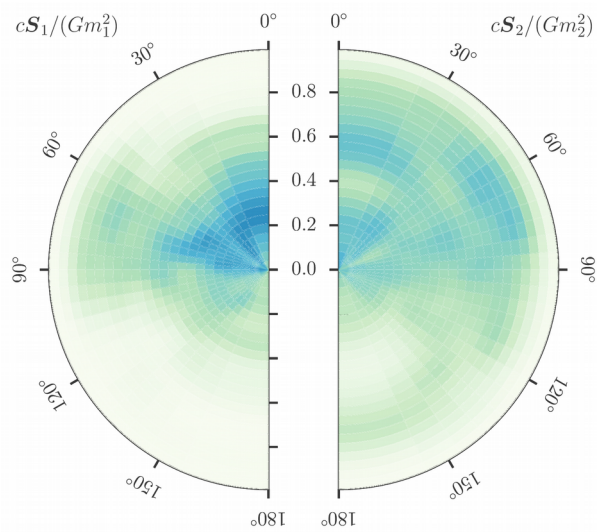
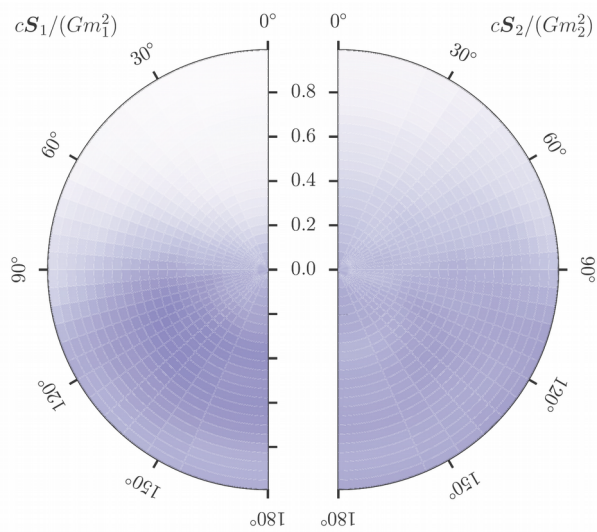
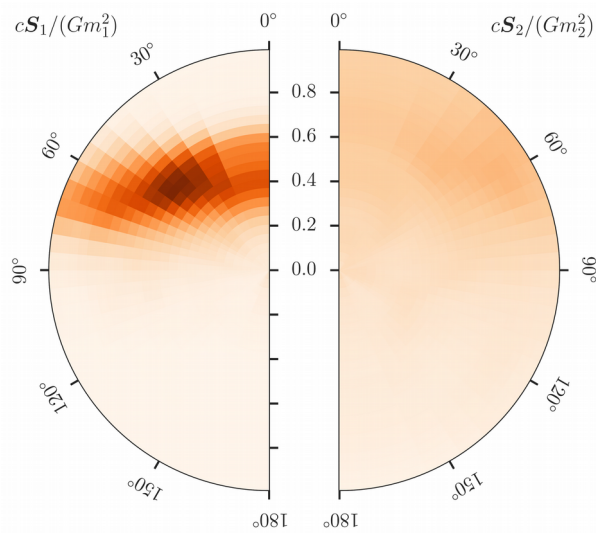
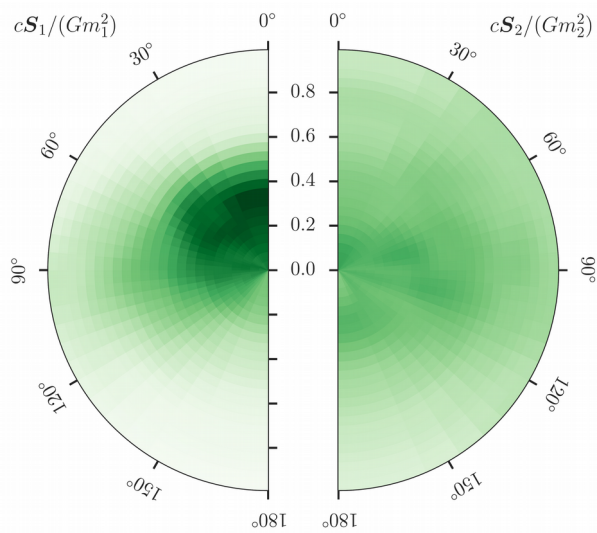
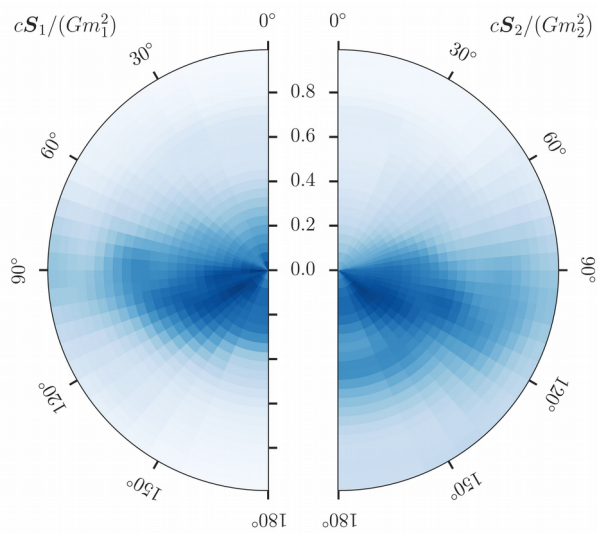
Black holes have:

1. Mass
2. Spin
3. Electric charge

Credit: Matt Groening

Spin





LVC arXiv:1606.04856

arXiv:1706.01812

arXiv:1709.09660

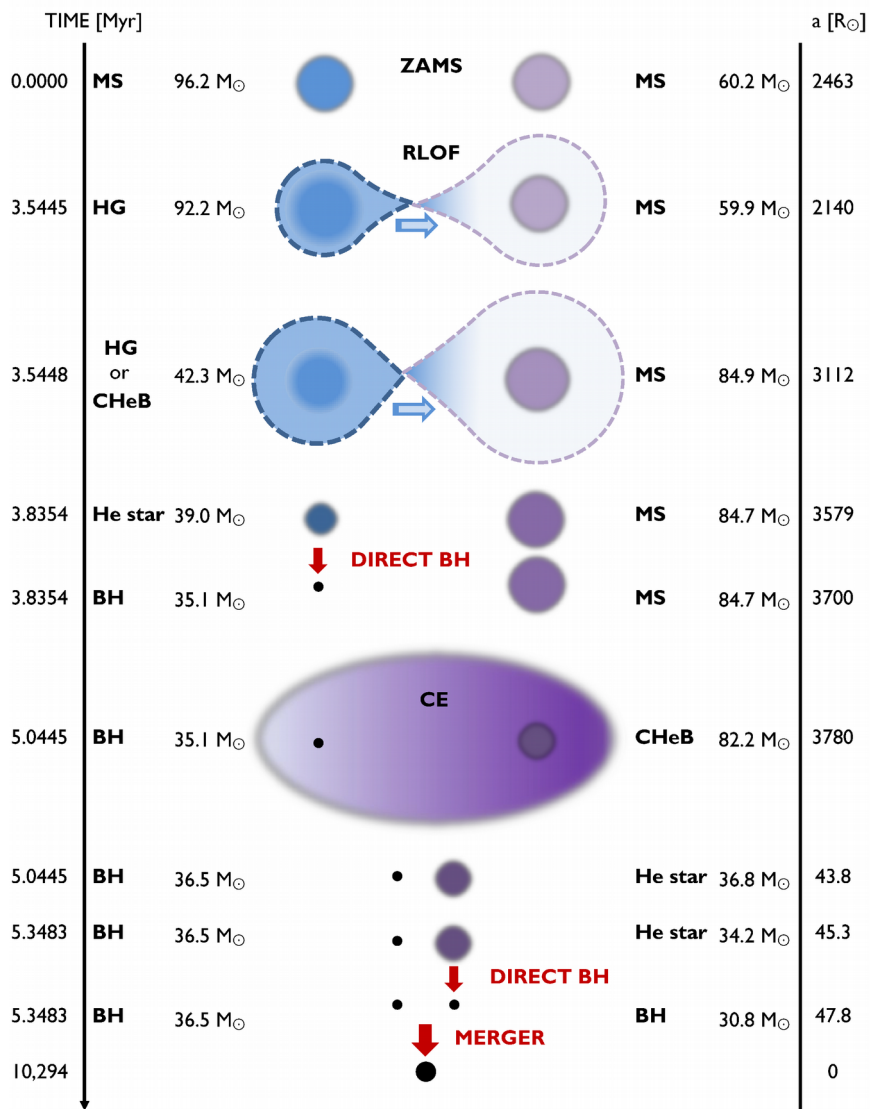
arXiv:1711.05578

How to infer source properties

Our measurements so far

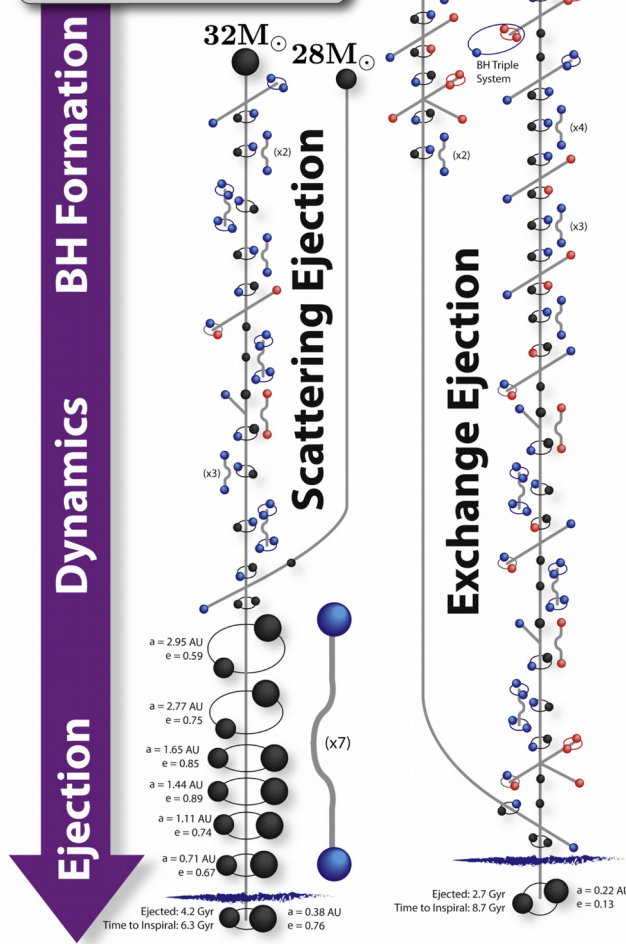
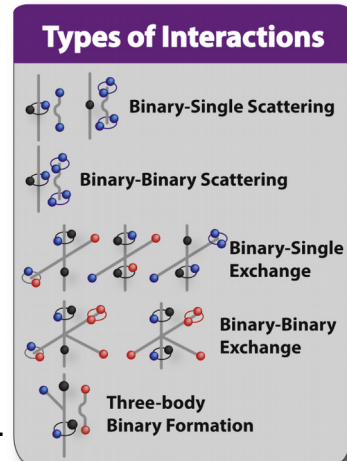
How we can use gravitational-wave
observations

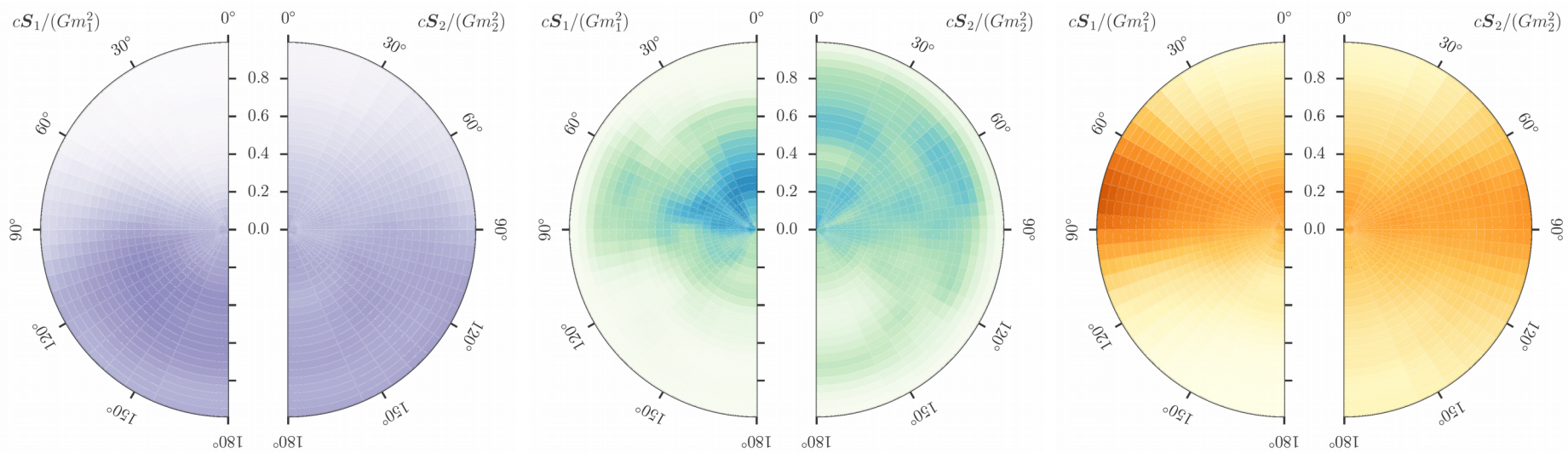
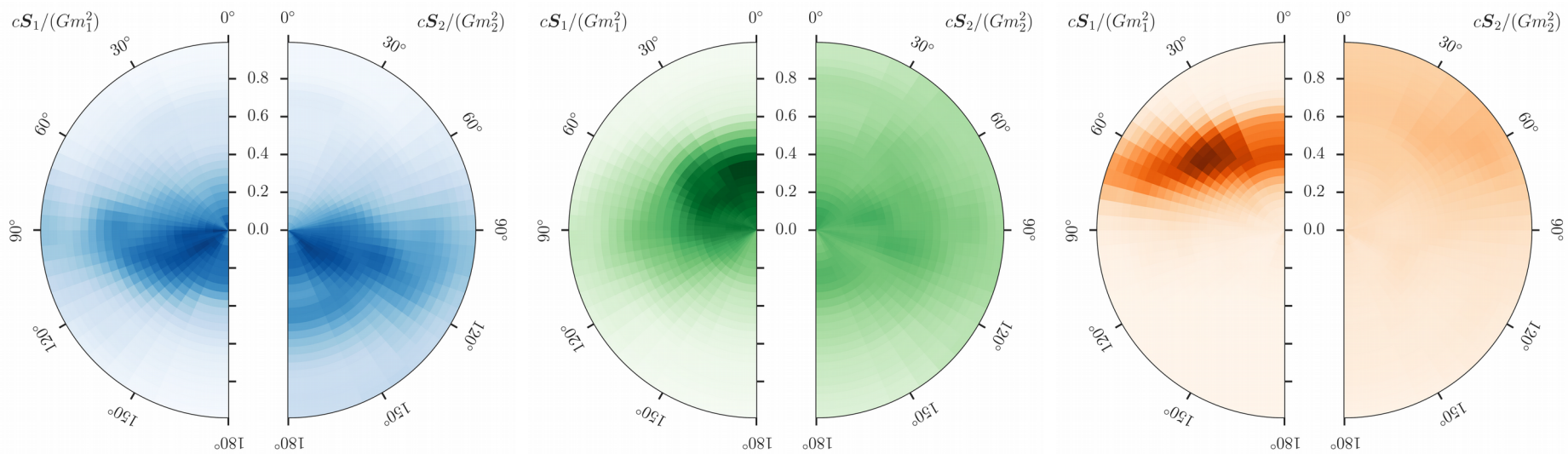
Binary formation



Rodriguez *et al.*
arXiv:1604.04254

Belczynski *et al.*
arXiv:1602.04531



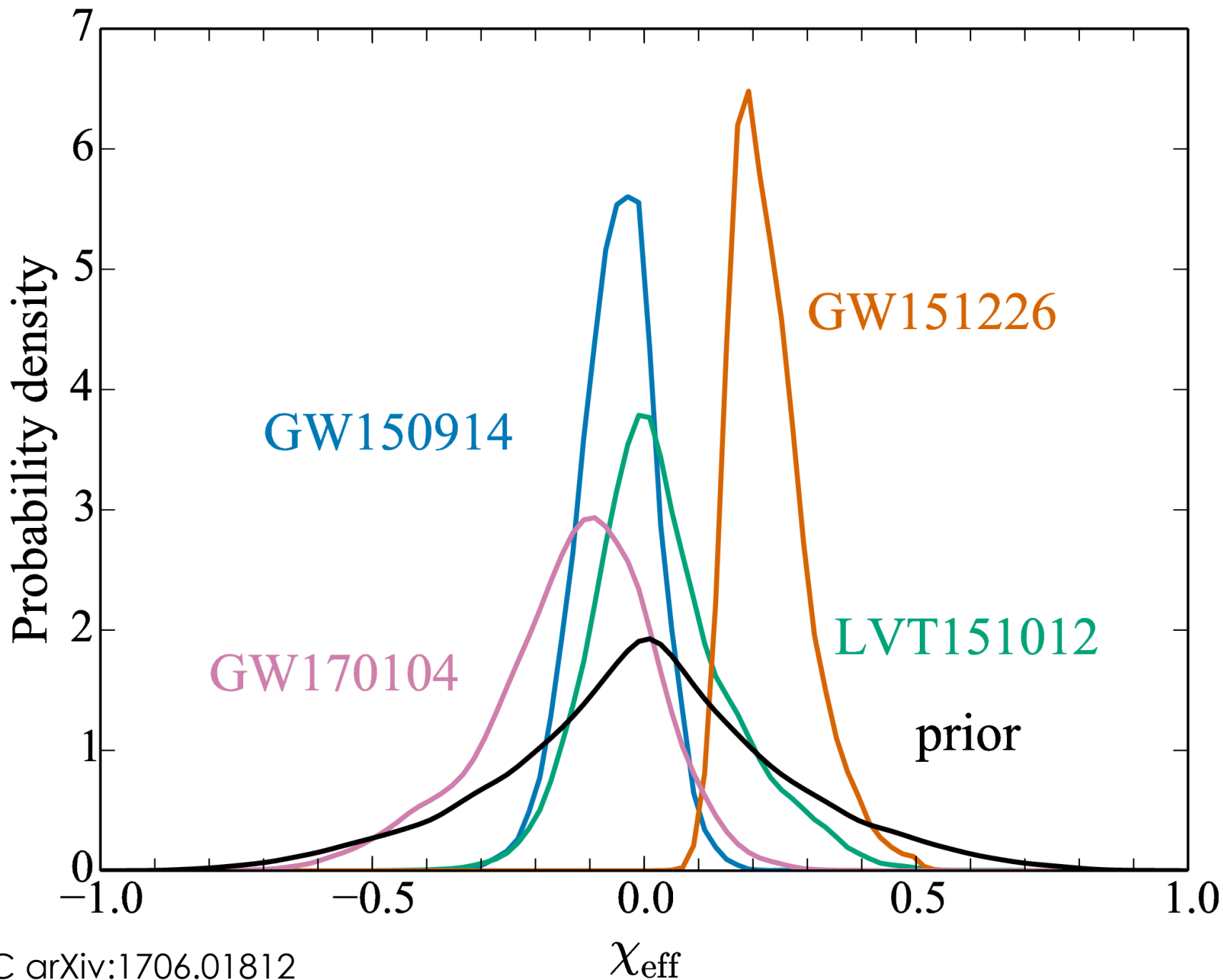


LVC arXiv:1606.04856

arXiv:1706.01812

arXiv:1709.09660

arXiv:1711.05578



Distinguishing Spin-Aligned and Isotropic Black Hole Populations With Gravitational Waves

Will M. Farr, Simon Stevenson, M. Coleman Miller, Ilya Mandel, Ben Farr, Alberto Vecchio

(Submitted on 5 Jun 2017 (v1), last revised 6 Jun 2017 (this version, v2))

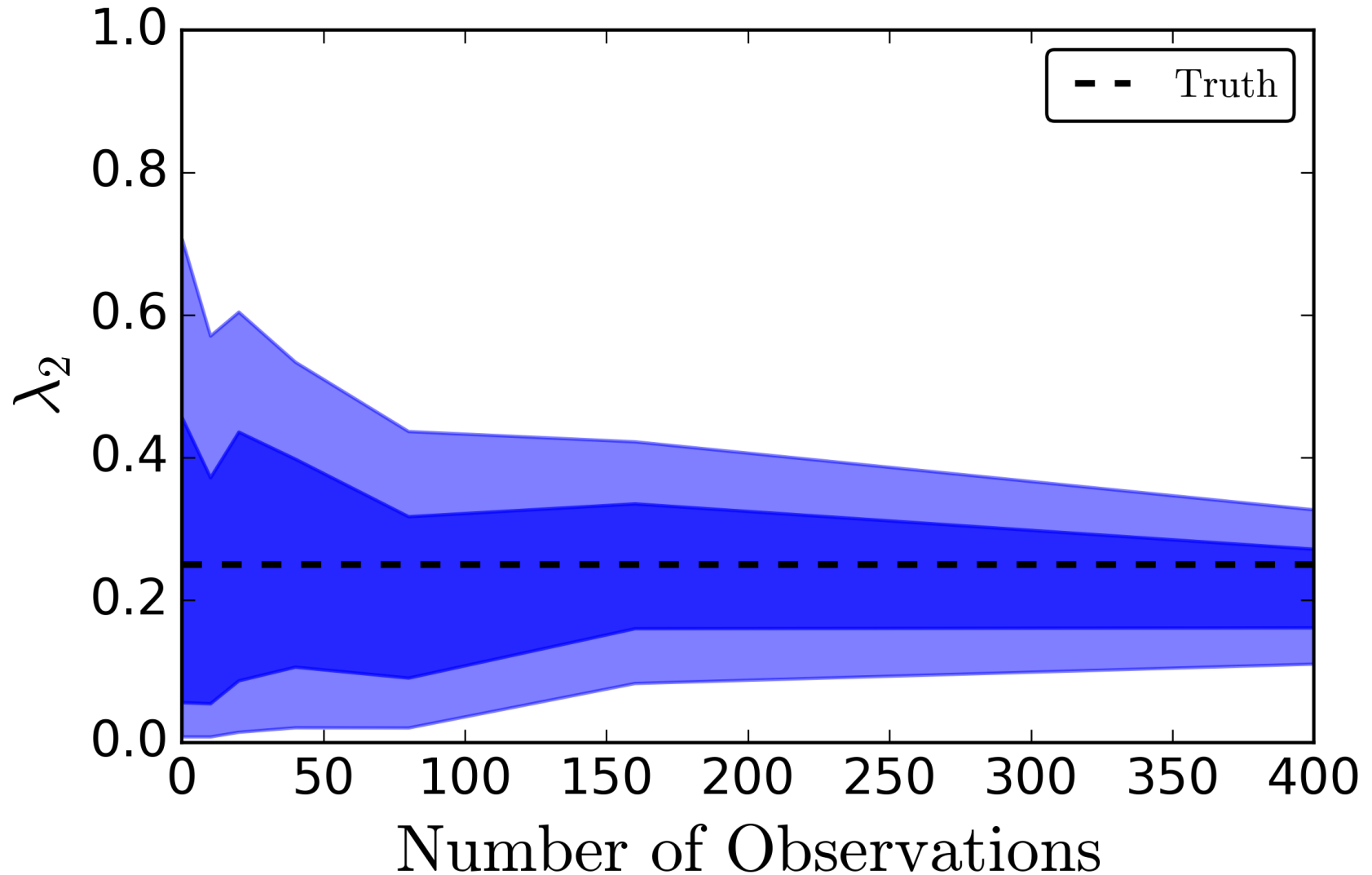
The first direct detections of gravitational waves from merging binary black holes open a unique window into the binary black hole formation environment. One promising environmental signature is the angular distribution of the black hole spins; systems formed through dynamical interactions among already-compact objects are expected to have isotropic spin orientations whereas binaries formed from pairs of stars born together are more likely to have spins preferentially aligned with the binary orbital angular momentum. We consider existing gravitational wave measurements of the binary effective spin, the best-measured combination of spin parameters, in the four likely binary black hole detections GW150914, LVT151012, GW151226, and GW170104. If binary black hole spin magnitudes extend to high values we show that the data exhibit a 2.4σ (0.015 odds ratio) preference for an isotropic angular distribution over an aligned one. By considering the effect of 10 additional detections, we show that such an augmented data set would enable in most cases a preference stronger than 5σ (2.9×10^{-7} odds ratio). The existing preference for either an isotropic spin distribution or low spin magnitudes for the observed systems will be confirmed (or overturned) confidently in the near future.

Comments: 32 pages, 9 figures, code and documents
Subjects: **High Energy Astrophysical Phenomena**
Report number: LIGO-P1700067
Cite as: [arXiv:1706.01385](https://arxiv.org/abs/1706.01385) [astro-ph.HE]
(or [arXiv:1706.01385v2](https://arxiv.org/abs/1706.01385v2) [astro-ph.HE])

Vitale *et al.* arXiv: 1503.04307
Gerosa & Berti arXiv: 1703.06223
Fishbach, Holz & Farr arXiv:1703.06869
Stevenson, **CPLB** & Mandel: 1703.06873
Talbot & Thrane arXiv:1704.08370

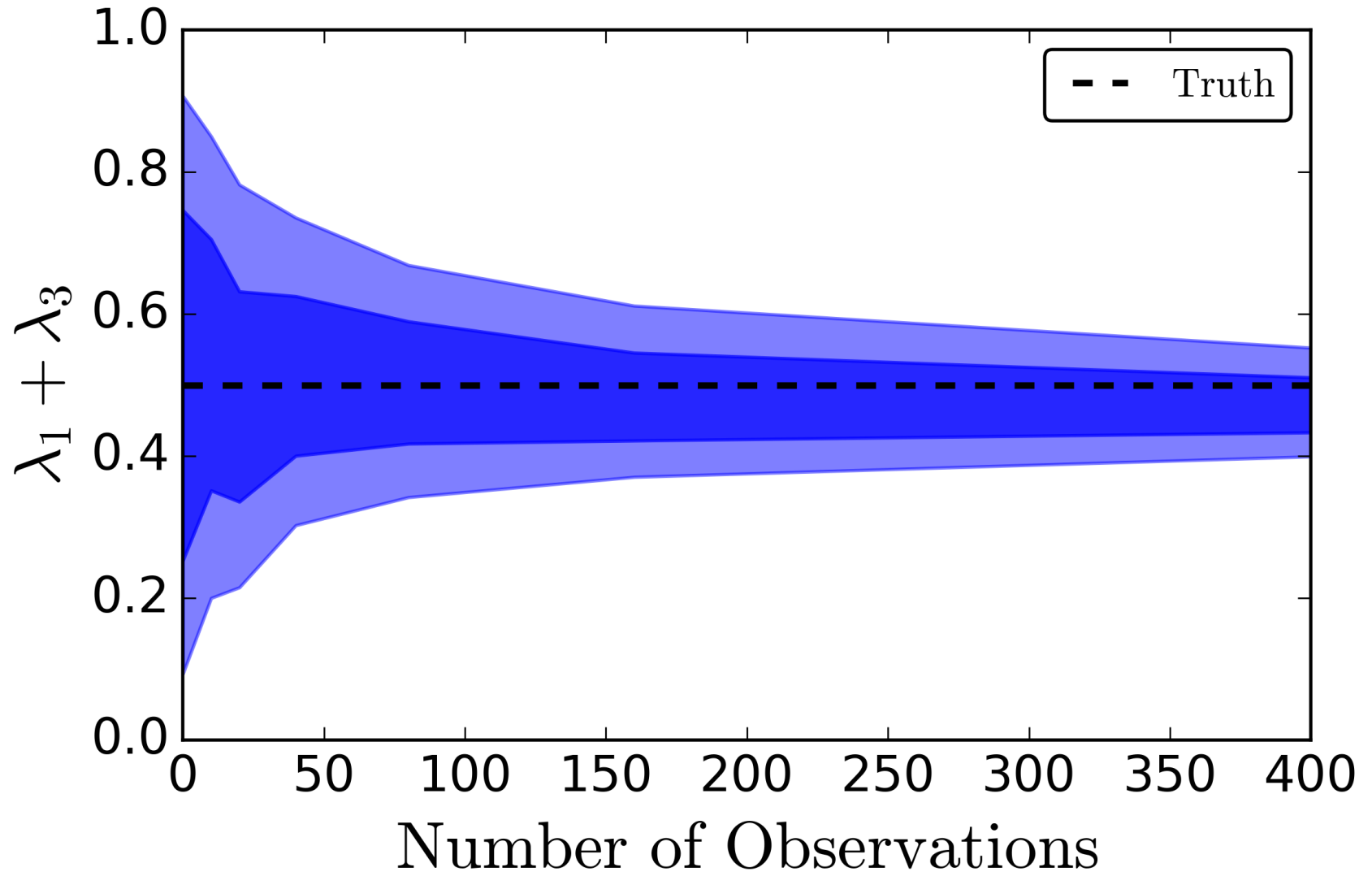
Model inference

Stevenson, CPLB & Mandel
arXiv:1703.06873

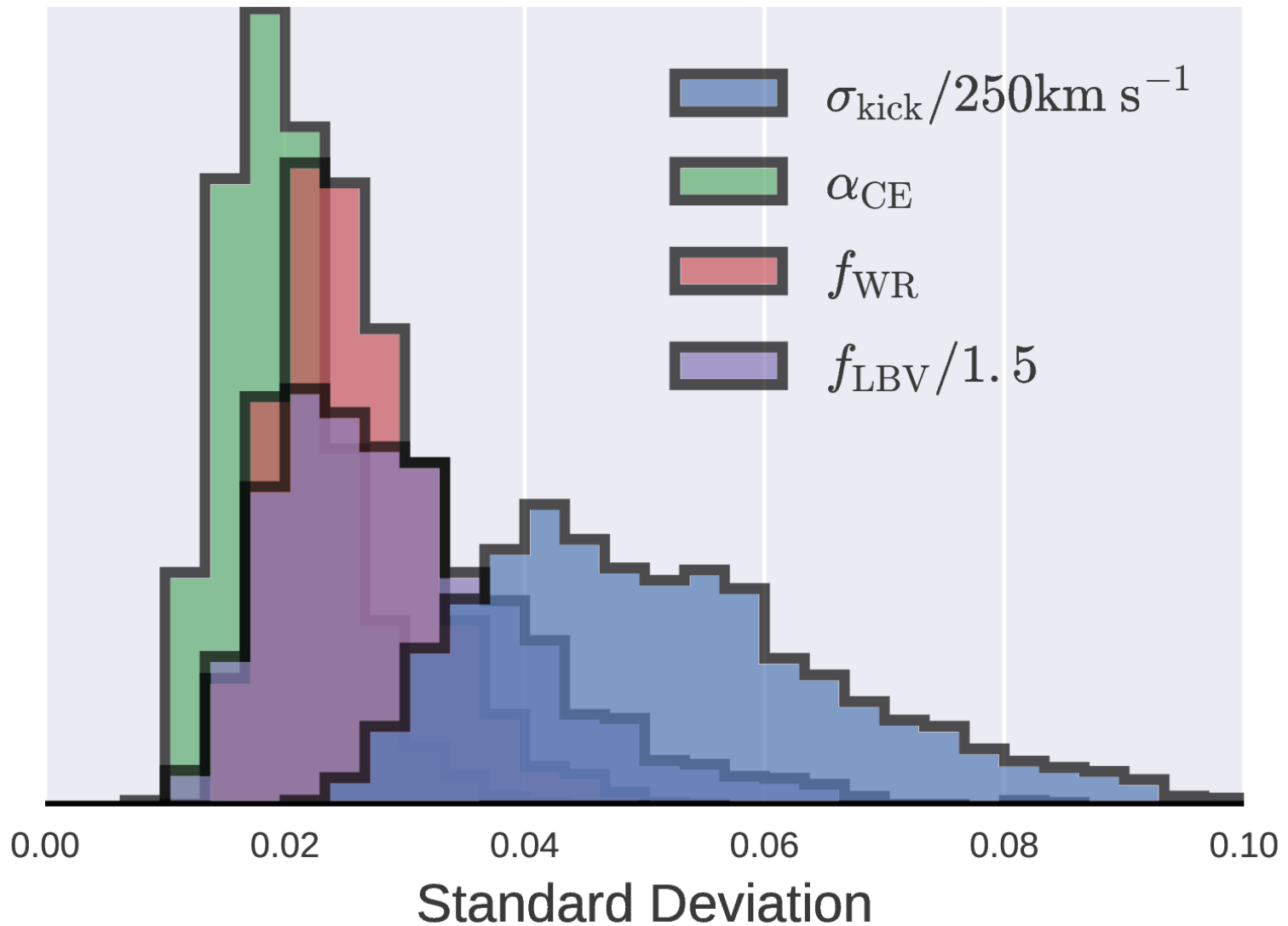


Model inference

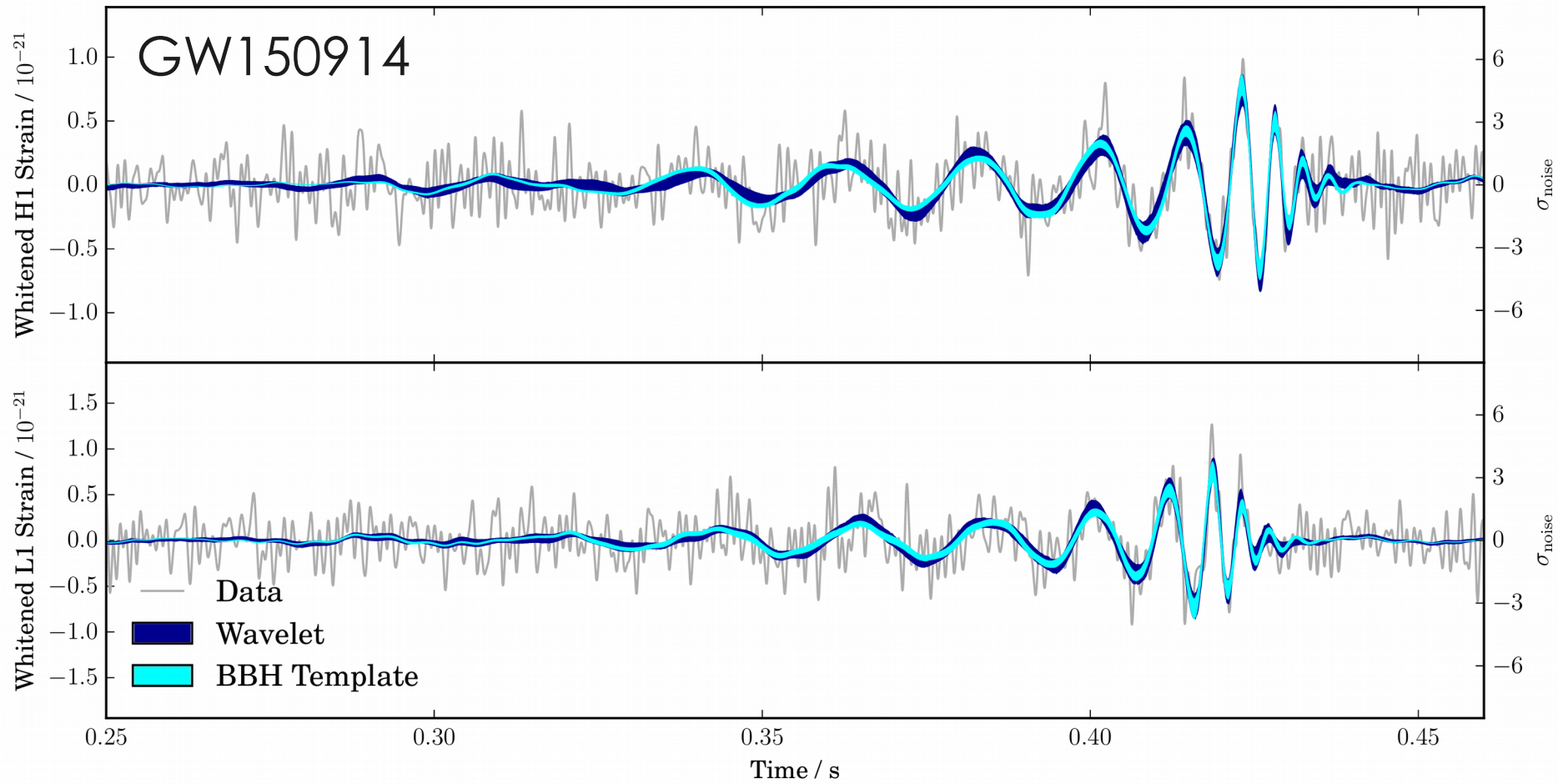
Stevenson, CPLB & Mandel
arXiv:1703.06873



Binary evolution

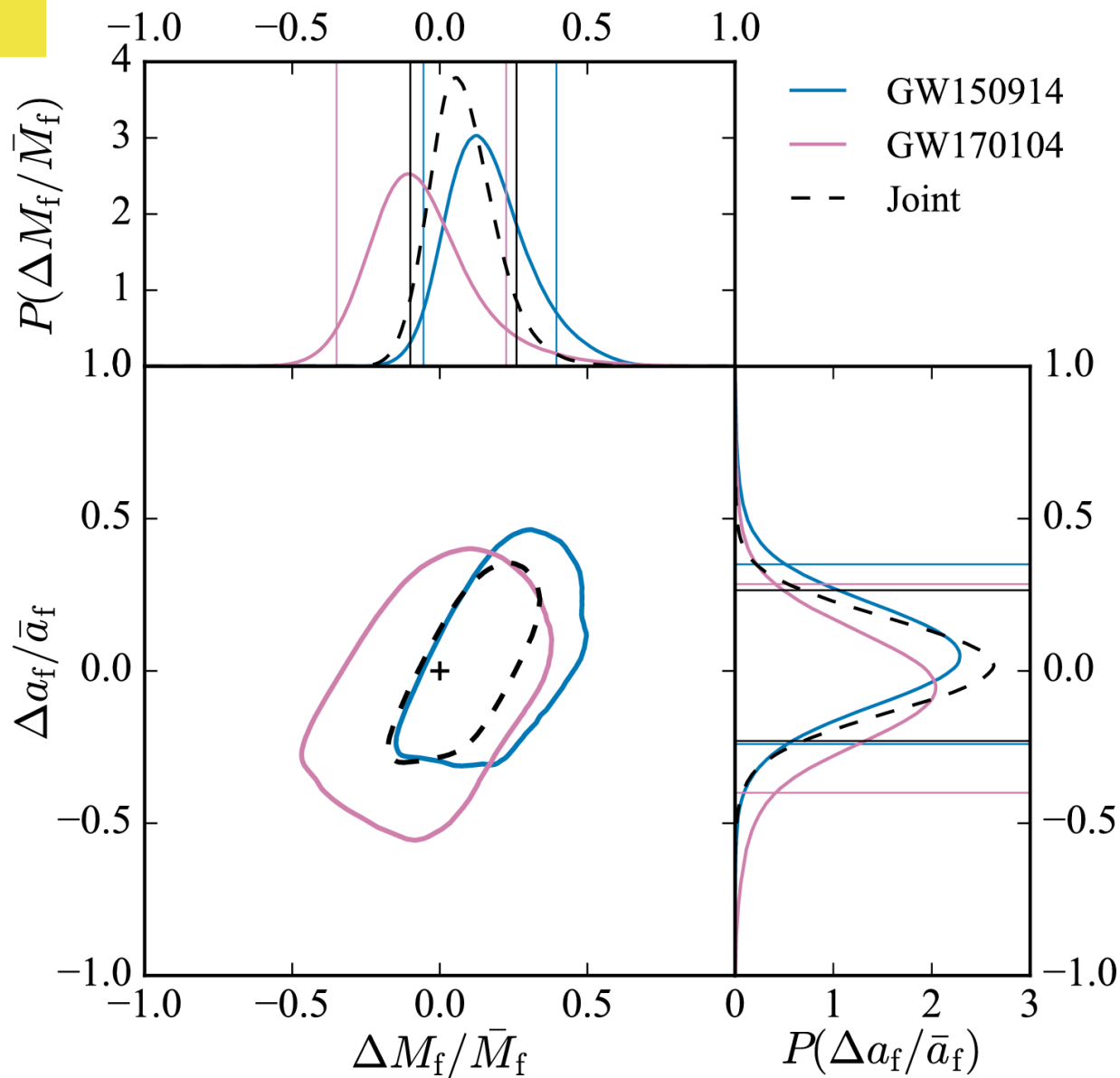


Waveform



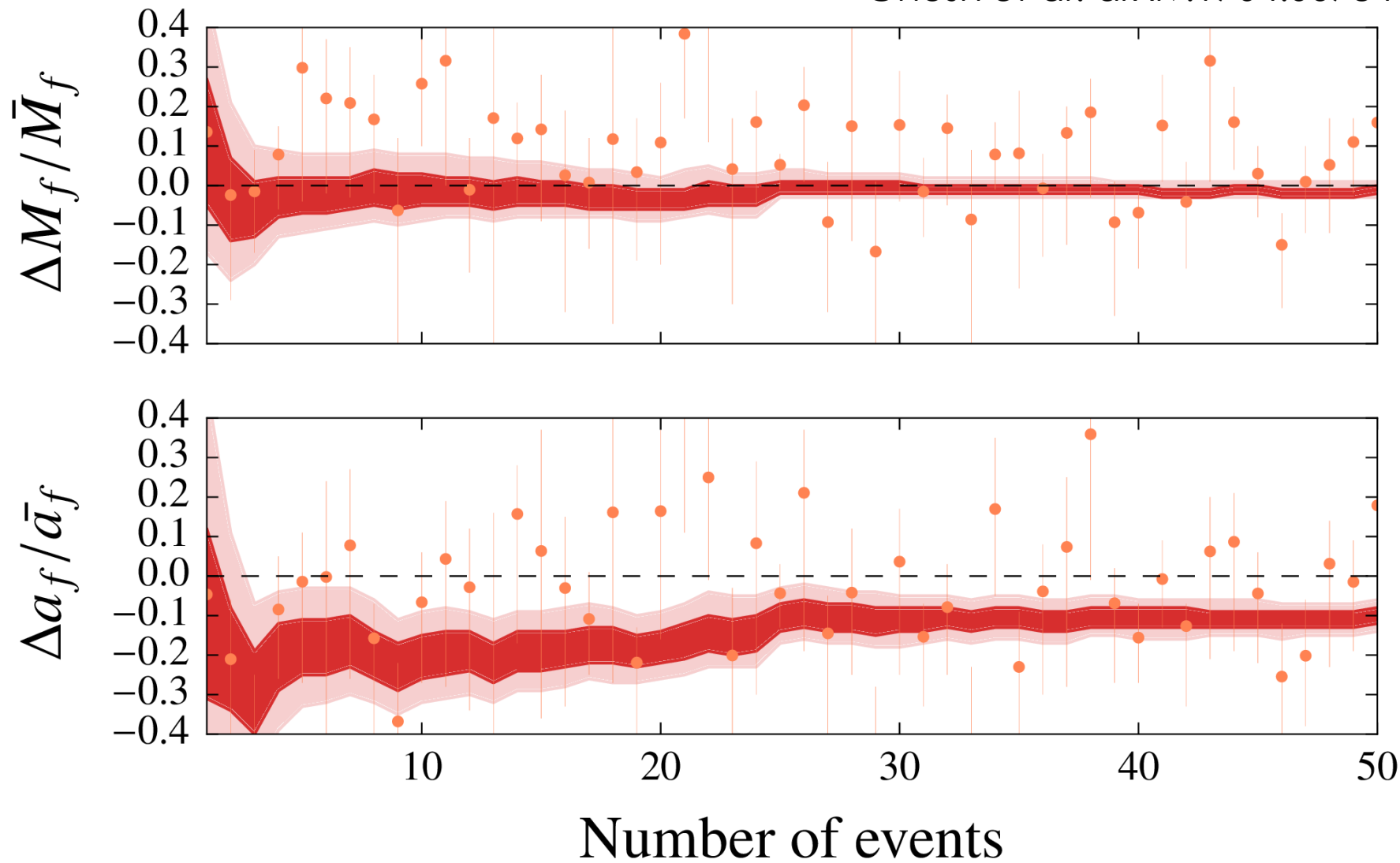
Testing GR

LVC arXiv:1602.03841
arXiv:1706.01812



Testing GR

Ghosh *et al.* arXiv:1704.06784



Gravitational waves provide a new tool
for astronomy

We are learning about the population
of binary black holes

Combining measurements lets us test
binary physics and general relativity

- Infer source properties by comparing waveform templates to data
- Some parameter (like chirp mass) measured well, others (like in-plane spins) remain uncertain
- Parameters (masses, spins, redshifts) could give insight into evolution
- Need a hierarchical analysis of a population of ~100–1000 detections

arXiv:1602.03837

arXiv:1602.03839

arXiv:1606.04855

arXiv:1706.01812

arXiv:1711.05578

arXiv:1709.09660

arXiv:1710.05832

Image: NSF/LIGO/Sonoma
State University/A. Simonnet

Thank you

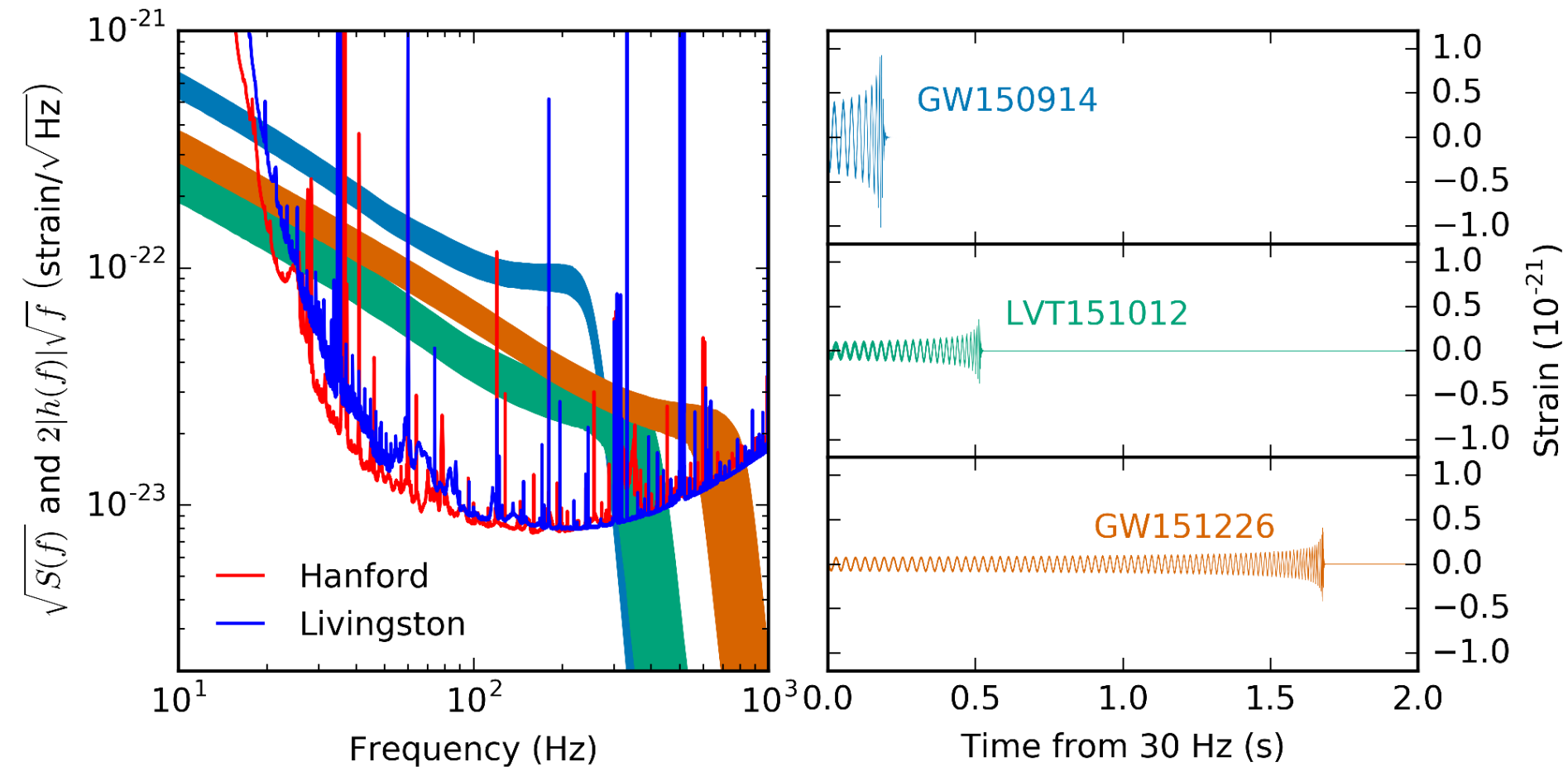
cplberry.com • @cplberry



Detector network



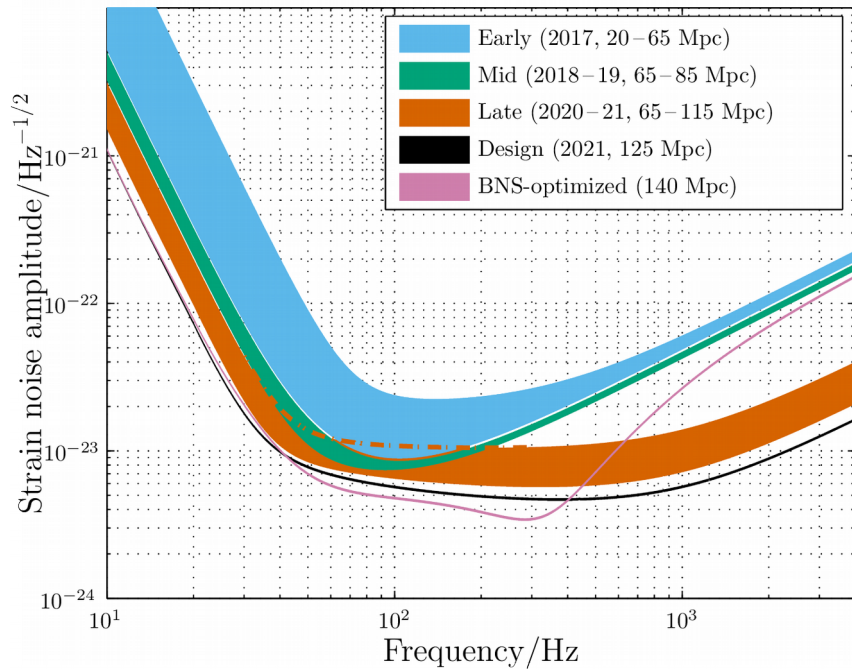
Detection



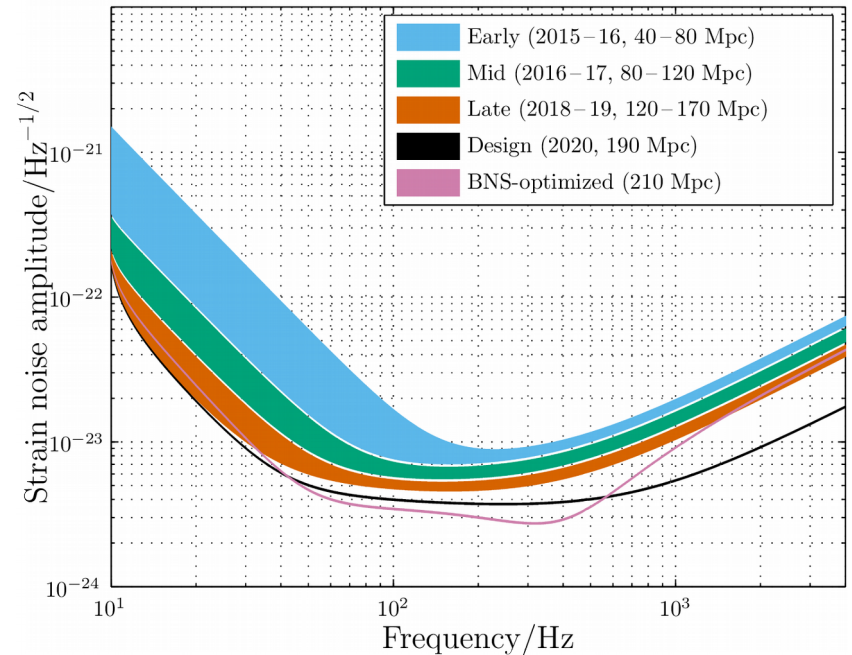
Plausible detector sensitivities

LVKC arXiv:1304.0670

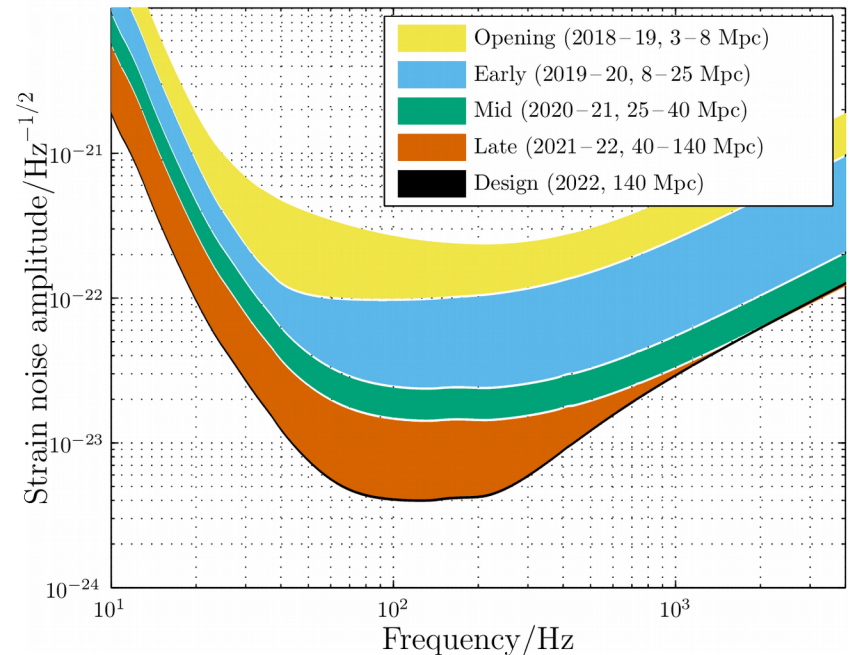
Advanced Virgo



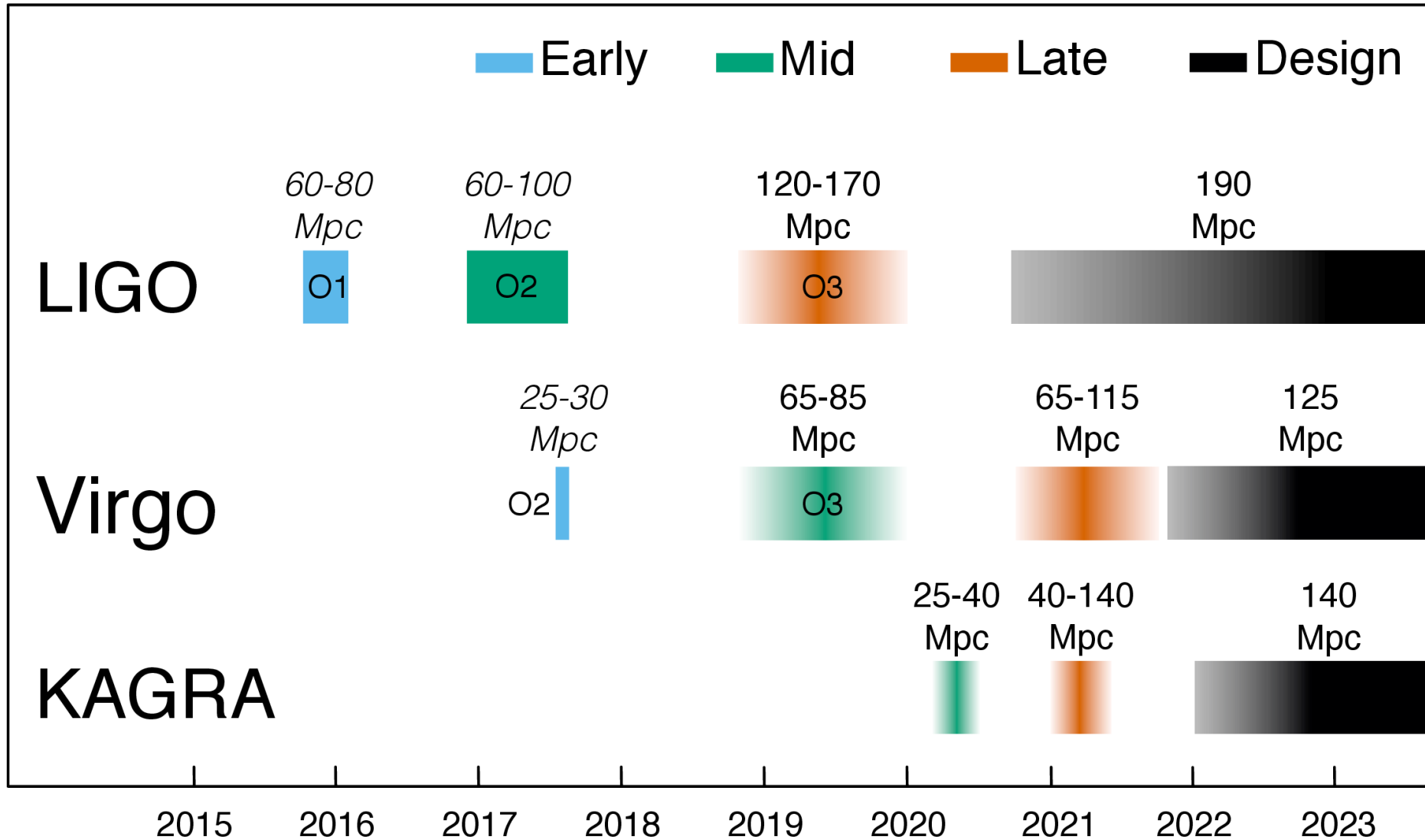
Advanced LIGO



KAGRA



Observing timetable



Ranges

Table 1 Plausible target detector sensitivities. The different phases match those in Figure 1. We quote the range, the average distance to which a signal could be detected, for a $1.4M_{\odot}+1.4M_{\odot}$ binary neutron star (BNS) system and a $30M_{\odot}+30M_{\odot}$ binary black hole (BBH) system.

	LIGO		Virgo		KAGRA	
	BNS range/Mpc	BBH range/Mpc	BNS range/Mpc	BBH range/Mpc	BNS range/Mpc	BBH range/Mpc
Early	40–80	415–775	20–65	220–615	8–25	80–250
Mid	80–120	775–1110	65–85	615–790	25–40	250–405
Late	120–170	1110–1490	65–115	610–1030	40–140	405–1270
Design	190	1640	125	1130	140	1270

Observing scenarios

Epoch			2015–2016	2016–2017	2018–2019	2020+	2024+
Planned run duration			4 months	9 months	12 months	(per year)	(per year)
Expected burst range/Mpc	LIGO		40–60	60–75	75–90	105	105
	Virgo		—	20–40	40–50	40–70	80
	KAGRA		—	—	—	—	100
Expected BNS range/Mpc	LIGO		40–80	80–120	120–170	190	190
	Virgo		—	20–65	65–85	65–115	125
	KAGRA		—	—	—	—	140
Achieved BNS range/Mpc	LIGO		60–80	60–100	—	—	—
	Virgo		—	25–30	—	—	—
	KAGRA		—	—	—	—	—
Estimated BNS detections			0.05–1	0.2–4.5	1–50	4–80	11–180
Actual BNS detections			0	1	—	—	—
90% CR	% within	5 deg ²	< 1	1–5	1–4	3–7	23–30
		20 deg ²	< 1	7–14	12–21	14–22	65–73
		median/deg ²	460–530	230–320	120–180	110–180	9–12
Searched area	% within	5 deg ²	4–6	15–21	20–26	23–29	62–67
		20 deg ²	14–17	33–41	42–50	44–52	87–90



LVT151012

**I WANT TO
BELIEVE**

Bayes' theorem

$$p(\theta|d) = \frac{p(d|\theta) p(\theta)}{p(d)}$$

Bayes' theorem

The diagram illustrates Bayes' theorem with the following components:

- Posterior:** $p(\theta|d)$ (blue box)
- Likelihood:** $p(d|\theta)$ (pink box)
- Prior:** $p(\theta)$ (orange box)
- Evidence:** $p(d)$ (green box)

$$p(\theta|d) = \frac{p(d|\theta)p(\theta)}{p(d)}$$

Likelihood

$$p(d|\theta) \propto \exp \left[-\frac{1}{2} \sum_k \langle h_k(\theta) - d_k | h_k(\theta) - d_k \rangle \right]$$

Likelihood

$$p(d|\theta) \propto \exp \left[-\frac{1}{2} \sum_k \langle h_k(\theta) - d_k | h_k(\theta) - d_k \rangle \right]$$

Noise-weighting

Likelihood

$$p(d|\theta) \propto \exp \left[-\frac{1}{2} \sum_k \langle h_k(\theta) - d_k | h_k(\theta) - d_k \rangle \right]$$

Noise-weighting

$$h_k(\theta) \rightarrow h_k(\theta) [1 + \delta A_k] \exp [i\delta\phi_k]$$

Likelihood

$$p(d|\theta) \propto \exp \left[-\frac{1}{2} \sum_k \langle h_k(\theta) - d_k | h_k(\theta) - d_k \rangle \right]$$

Noise-weighting

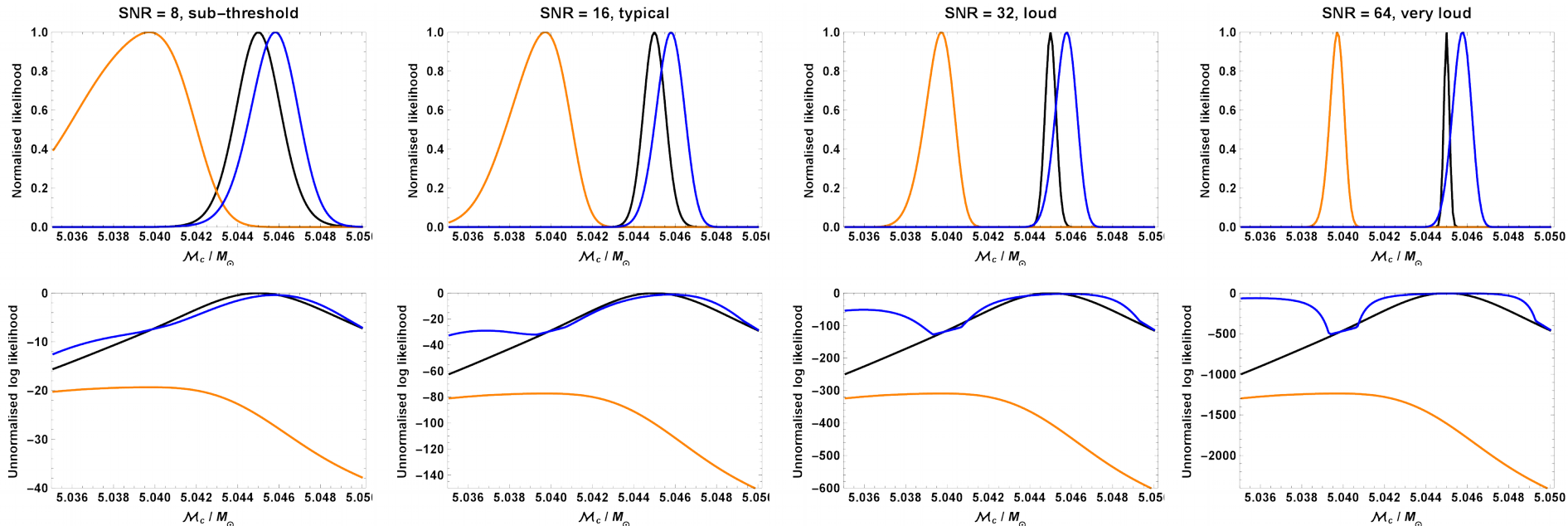
$$h_k(\theta) \rightarrow h_k(\theta) [1 + \delta A_k] \exp [i\delta\phi_k]$$

Calibration

Waveform

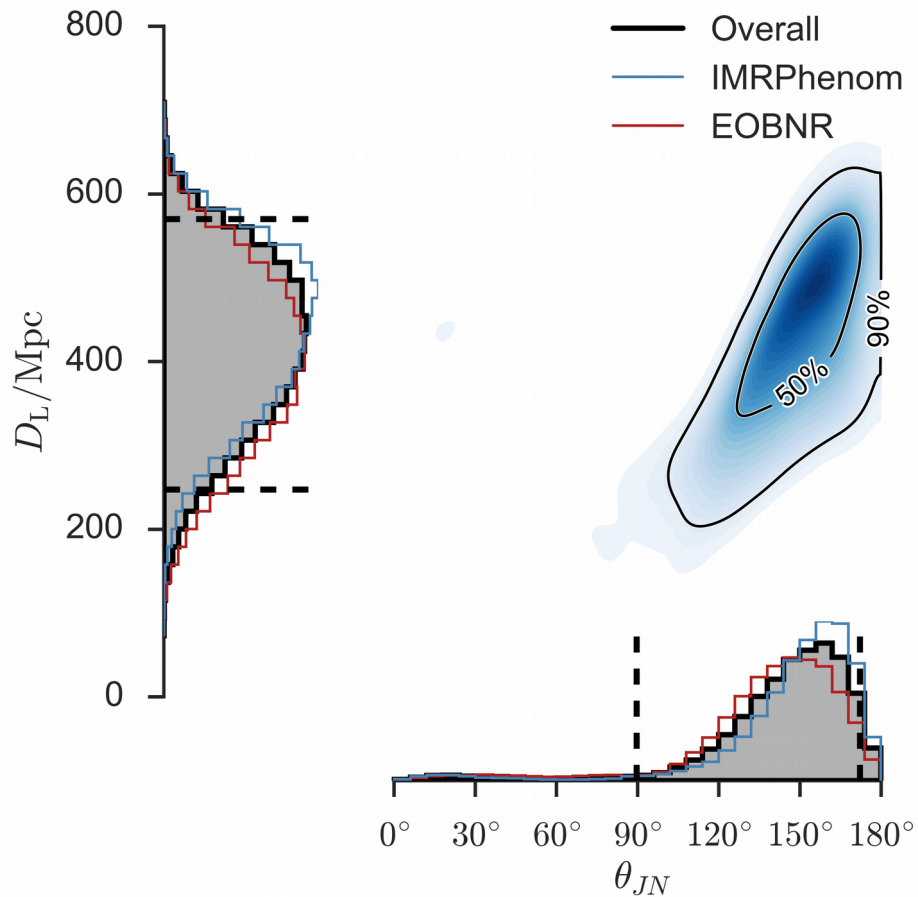
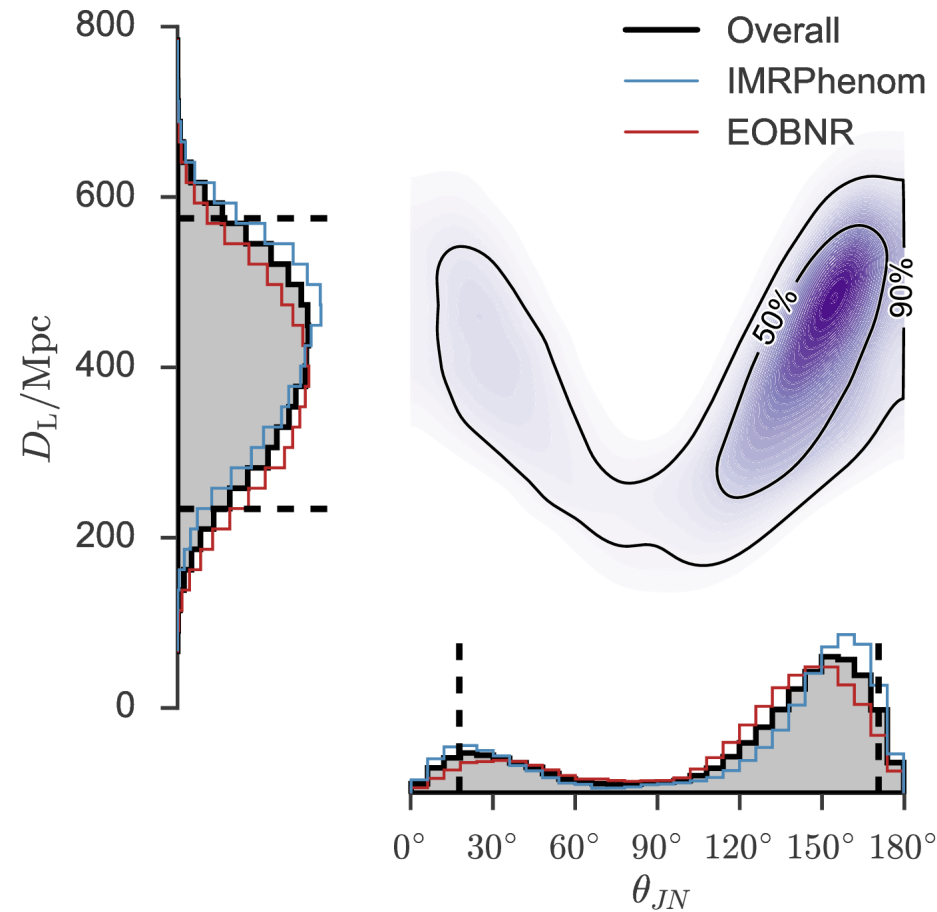
Waveform error

Waveforms introduce theoretical error (arXiv:0707.2982).
Mitigated using Gaussian processes (arXiv:1509.04066).

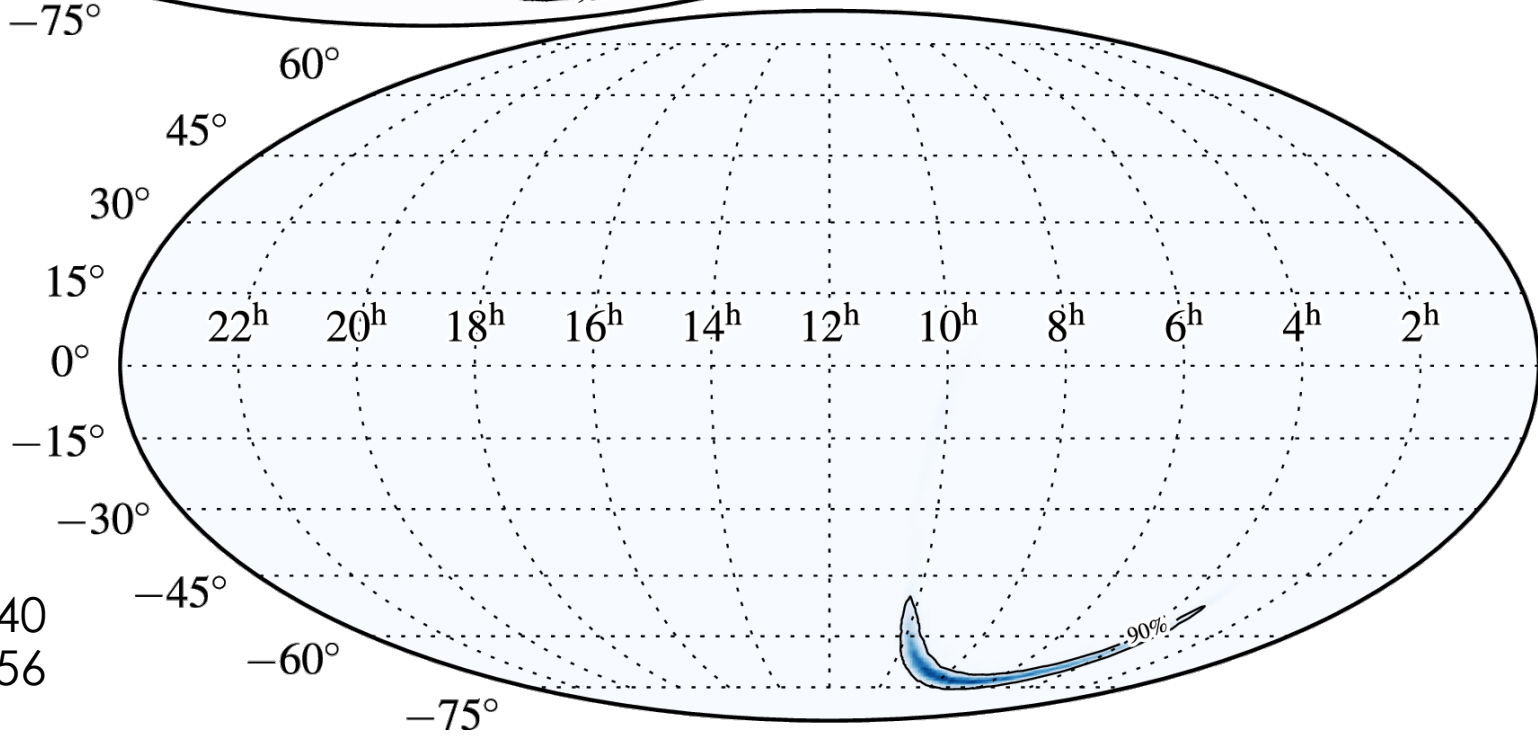
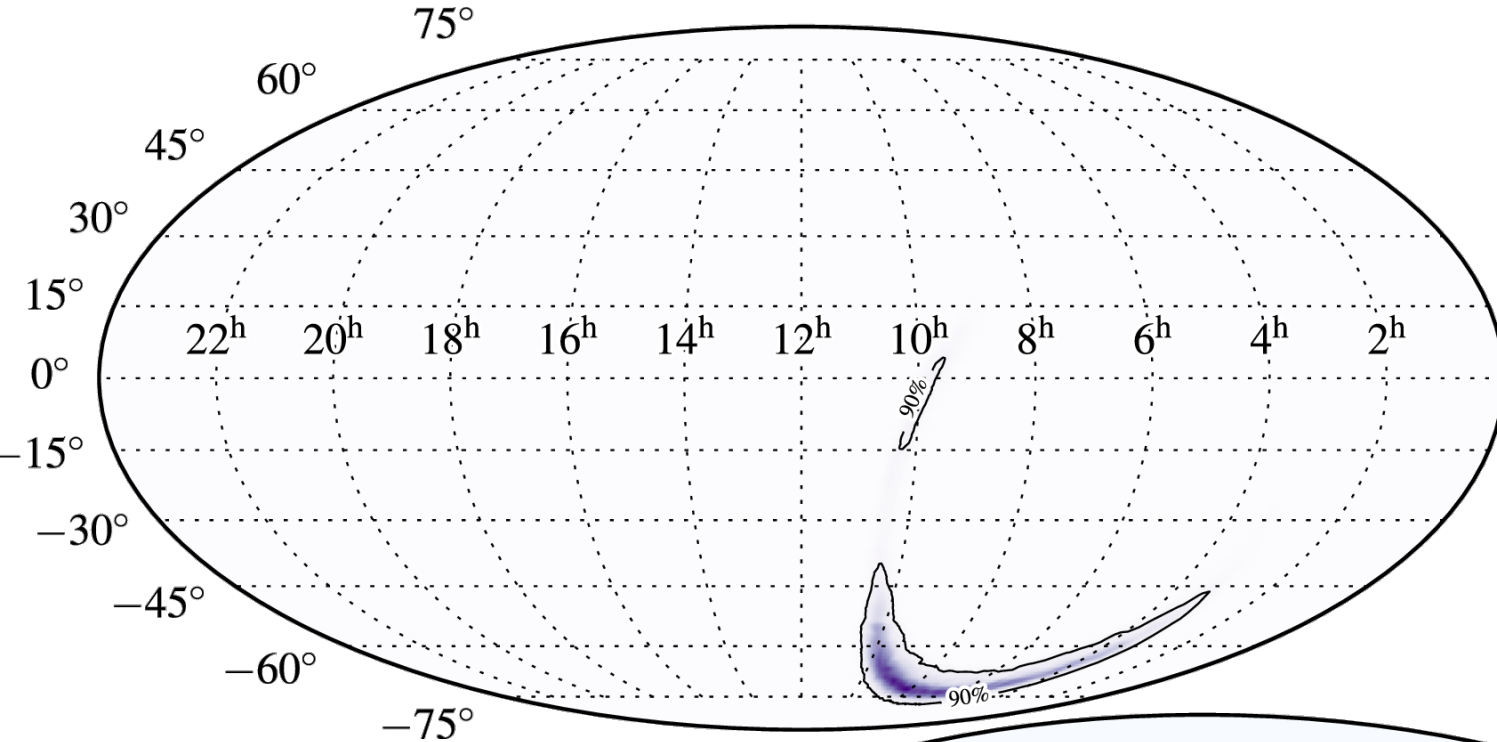


Moore *et al.* arXiv:1509.04066

Inclination

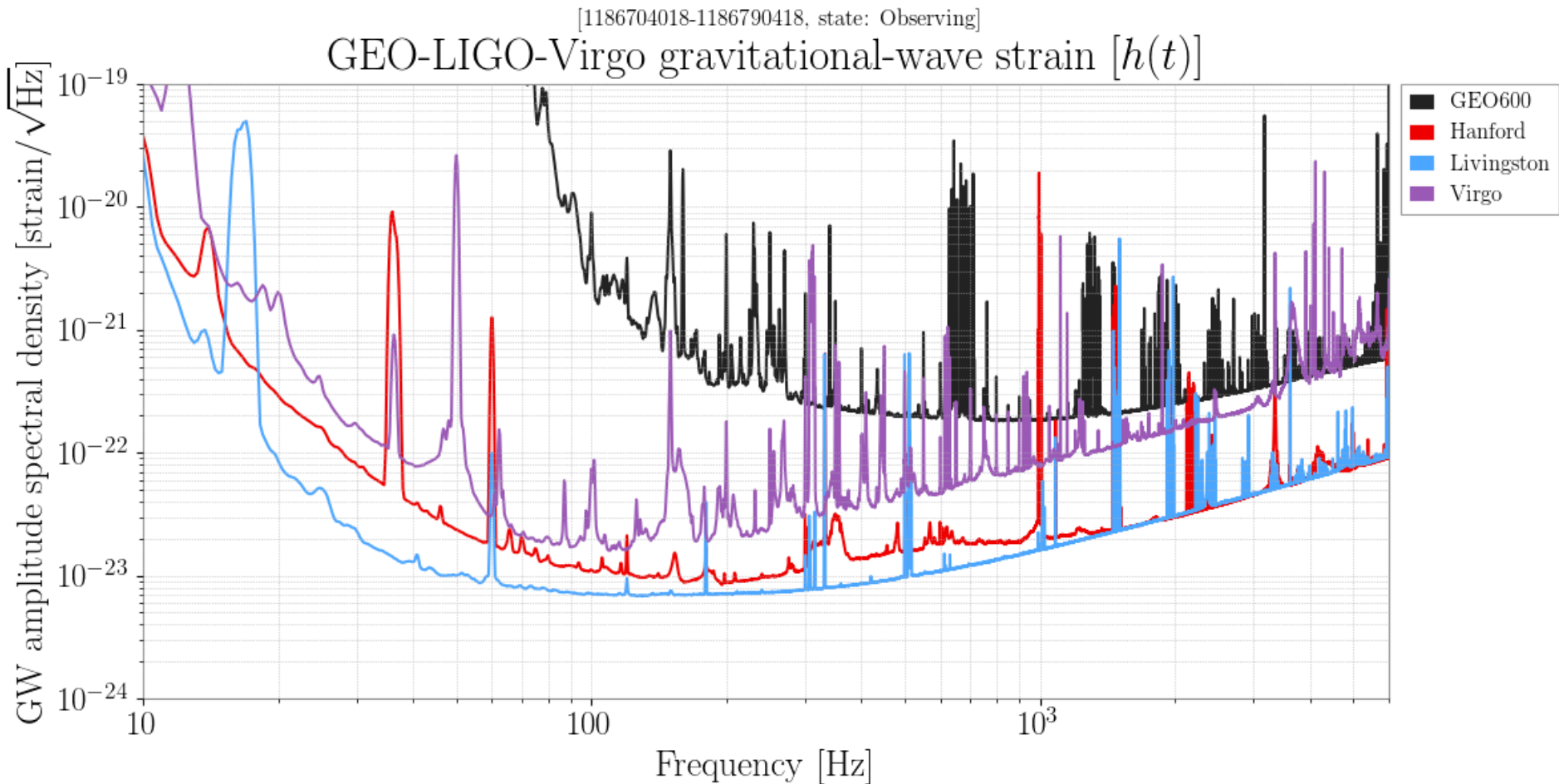


LVC
arXiv:1602.03840
arXiv:1606.04856



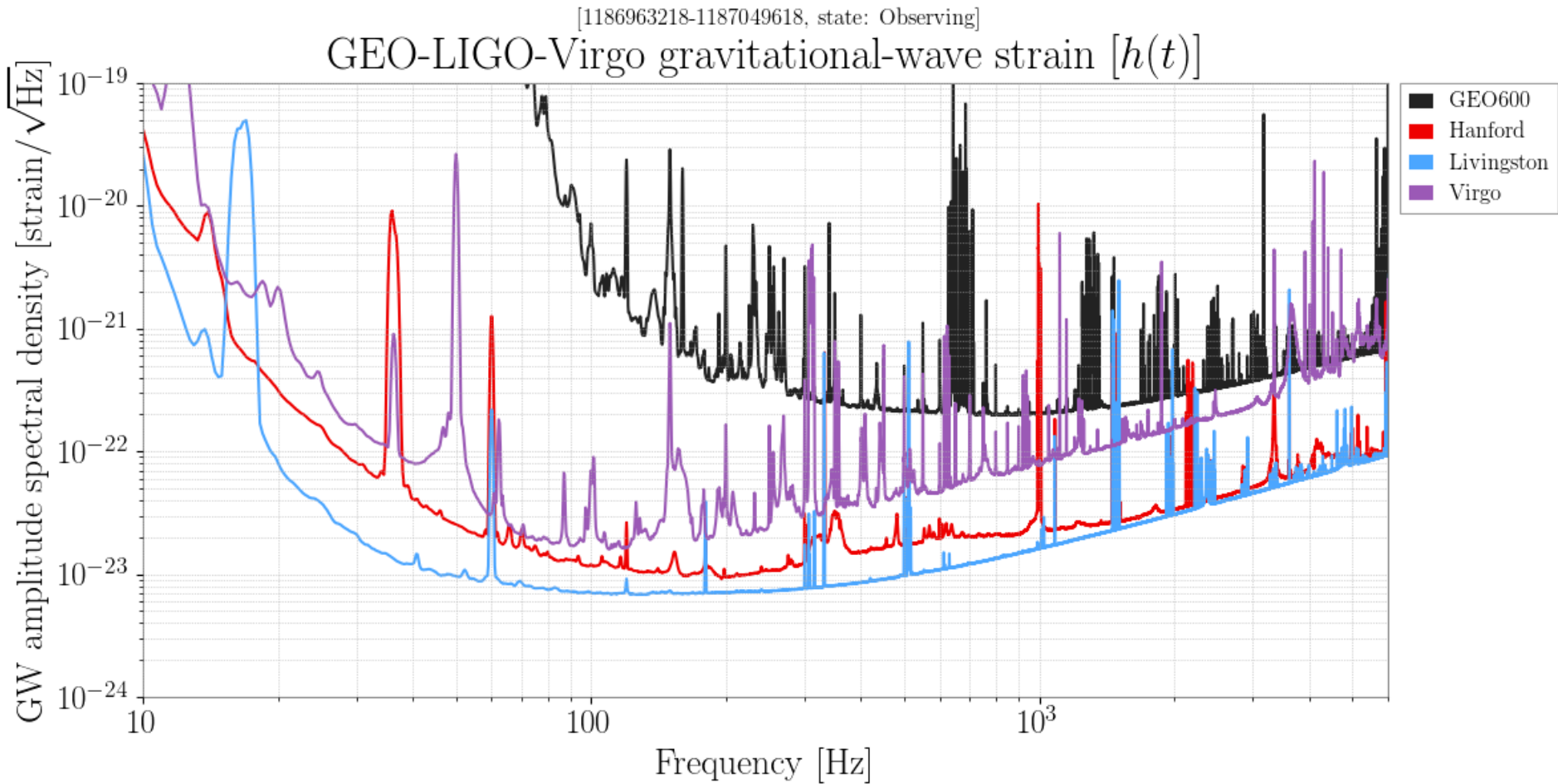
LVC
arXiv:1602.03840
arXiv:1606.04856

Stationarity



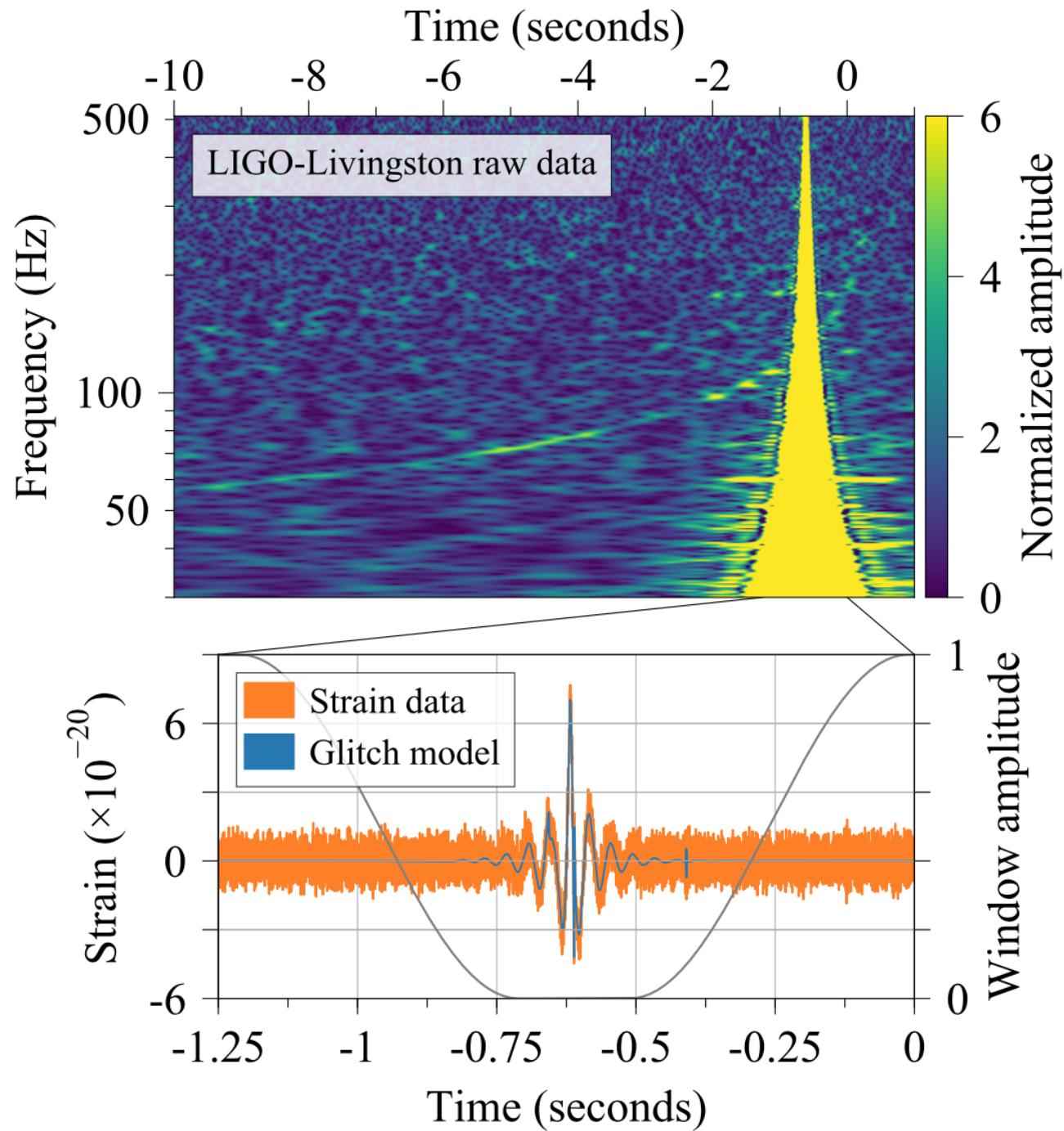
losc.ligo.org/detector_status/day/20170814/

Stationarity



losc.ligo.org/detector_status/day/20170817/

Glitch



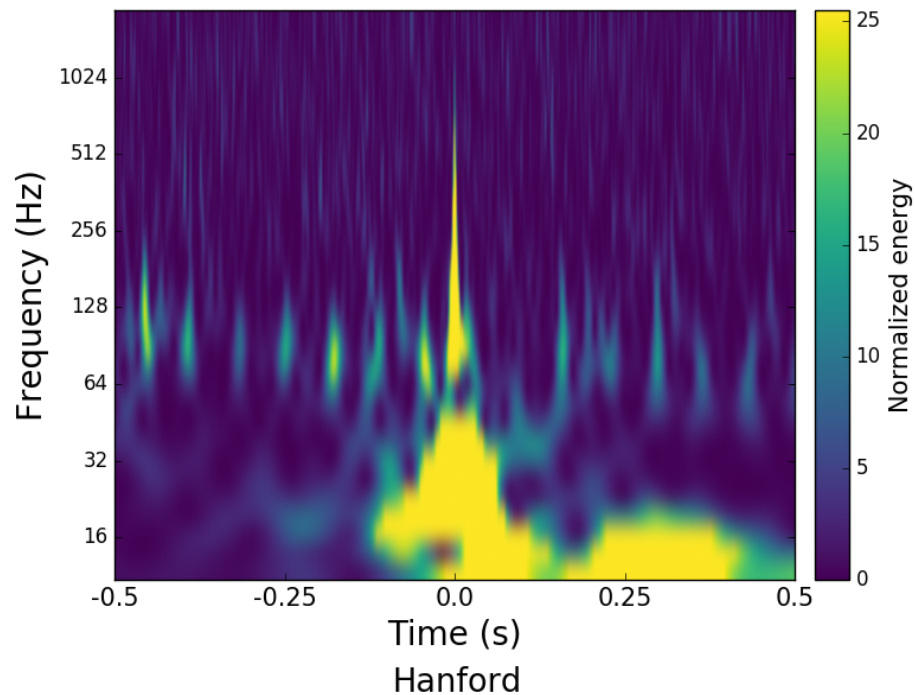
Glitch zoo

gravityspy.org

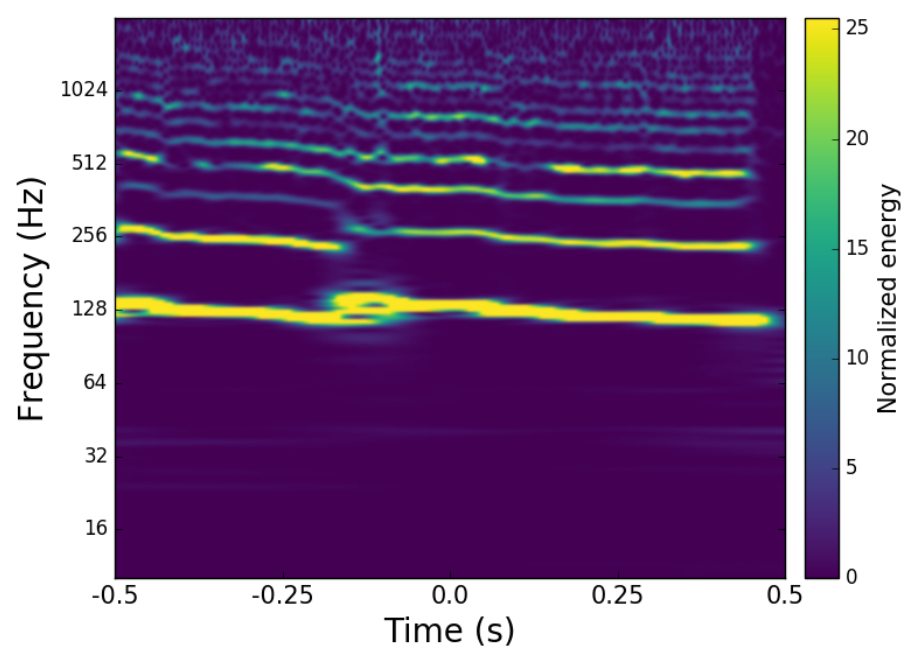
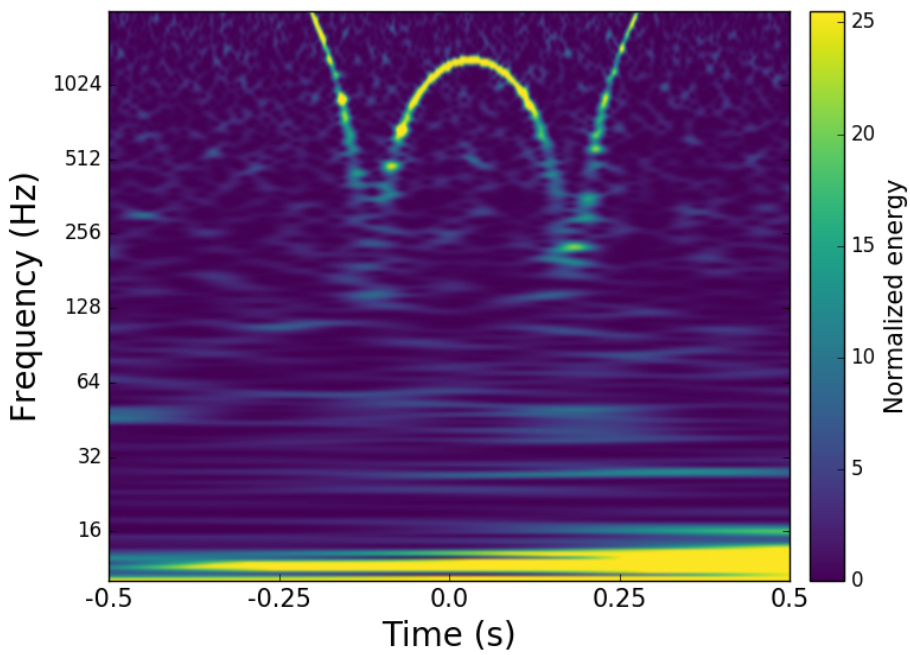
Zevin *et al.* arXiv:1611.04596

LVC arXiv:1602.03844

Livingston - O1



Livingston



Bayes' theorem

$$p(\theta|d) = \frac{p(d|\theta)p(\theta)}{p(d)}$$

Posterior

Likelihood

Prior

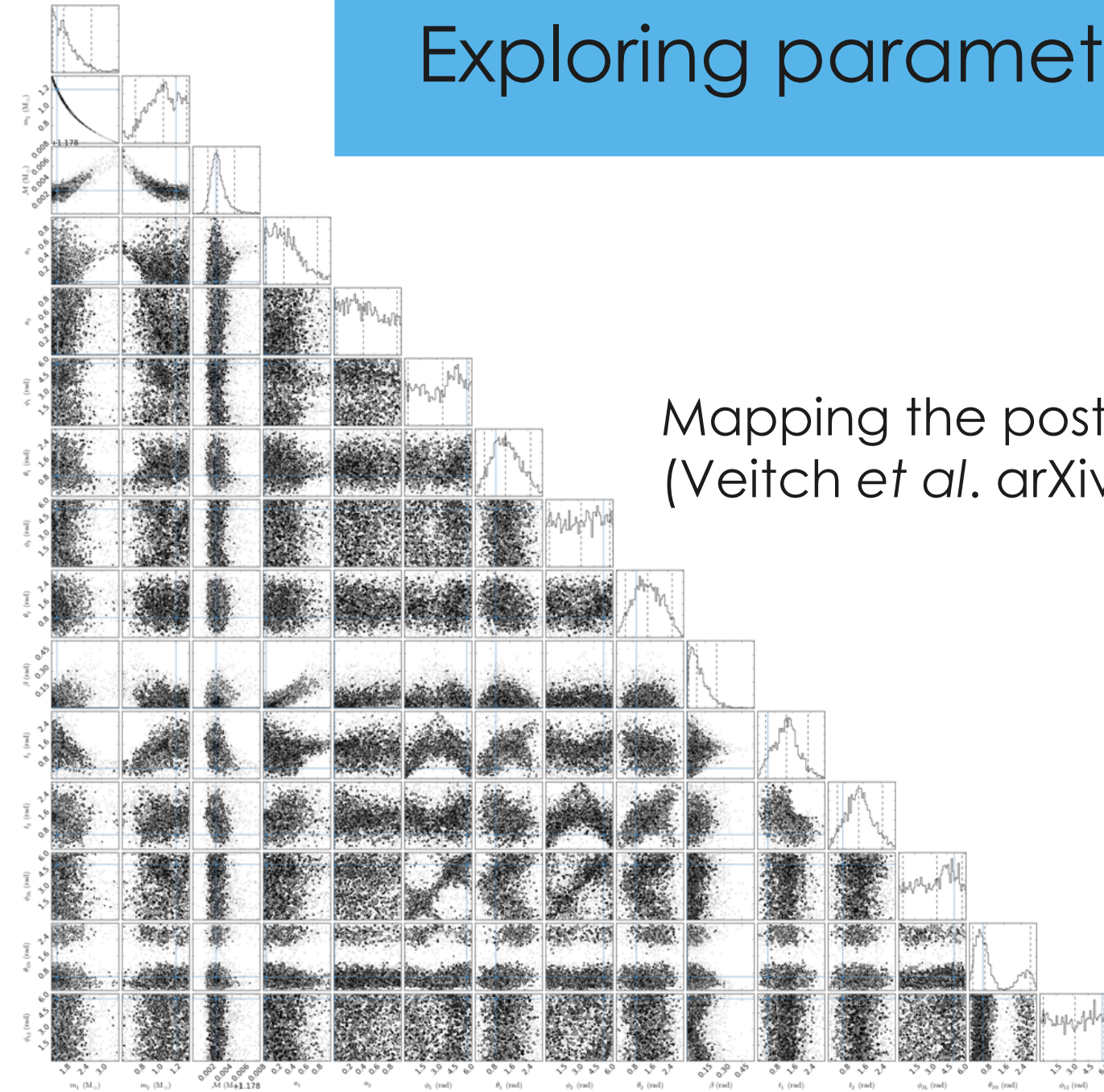
Evidence

The diagram illustrates Bayes' theorem with the following components:

- Posterior:** $p(\theta|d)$ (blue box)
- Likelihood:** $p(d|\theta)$ (pink box)
- Prior:** $p(\theta)$ (orange box)
- Evidence:** $p(d)$ (green box)

Exploring parameter space

Mapping the posterior is difficult
(Veitch *et al.* arXiv:1409.7215)



Bayes' theorem

The diagram illustrates Bayes' theorem with the following components:

- Posterior:** $p(\theta|d)$ (blue box)
- Likelihood:** $p(d|\theta)$ (pink box)
- Prior:** $p(\theta)$ (orange box)
- Evidence:** $p(d)$ (green box)

$$p(\theta|d) = \frac{p(d|\theta)p(\theta)}{p(d)}$$

Bayes' theorem

$$p(\theta|d, \lambda) = \frac{p(d|\theta, \lambda) p(\theta|\lambda)}{p(d|\lambda)}$$

Posterior = Likelihood × Prior / Evidence

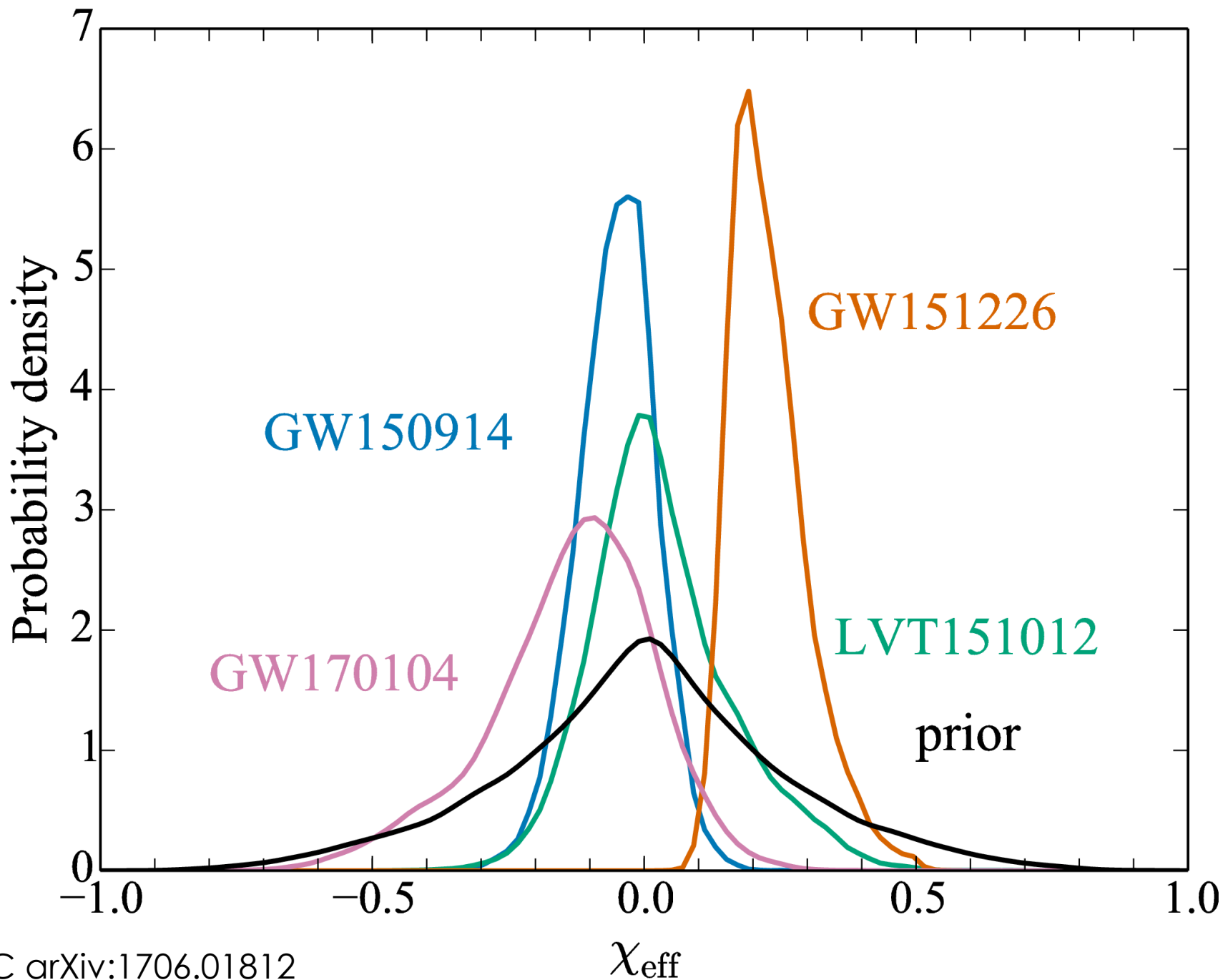
Bayes' theorem

$$p(\lambda|\{d\}) = \frac{p(\{d\}|\lambda) p(\lambda)}{p(\{d\})}$$

Evidence

Model prior

Model posterior



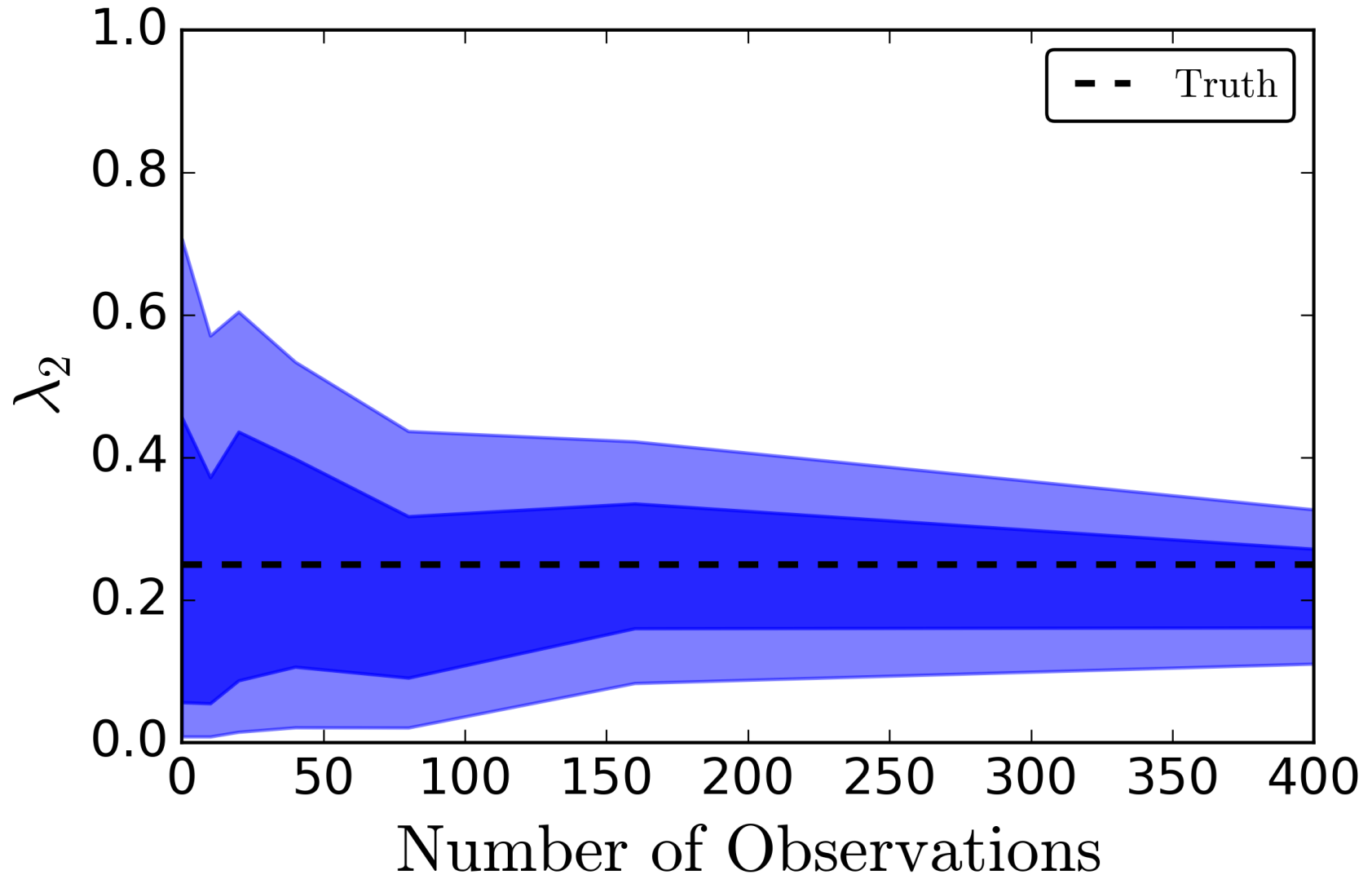
Effective inspiral spin

$$\chi_{\text{eff}} = \frac{c}{GM} \left(\frac{\mathbf{S}_1}{m_1} + \frac{\mathbf{S}_2}{m_2} \right) \cdot \hat{\mathbf{L}}$$

Most important combination of spins for evolution of inspiral (Ajith *et al.* arXiv:0909.2867, Santamaría *et al.* arXiv:1005.3306)

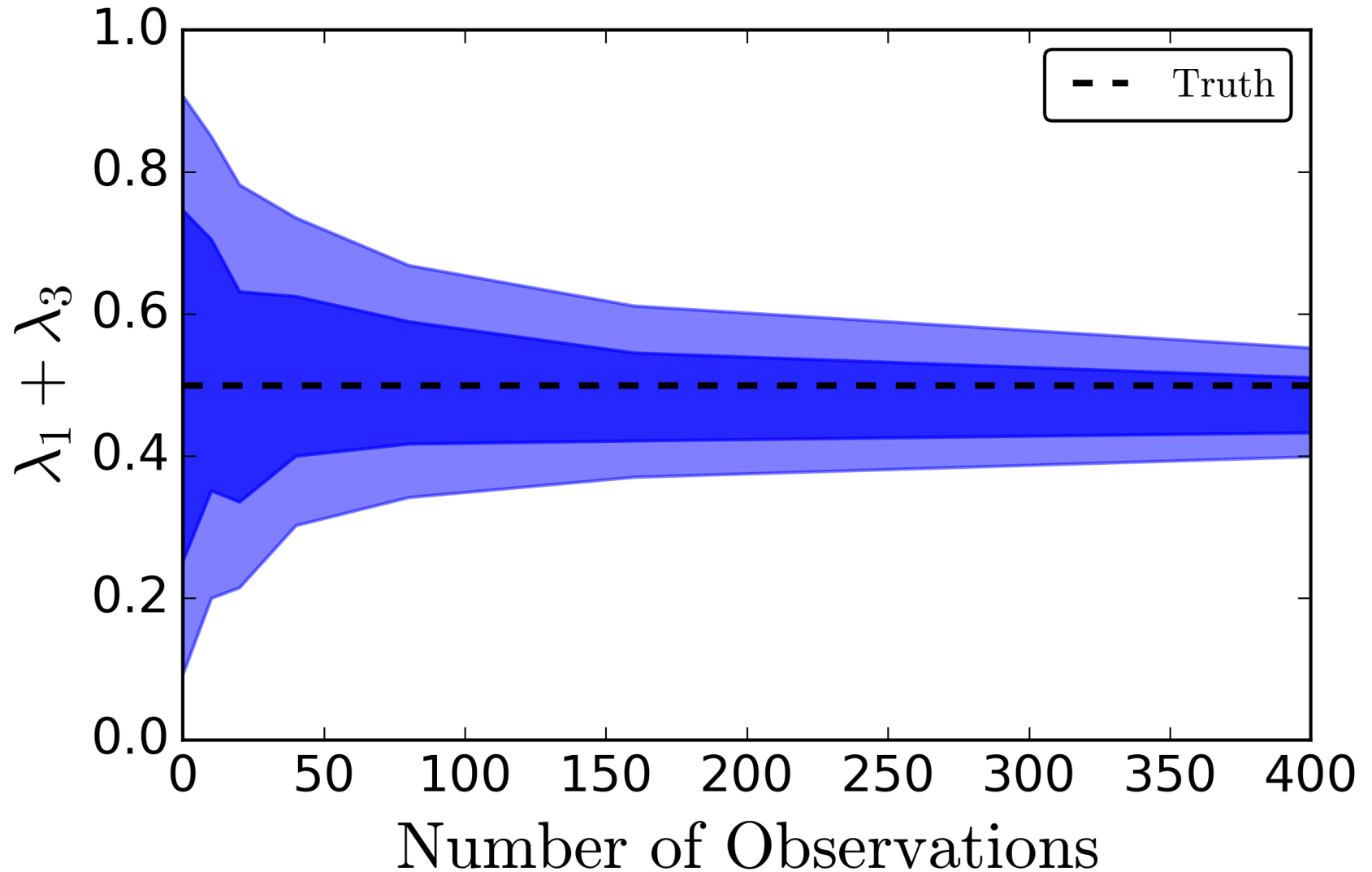
Model inference

Stevenson, CPLB & Mandel
arXiv:1703.06873



Model inference

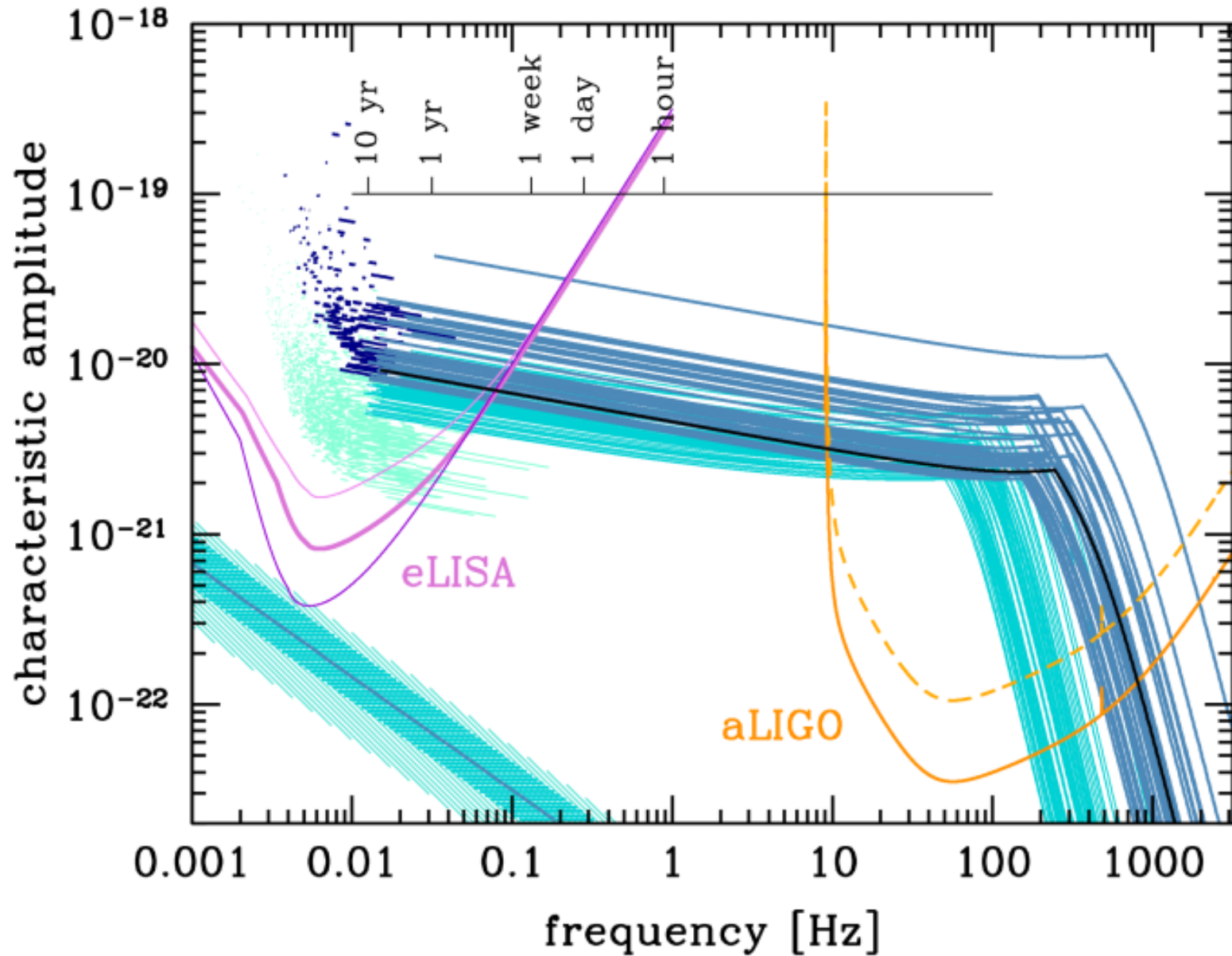
Stevenson, CPLB & Mandel
arXiv:1703.06873



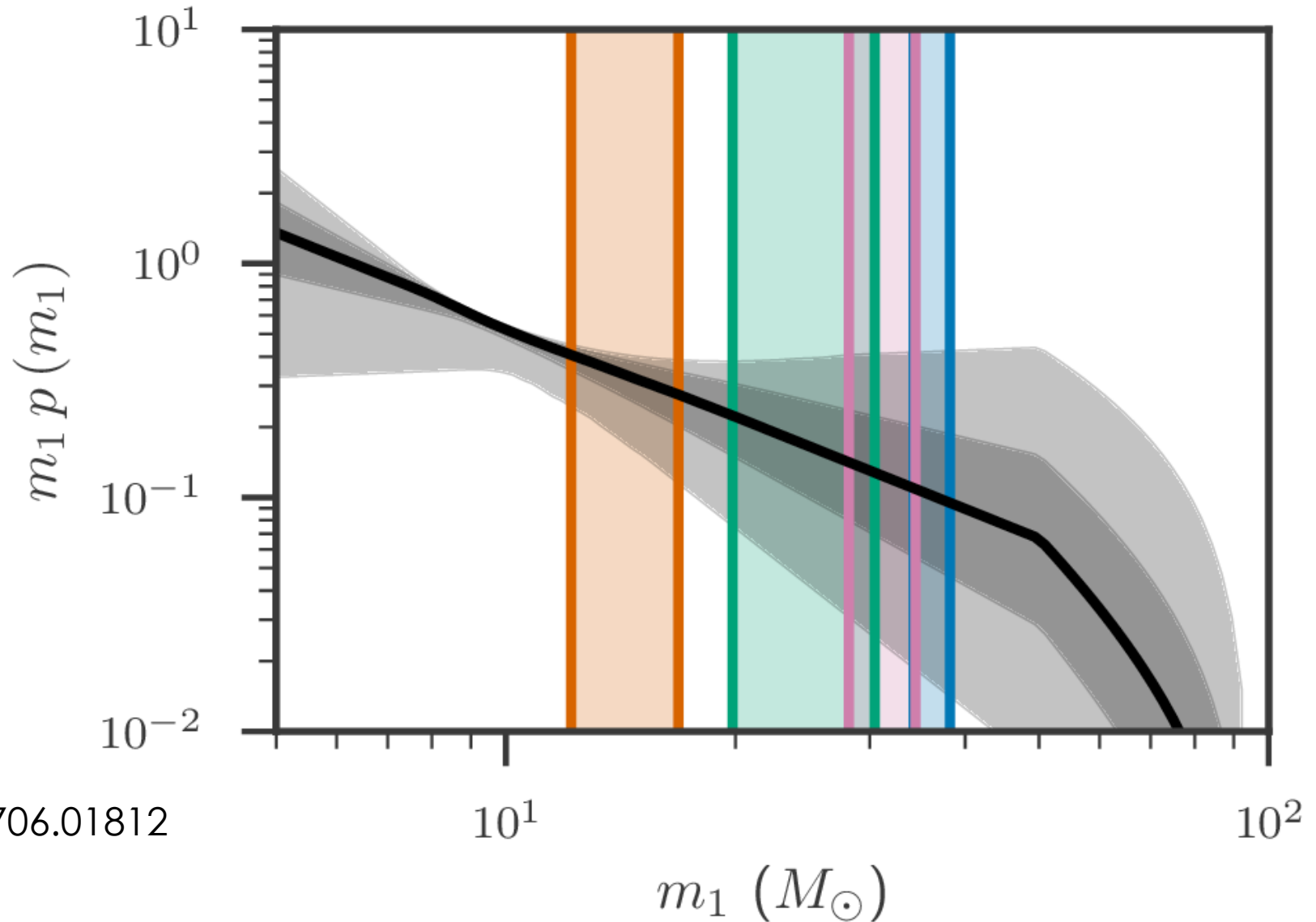
Chirp mass

$$\mathcal{M}_c = \frac{(m_1 m_2)^{3/5}}{(m_1 + m_2)^{1/5}}$$

Chirp mass gives leading-order amplitude and phase evolution (Blanchet *et al.* arXiv:gr-qc/9501027 Poisson & Will arXiv:gr-qc/9502040)



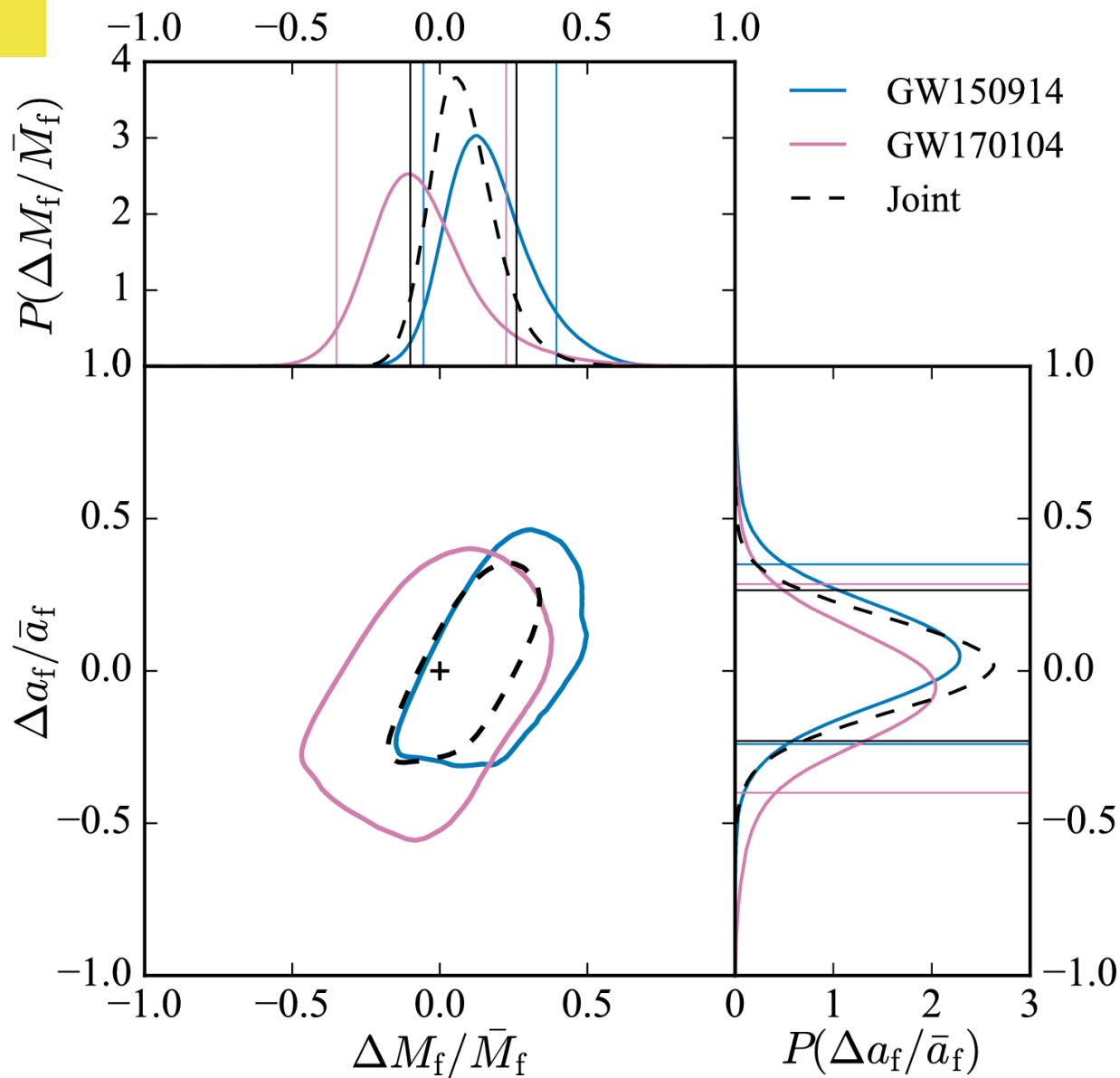
Mass distribution



LVC
arXiv:1706.01812

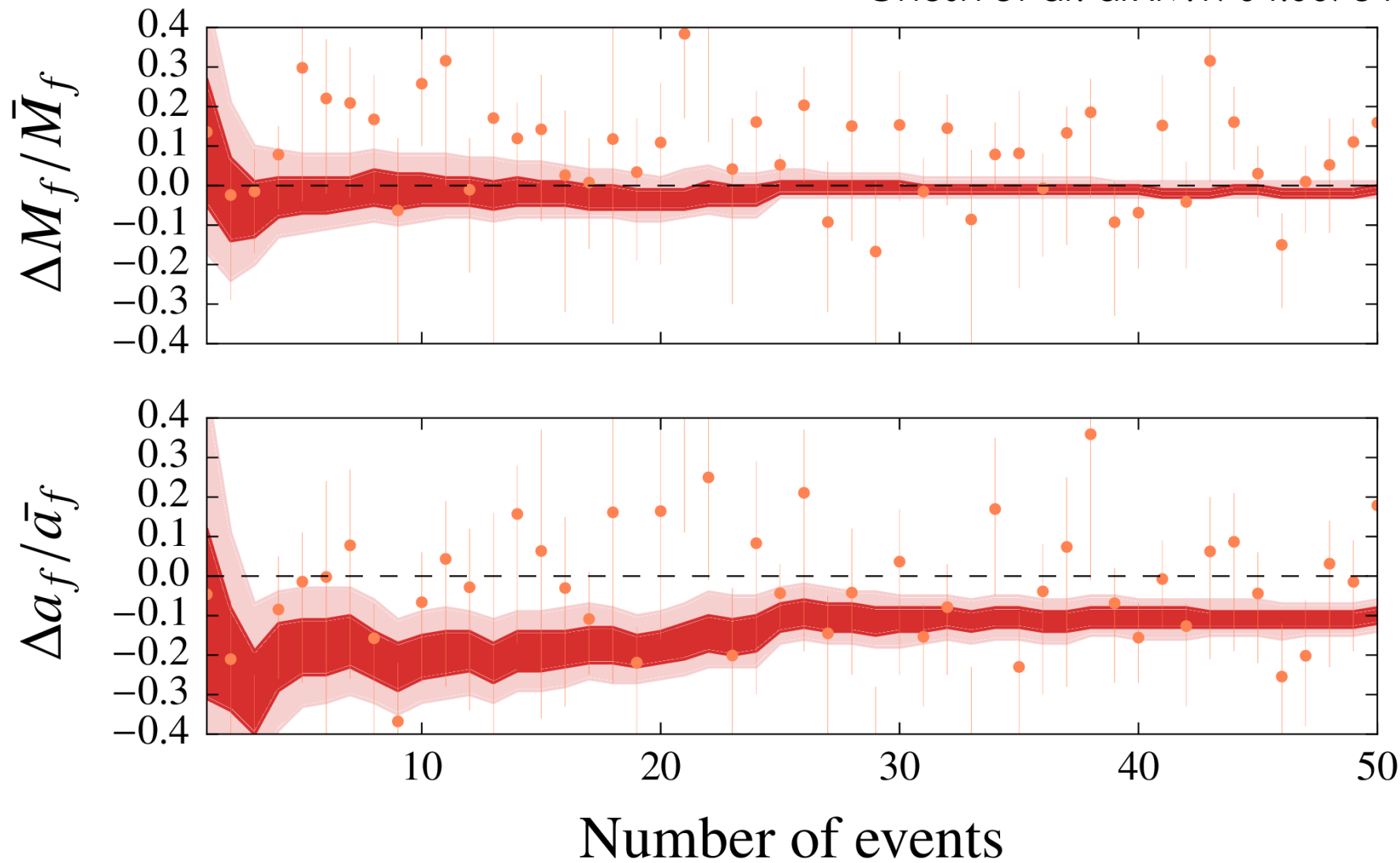
Testing GR

LVC arXiv:1602.03841
arXiv:1706.01812



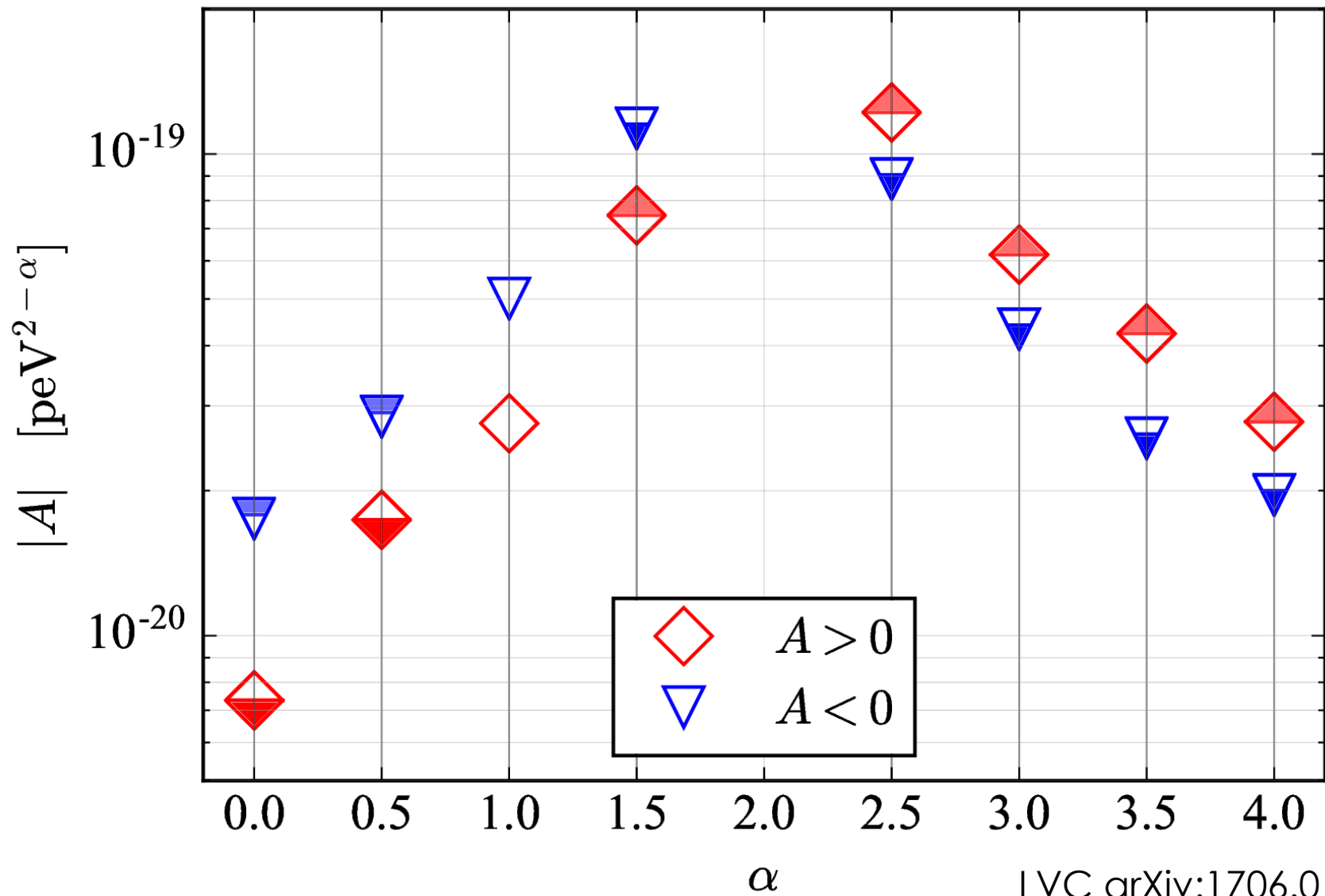
Testing GR

Ghosh *et al.* arXiv:1704.06784



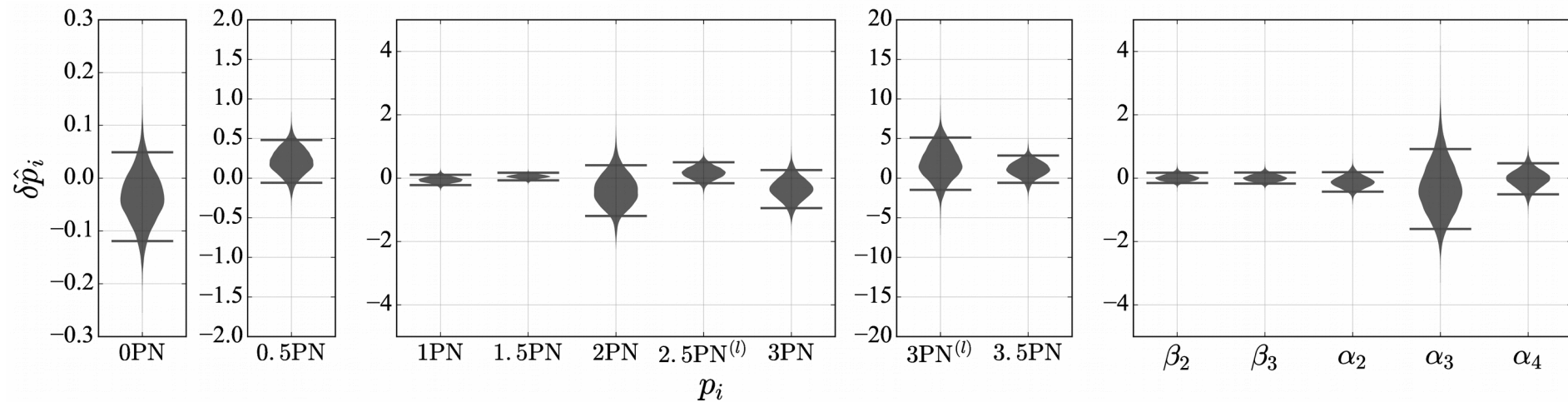
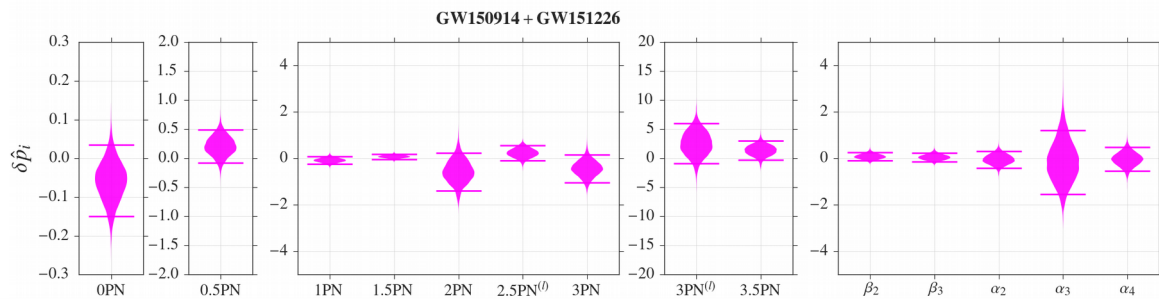
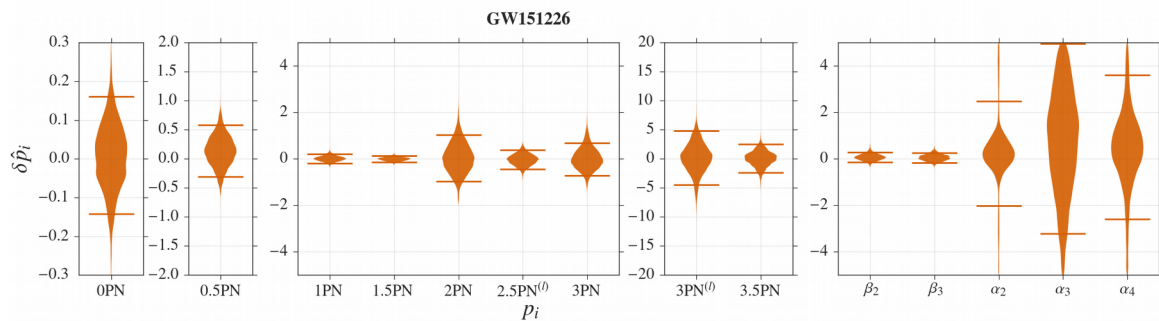
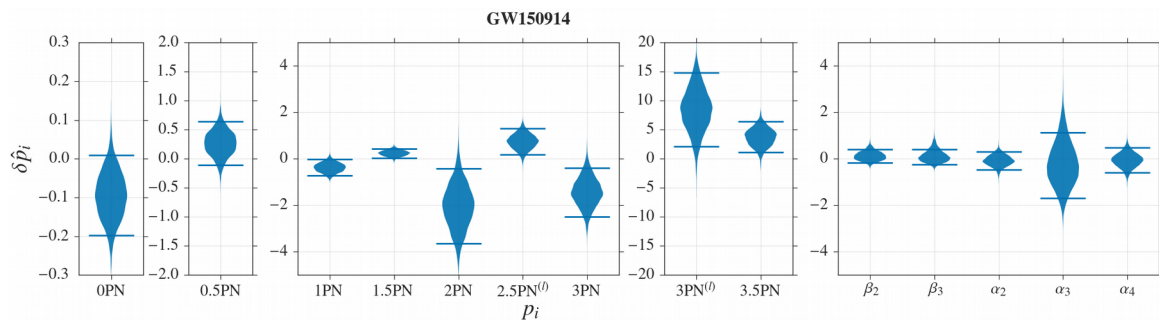
Dispersion

$$E^2 = p^2 c^2 + A p^\alpha c^\alpha$$

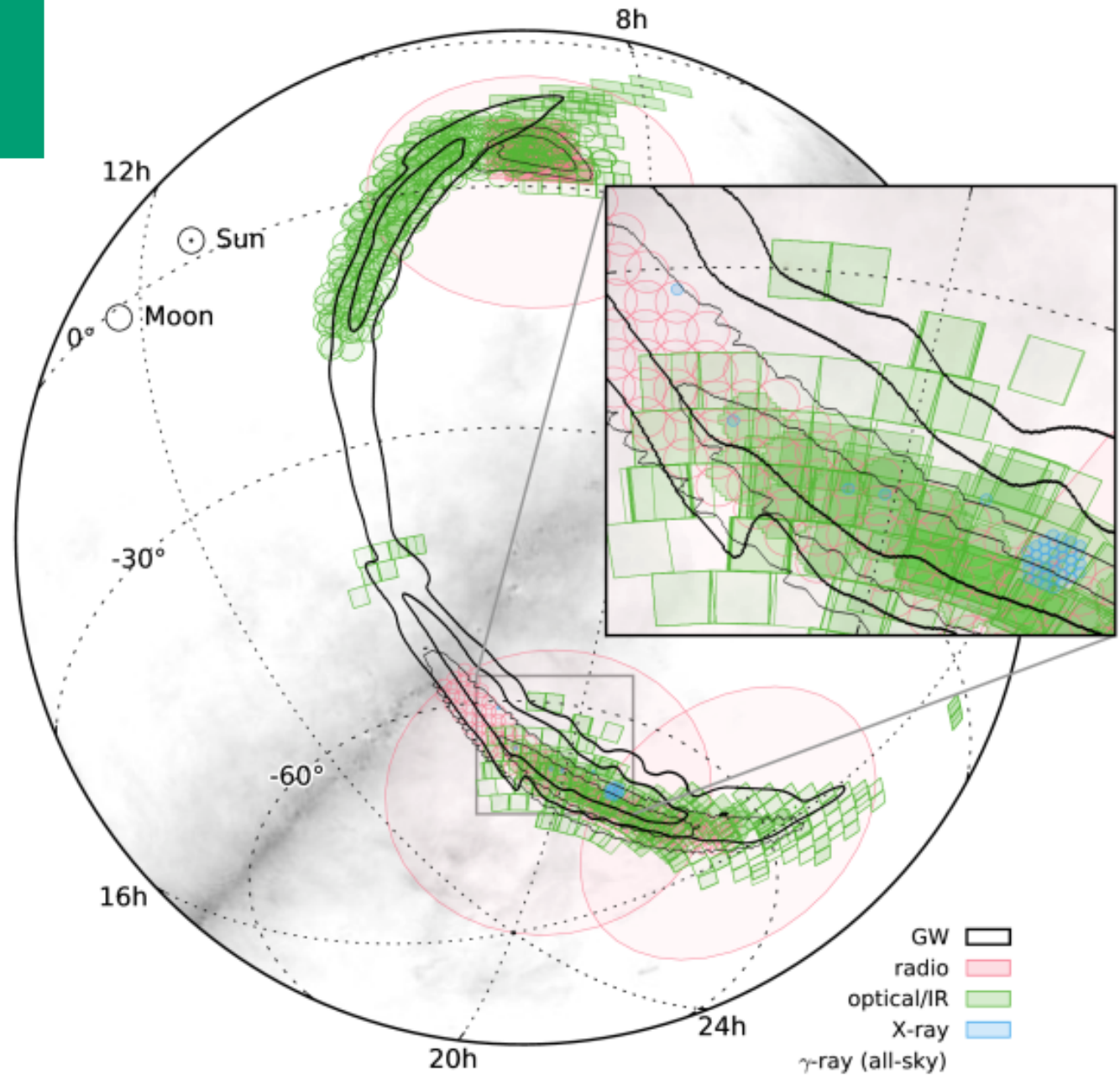


Testing GR

LVC arXiv:1606.04856
arXiv:1706.01812

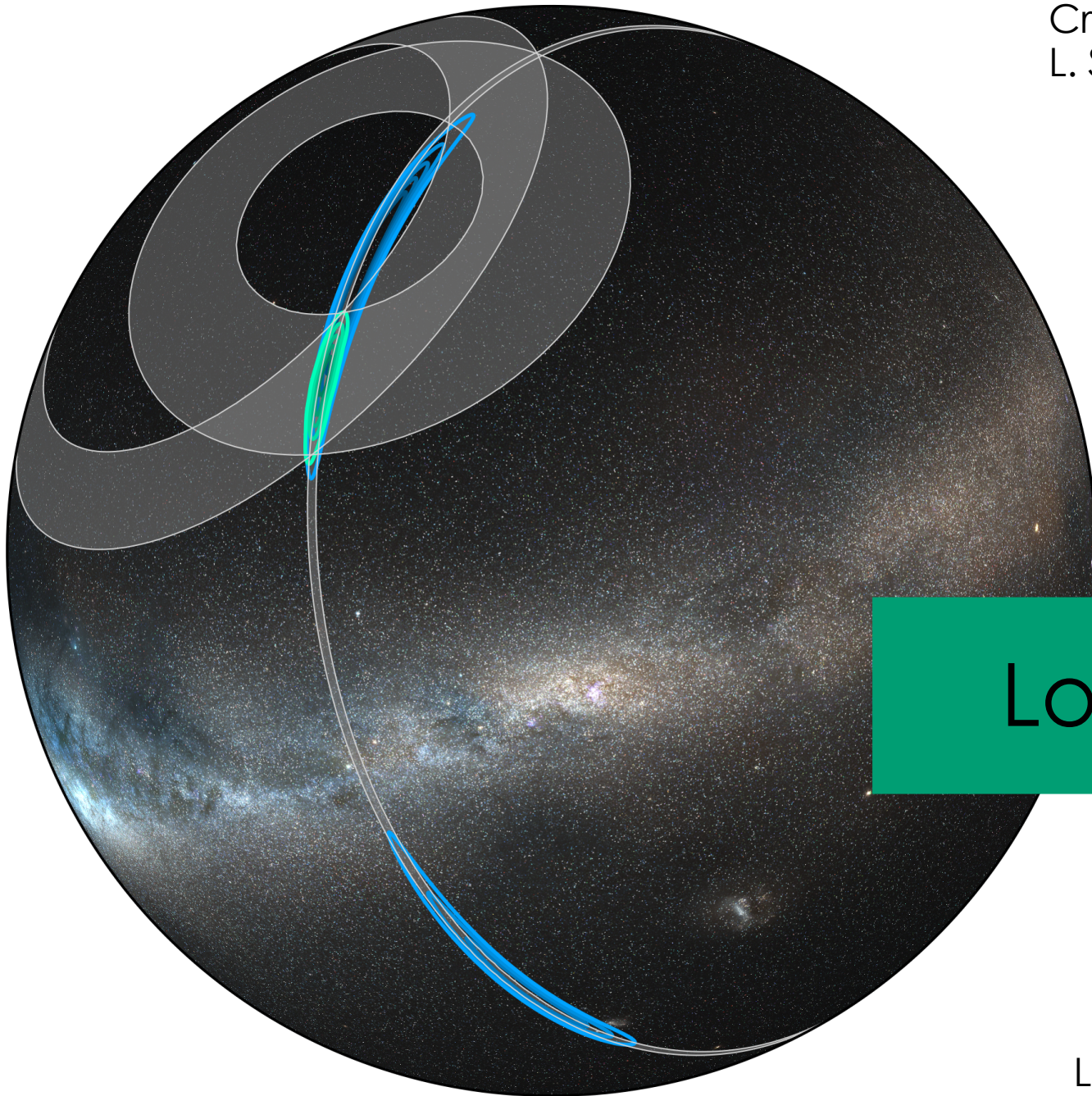


Follow-up



LVC
arXiv:1602.08492
arXiv:1604.07864


Credit: LVC/NASA/
L. Singer/A. Mellinger




Location




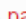
LVC arXiv:1710.05832

The First Two Years of Electromagnetic Follow-Up with Advanced LIGO and Virgo

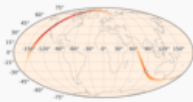
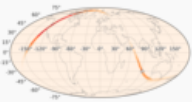
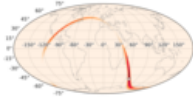
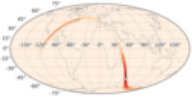


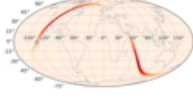
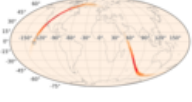
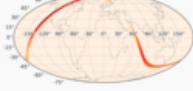
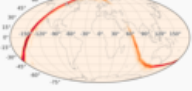
 [Singer et al. 2014](#)
arXiv:1404.5623

 [Berry et al. 2015](#)
arXiv:1411.6934

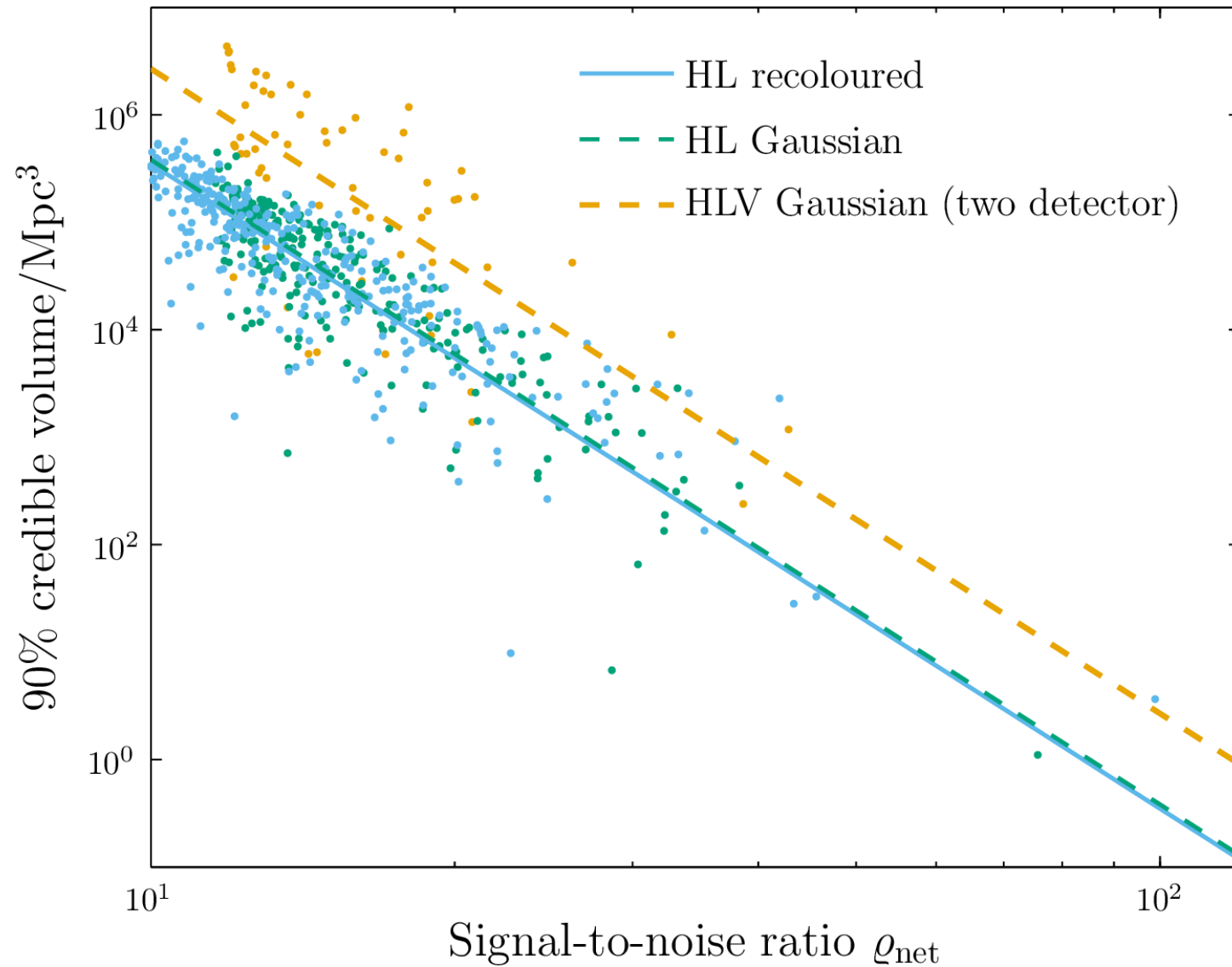
www.ligo.org/scientists/first2years/
asd.gsfc.nasa.gov/Leo.Singer/going-the-distance/

Catalog of simulated events and sky maps for two-detector, HL, 2015 configuration. This is the same configuration as the 2015 tab, except that the simulated detector noise is data from initial LIGO's  sixth science run, recoloured (filtered) to have the same PSD as the early Advanced LIGO configuration. See also ASCII tables of  simulated signals,  detections, and  parameter-estimation accuracies in [Machine Readable Table](#) format.

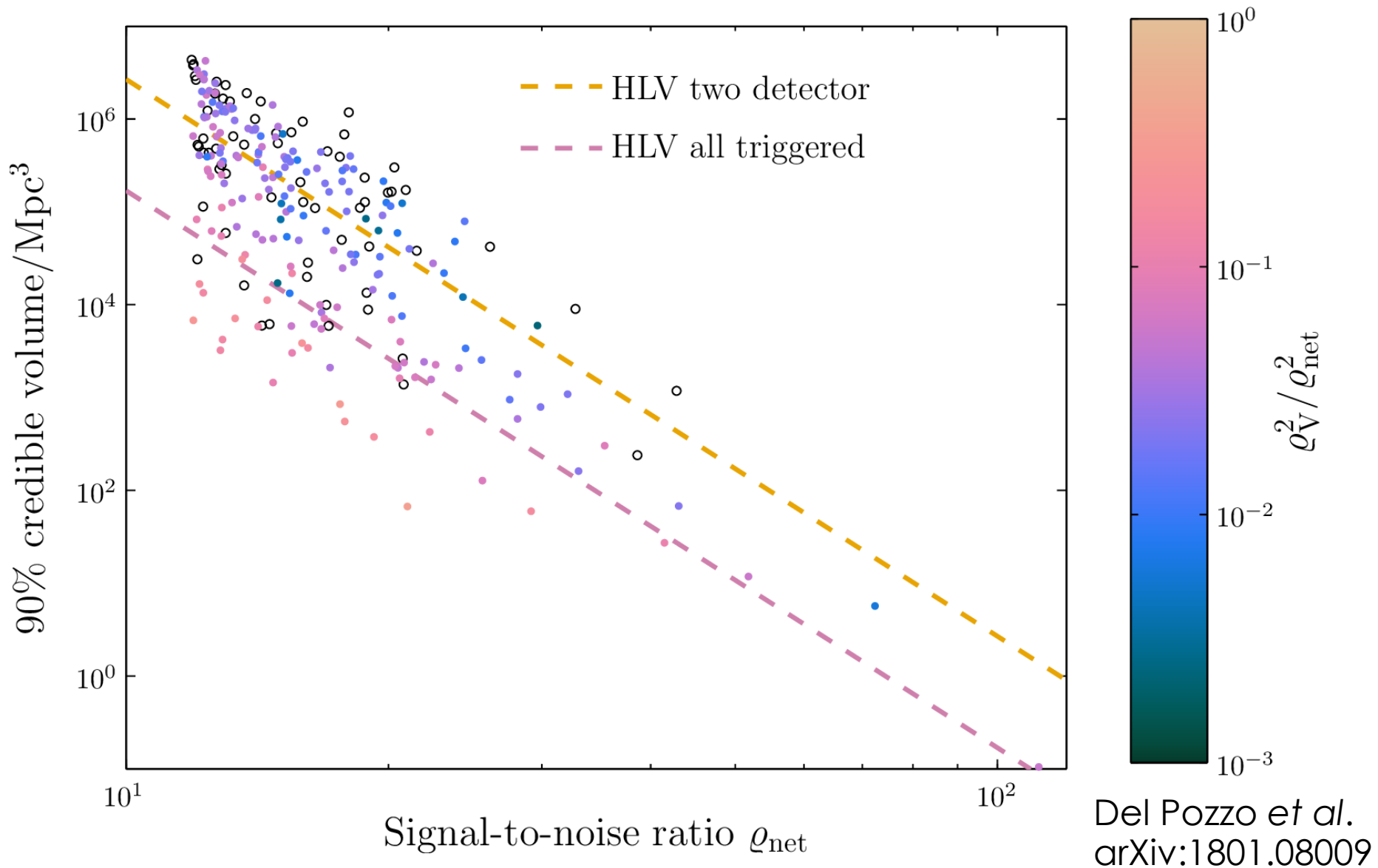
This web page provides additional online information related to the paper "Two Years of Electromagnetic Follow-Up with Advanced LIGO and Virgo" and the paper "Parameter Estimation for Binary Neutron Coalescences with

event ID	sim ID	network	SNR			BAYESTAR			LALINFERENCE_NEST			sky maps	
			net	H	L	50%	90%	searched	50%	90%	searched	BAYESTAR	LALINFERENCE_NEST
4532	899	HL	13.9	10.1	9.5	180	750	190	170	790	150		
4572	1243	HL	13.2	10.0	8.7	230	830	45	200	920	33		
4618	1768	HL	10.8	8.0	7.3	160	540	220	130	440	280		
4647	1964	HL	12.4	8.6	9.0	260	890	1200	190	780	780		
4711	2704	HL	10.7	8.0	7.1	370	1200	300	450	1600	520		

3-dimensional localization

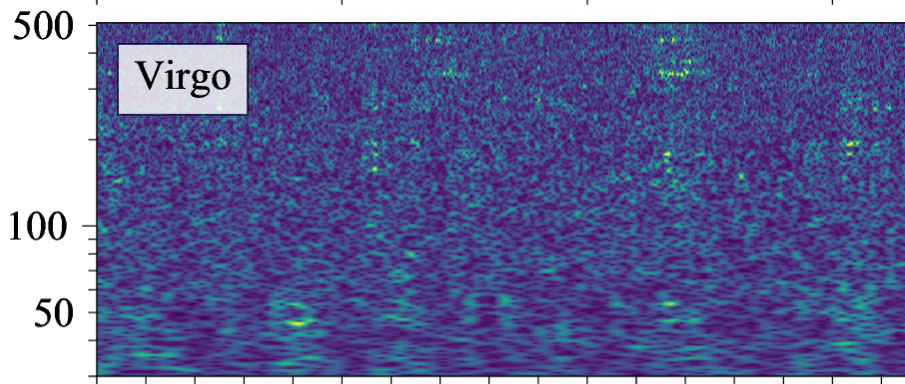
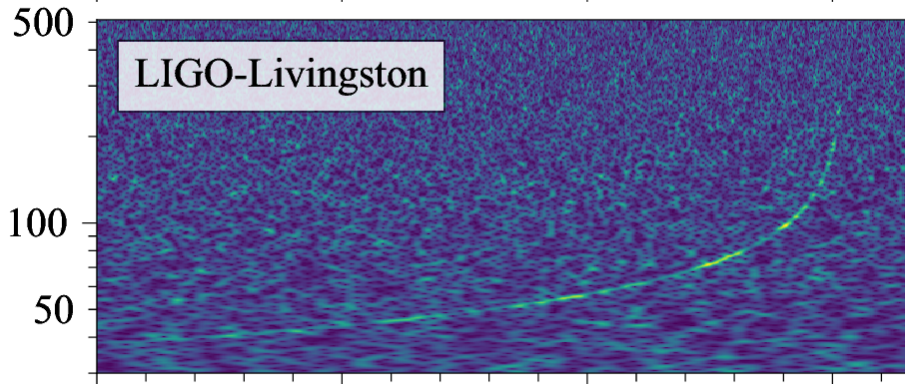
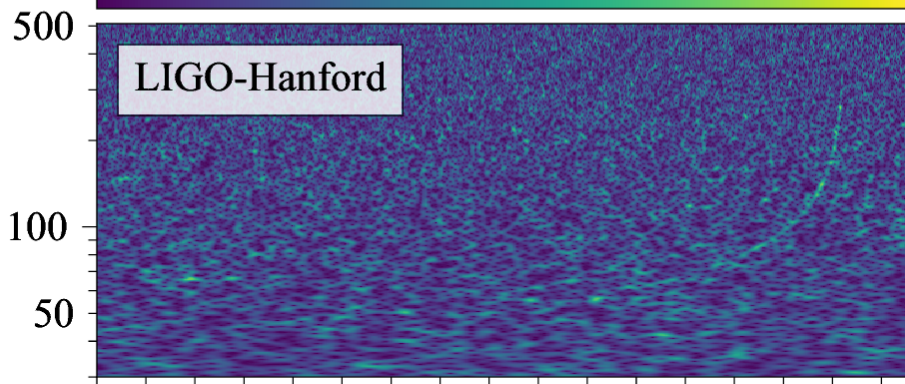


3-dimensional localization



Normalized amplitude

0 2 4 6



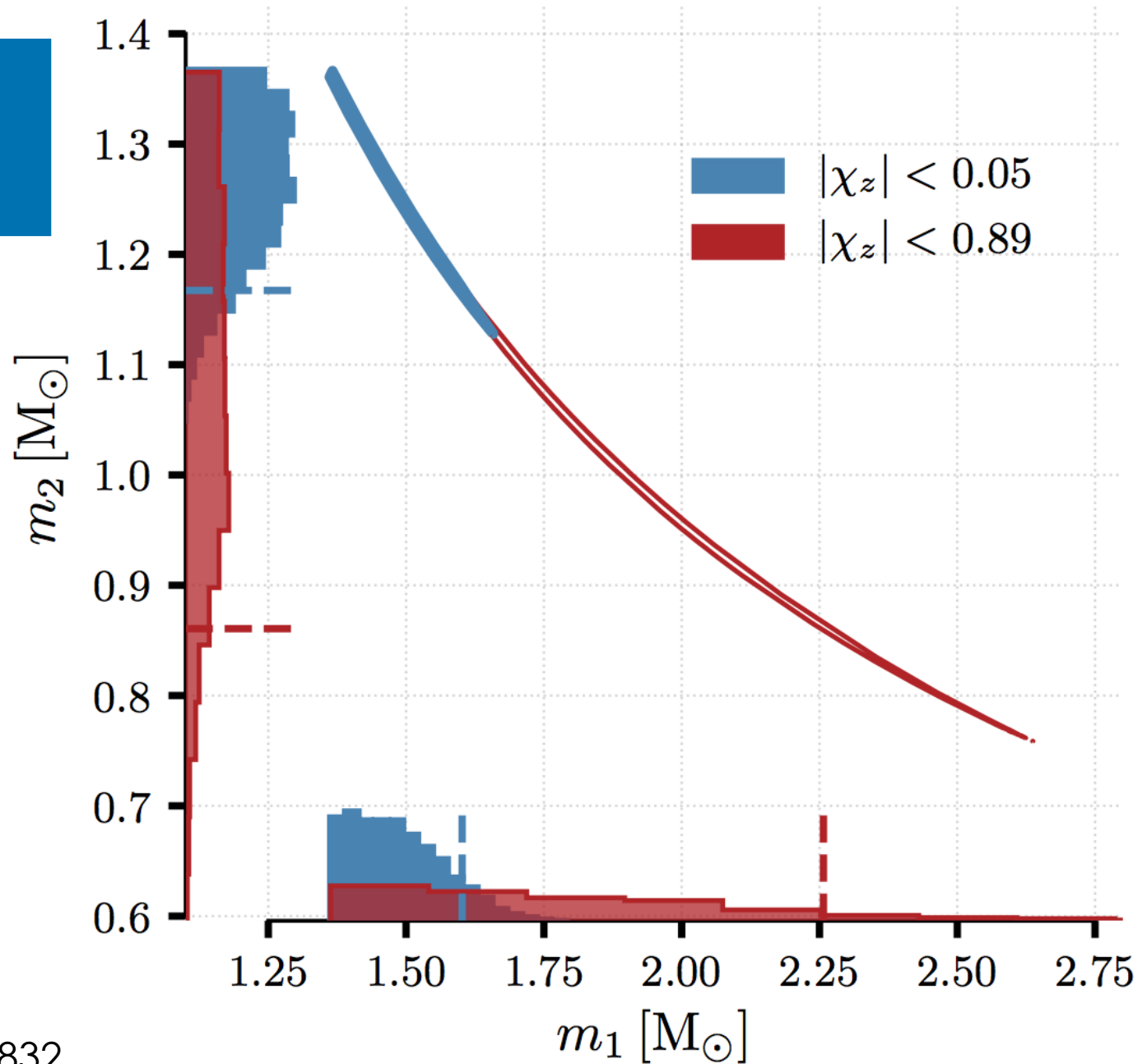
GW170817

13:41:04 BST 17 August 2017

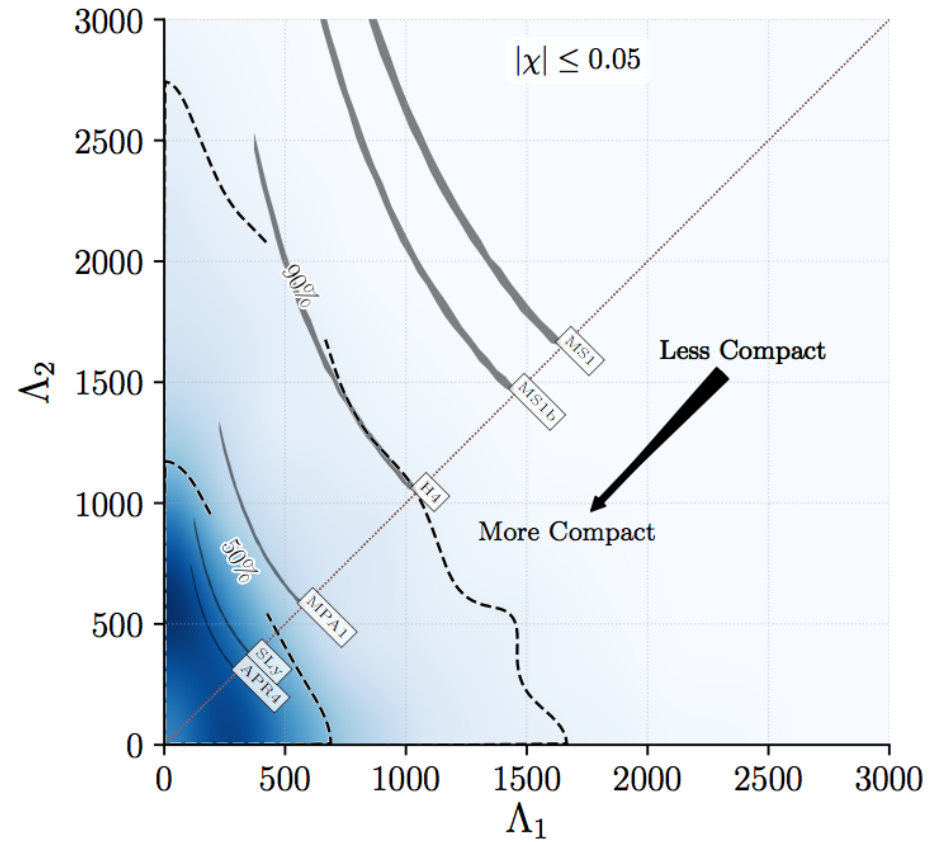
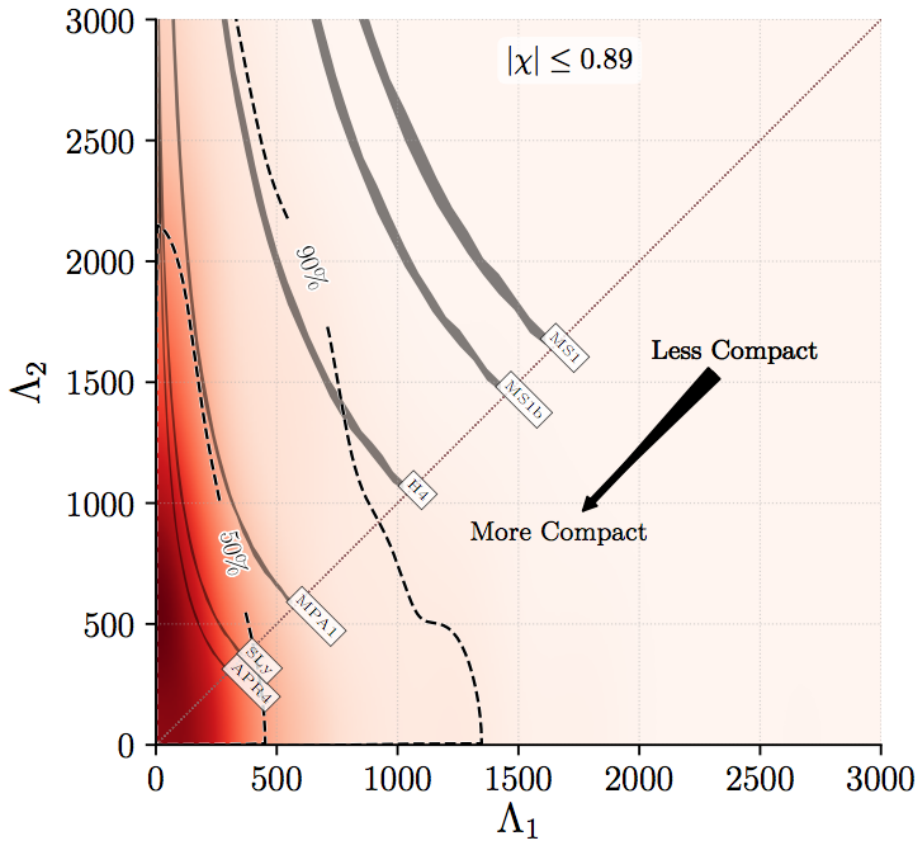
LVC arXiv:1710.05832

Time (seconds)

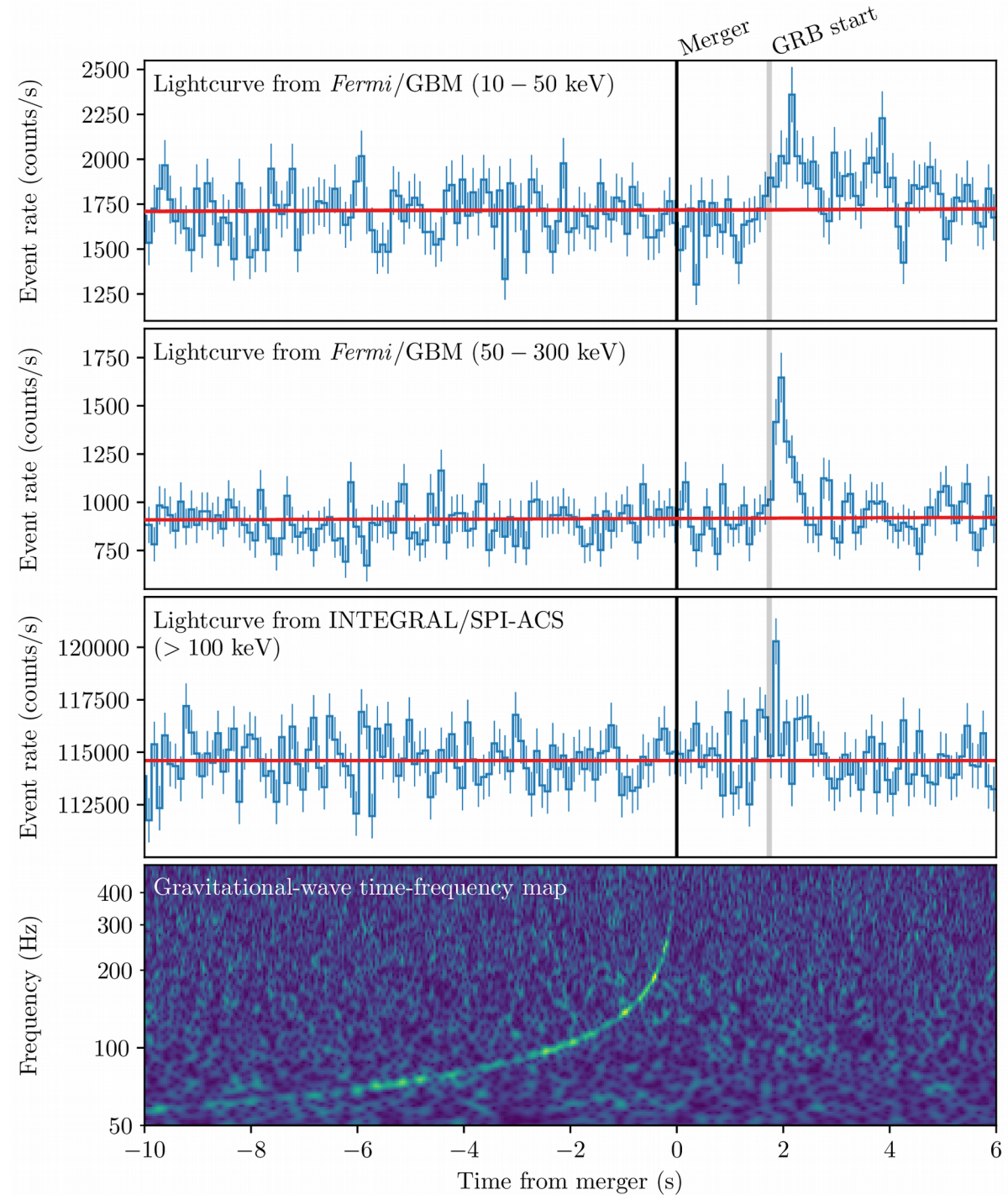
Masses



Tidal distortion



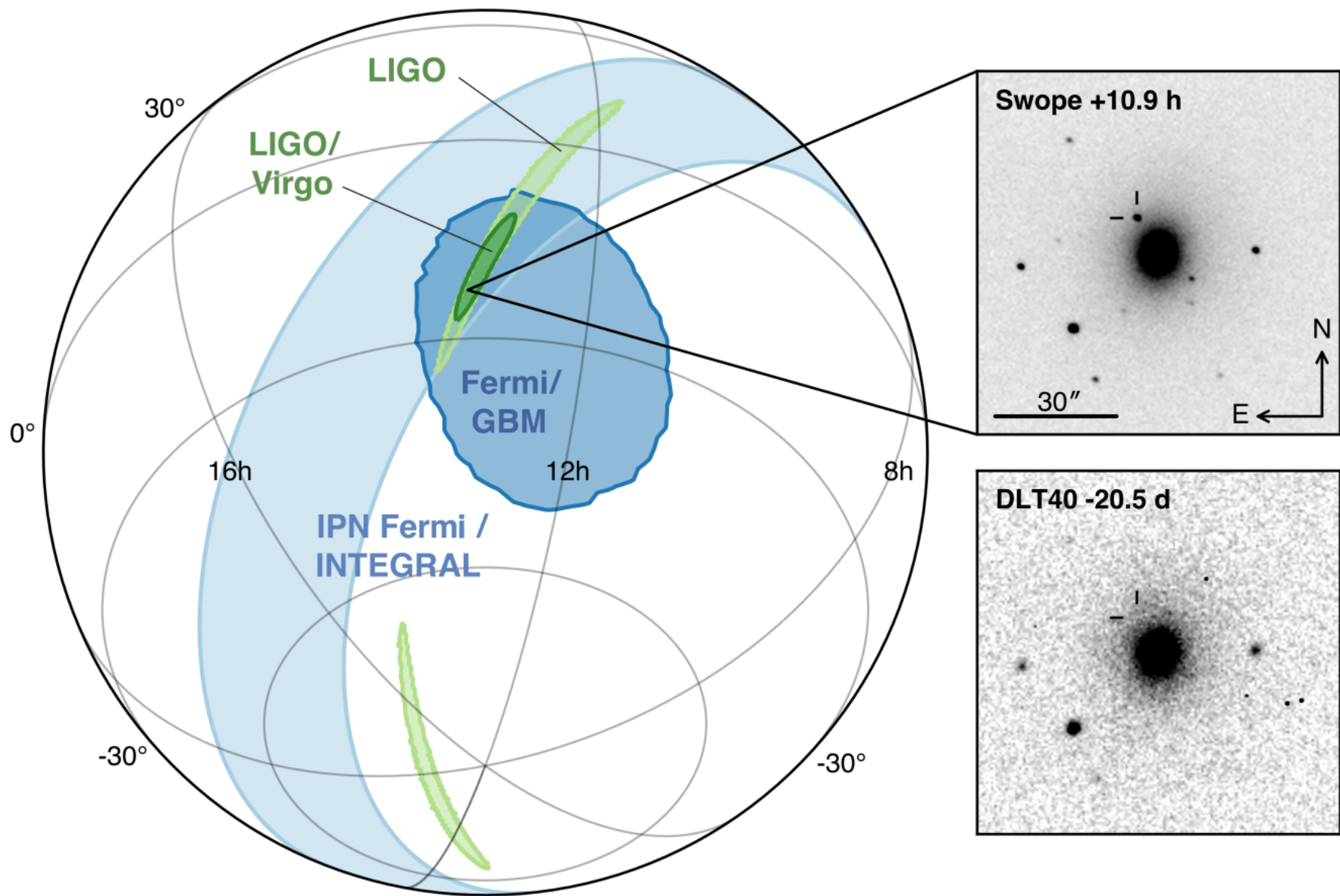
Gamma-rays



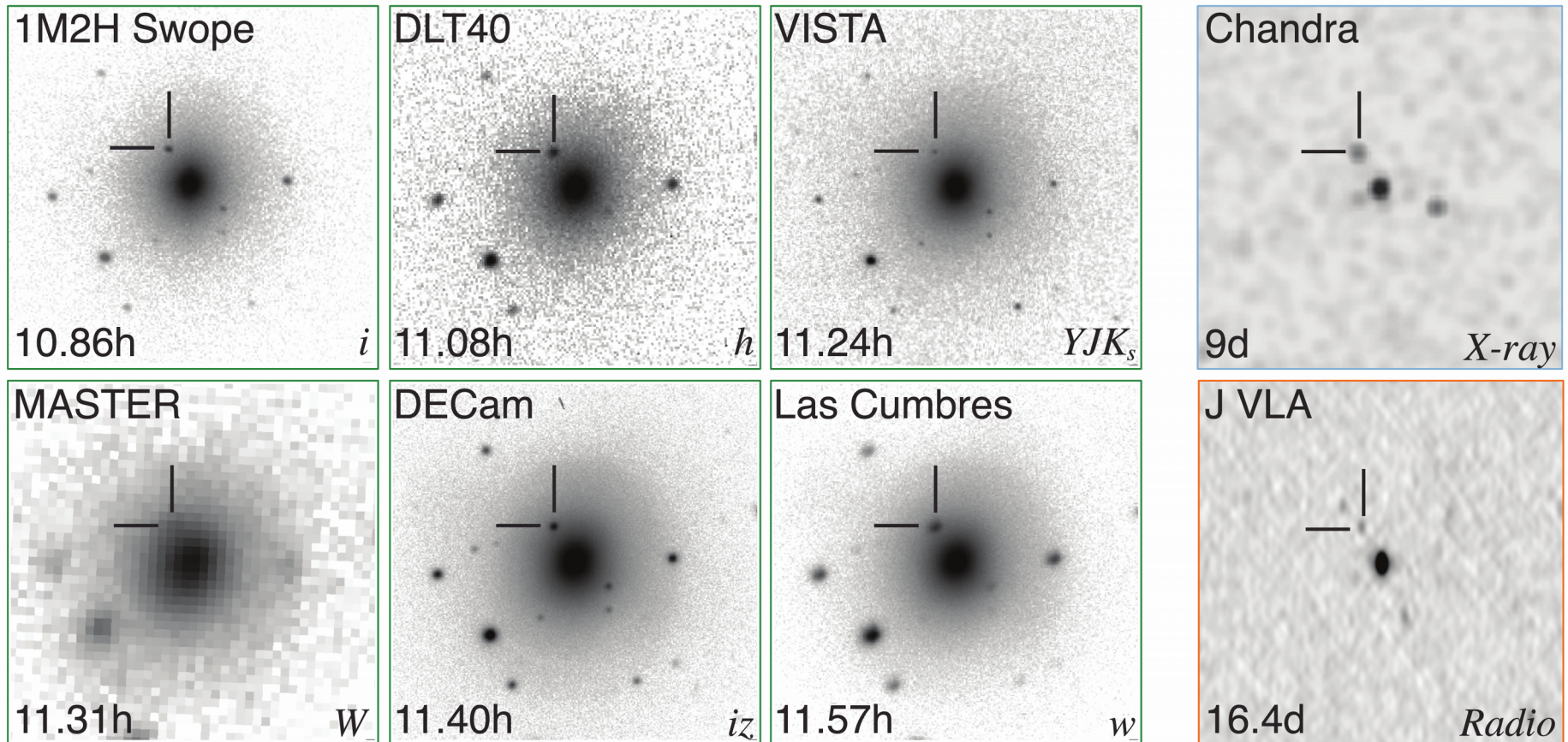
LVC, *Fermi* & INTEGRAL
arXiv:1710.05834

Gravity vs light

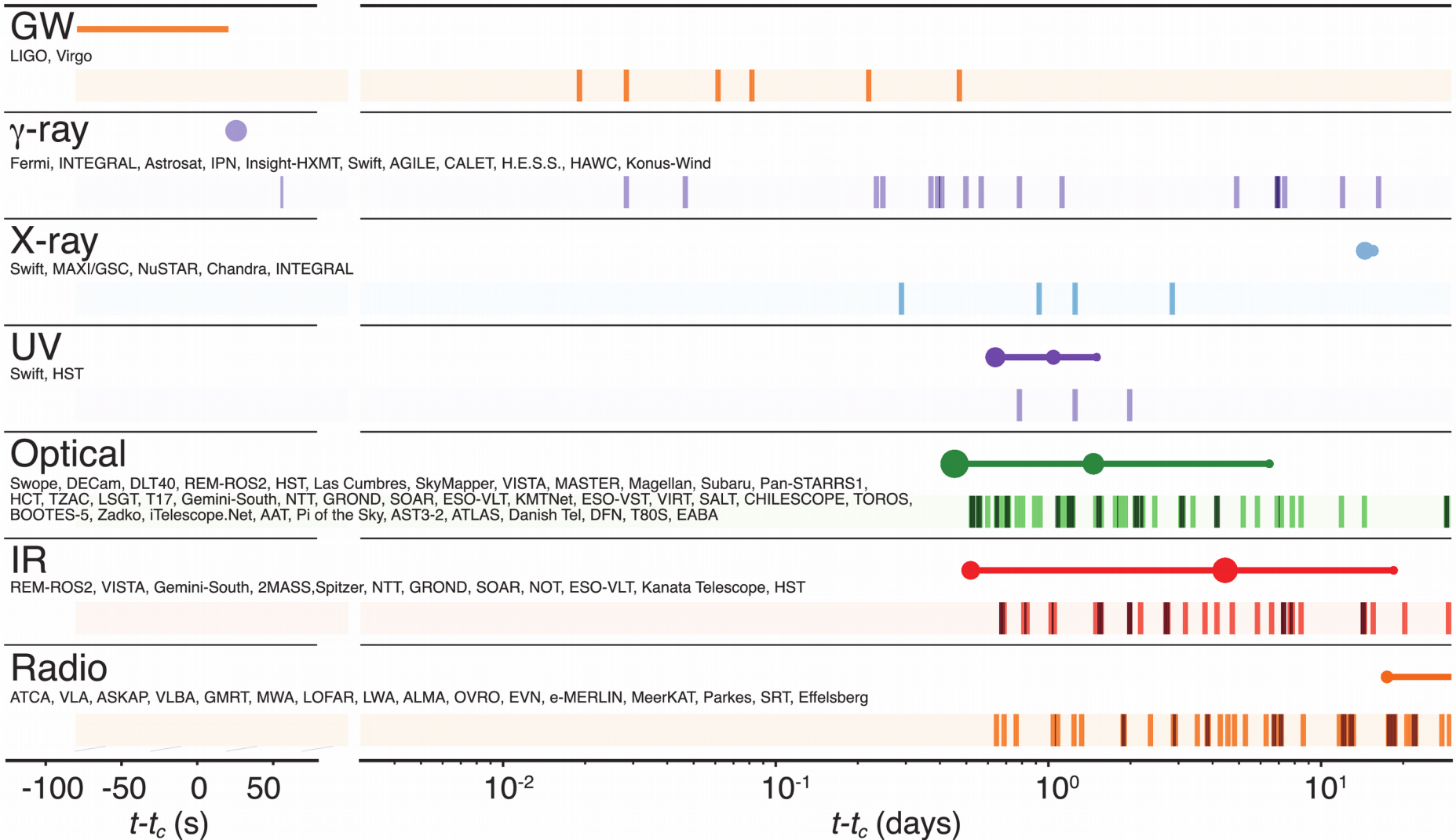
	$c_g = c$	$c_g \neq c$
Horndeski	<p>General Relativity</p> <p>quintessence/k-essence [46]</p> <p>Brans-Dicke/$f(R)$ [47, 48]</p> <p>Kinetic Gravity Braiding [50]</p>	<p>quartic/quintic Galileons [13, 14]</p> <p>Fab Four [15]</p> <p>de Sitter Horndeski [49]</p> <p>$G_{\mu\nu}\phi^\mu\phi^\nu$ [51], $f(\phi)\cdot$Gauss-Bonnet [52]</p>
beyond H.	<p>Derivative Conformal (19) [17]</p> <p>Disformal Tuning (21)</p> <p>quadratic DHOST with $A_1 = 0$</p>	<p>quartic/quintic GLPV [18]</p> <p>quadratic DHOST [20] with $A_1 \neq 0$</p> <p>cubic DHOST [23]</p>
	Viable after GW170817	Non-viable after GW170817



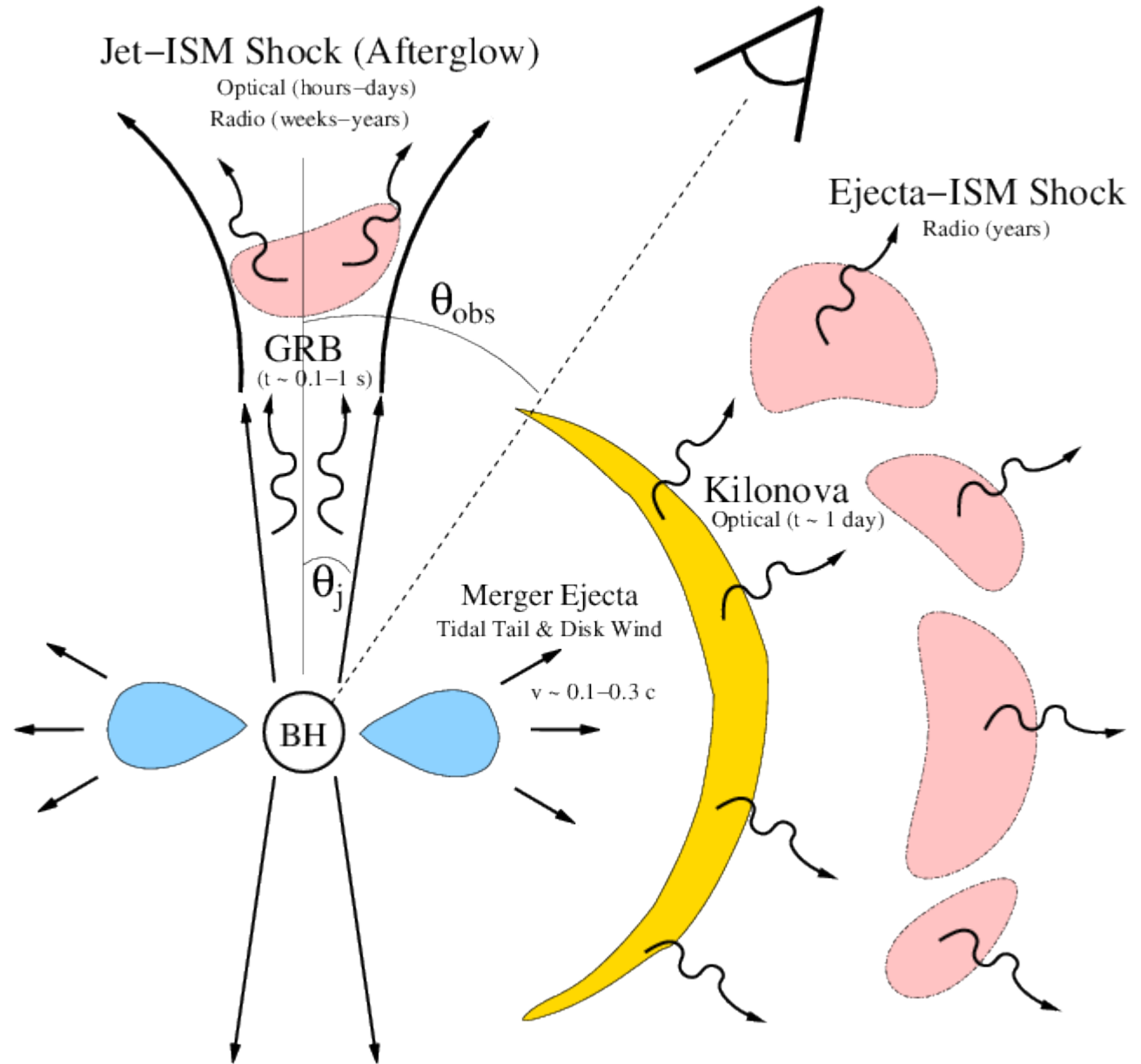
Spectrum of observations



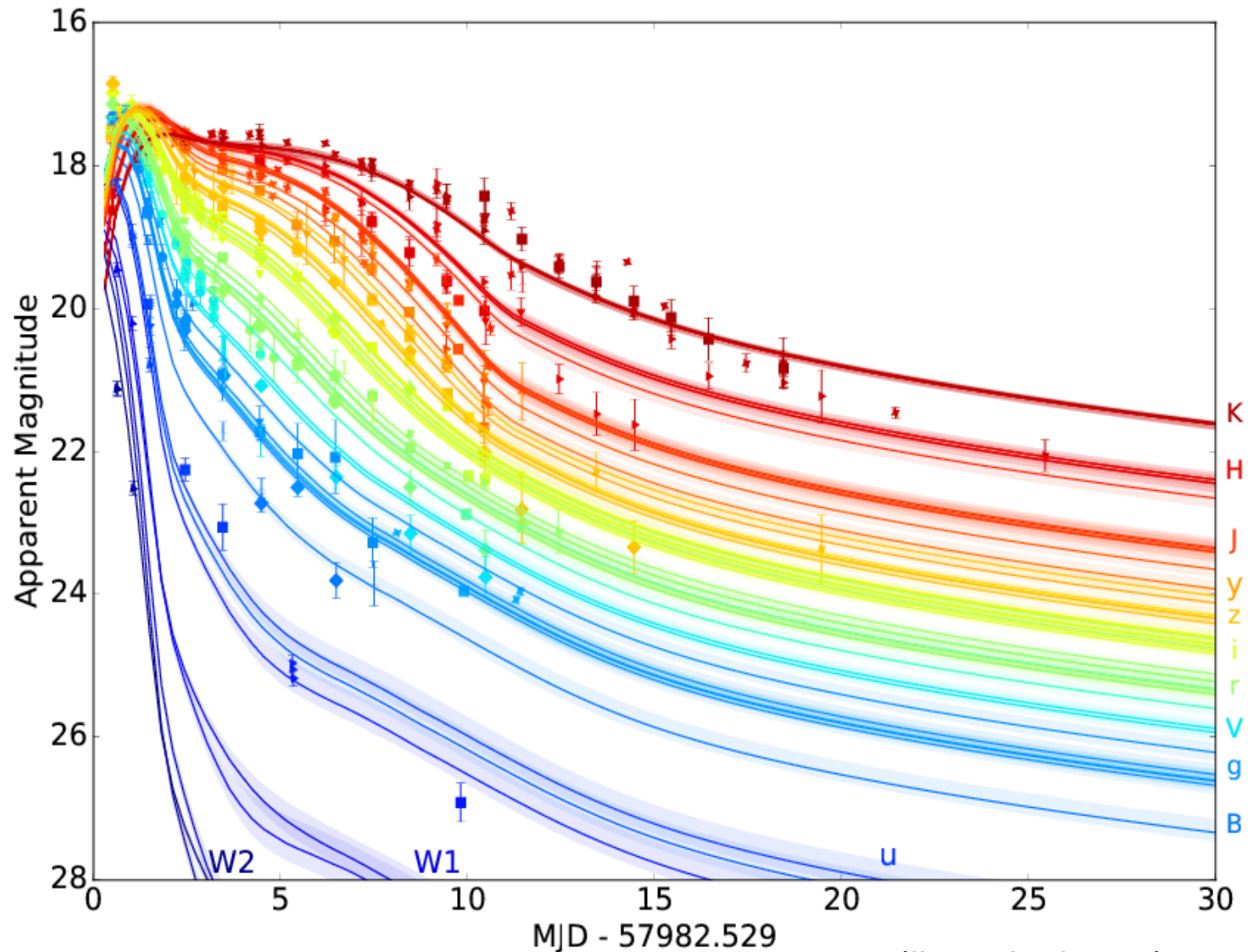
Spectrum of observations



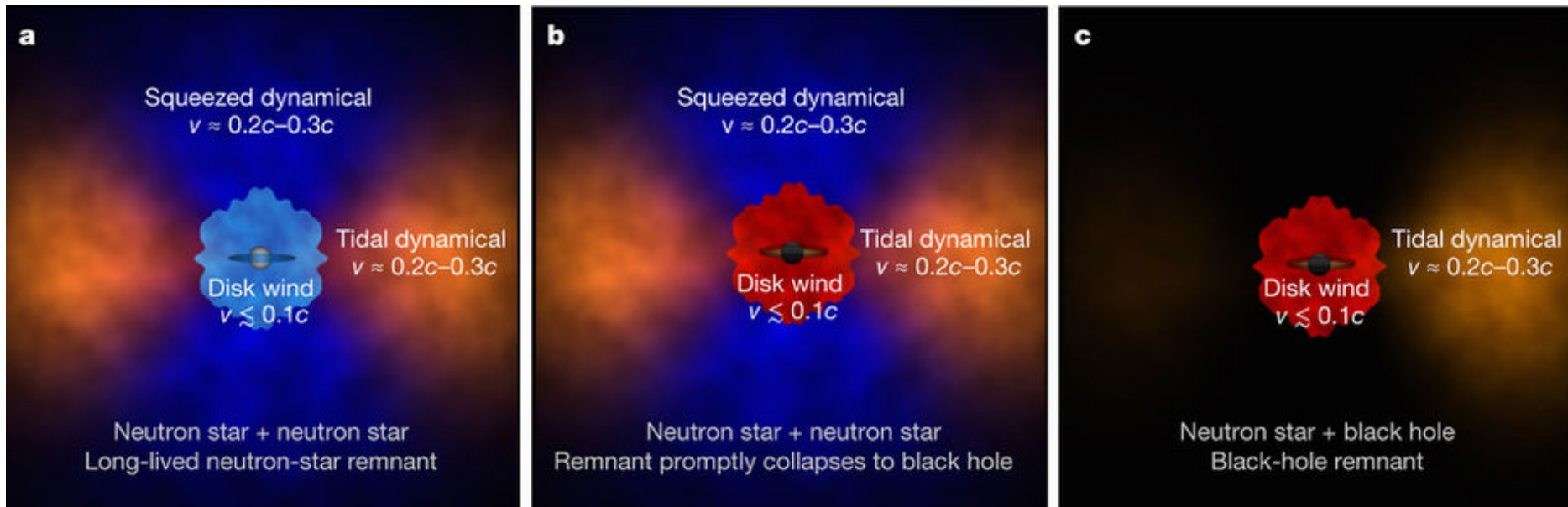
Light



Spectrum of observations



Kilonova



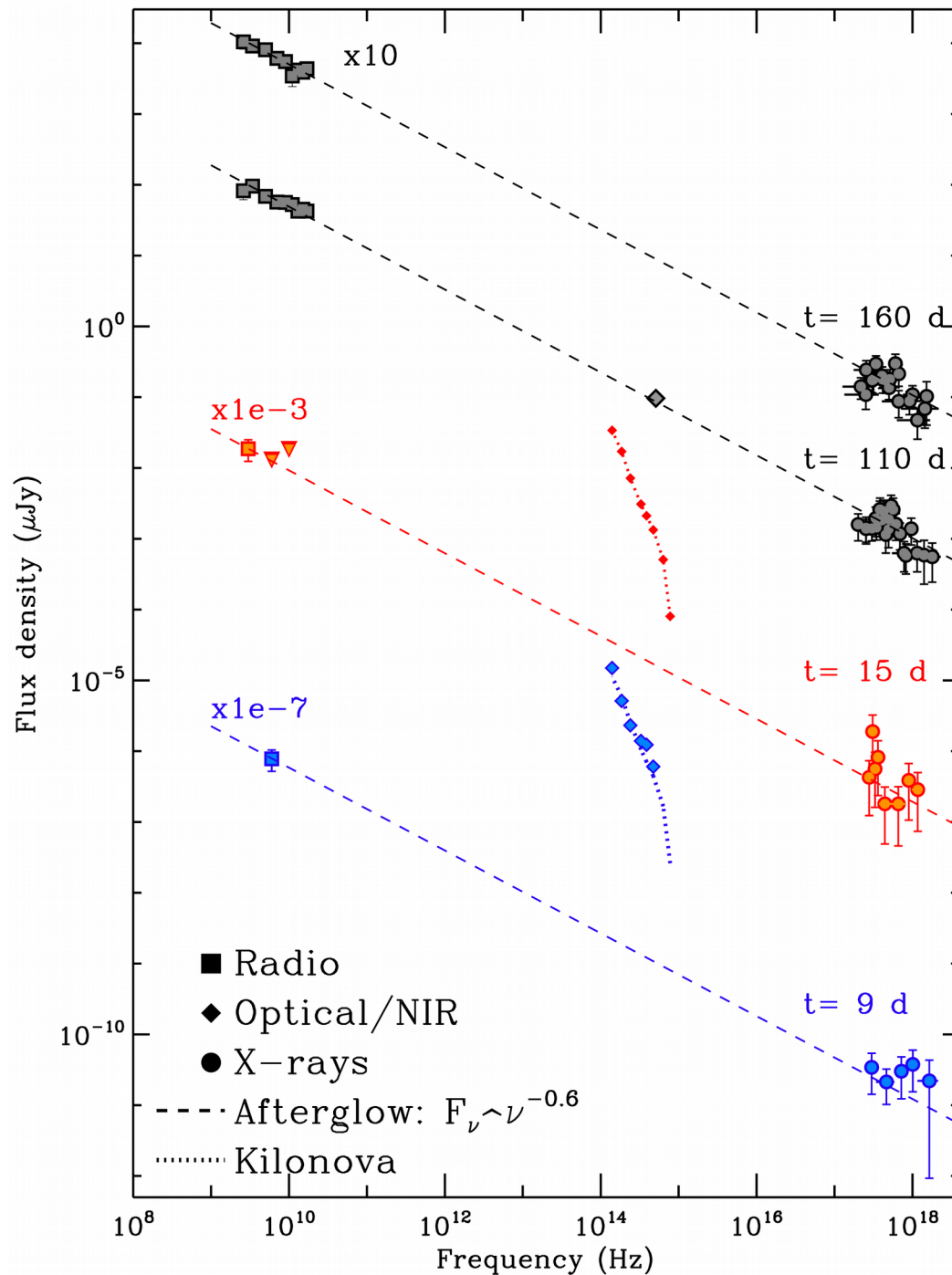
Kasen *et al.* arXiv:1710.05463

Heavy elements

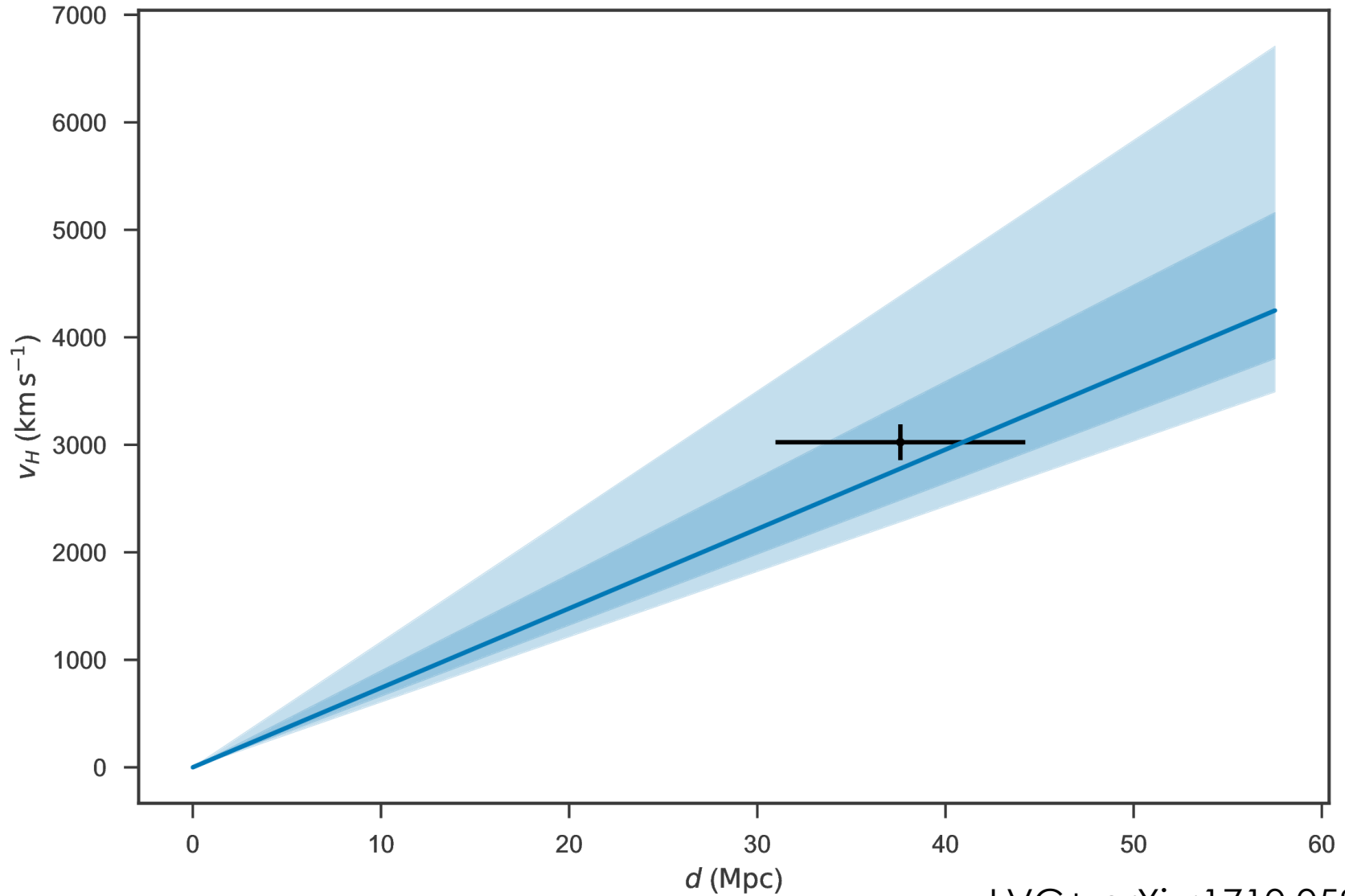


Credit: AP/F. Vergara

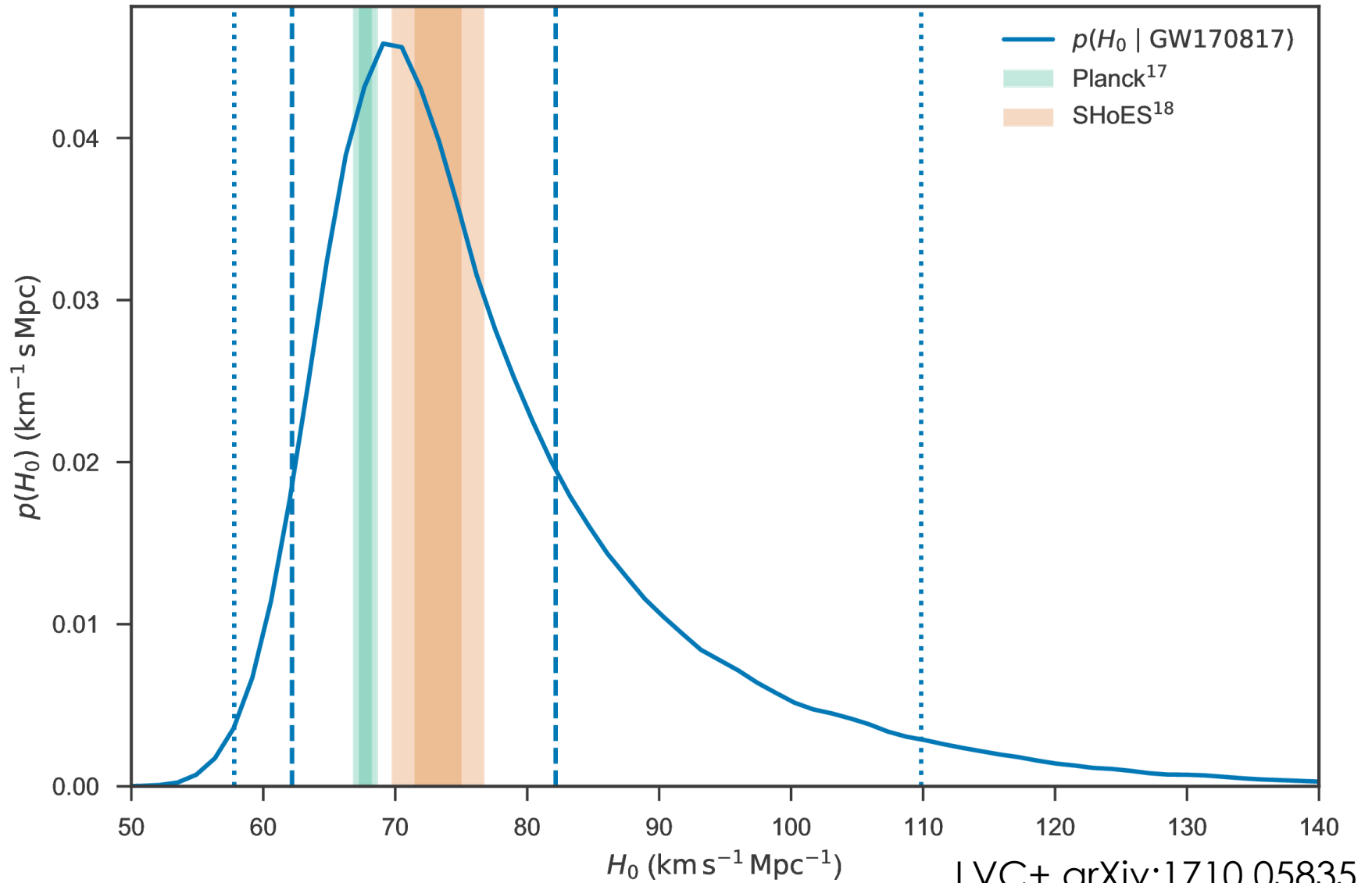
Afterglow



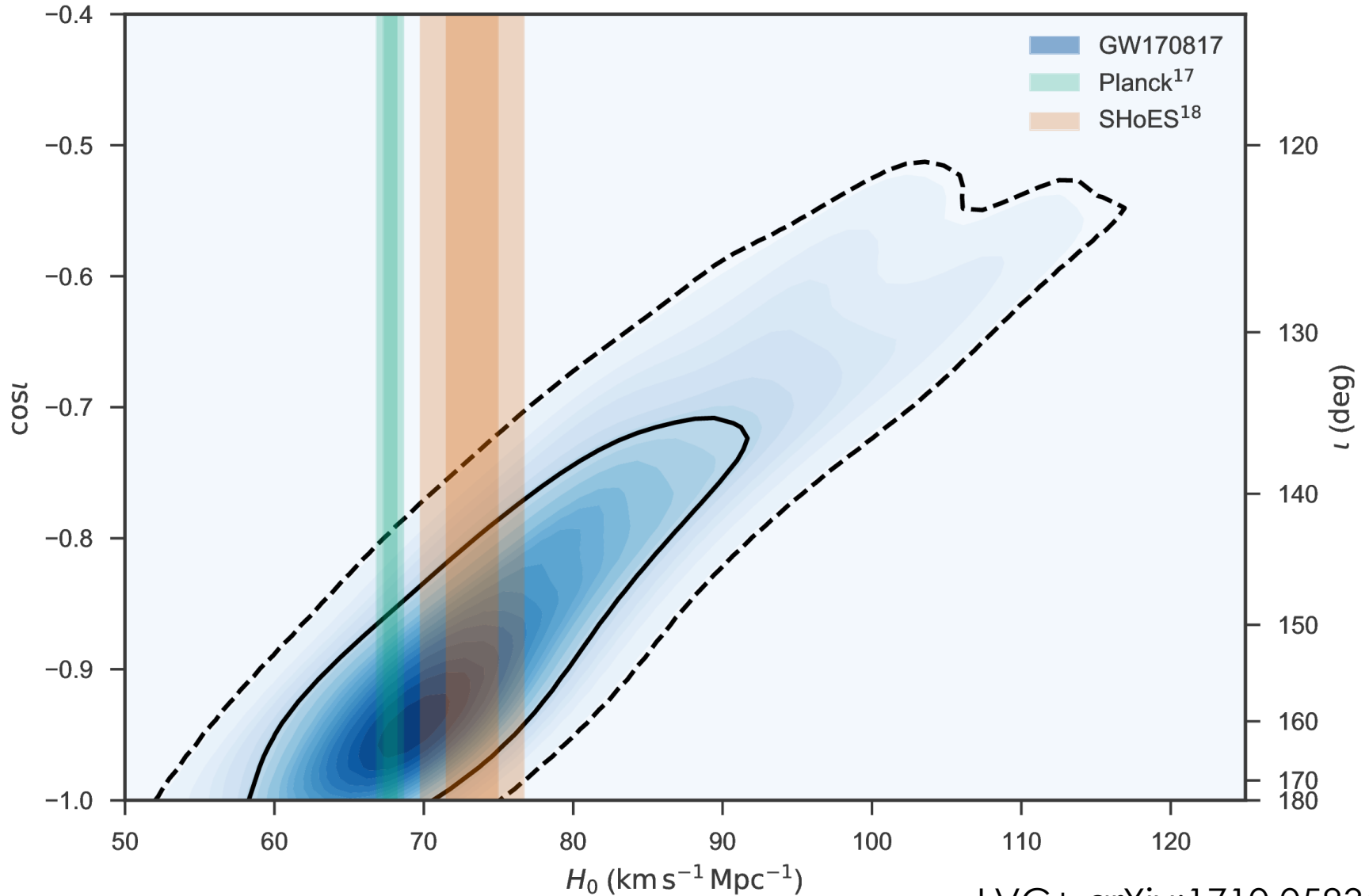
Expansion of the Universe



Hubble constant



Inclination



losc.ligo.org/events/
papers.ligo.org/

